

AD-A128 788

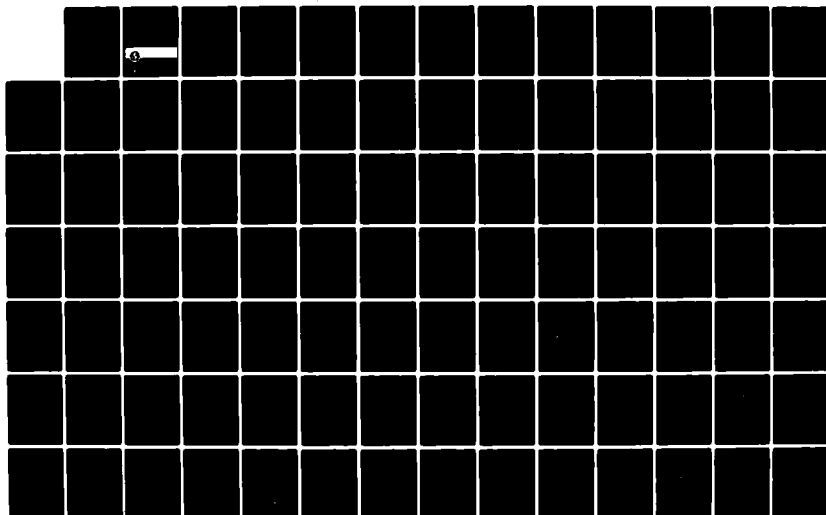
EVALUATION OF A NONLINEAR FINITE ELEMENT PROGRAM -  
ABAQUS(U) AKRON UNIV OH DEPT OF CIVIL ENGINEERING  
T Y CHANG ET AL. 15 MAR 83 AUE-821 N00014-78-C-0691

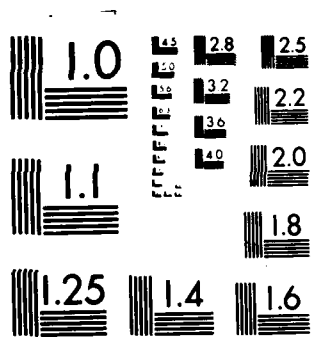
1/2

UNCLASSIFIED

F/G 9/2

NL





MICROCOPY RESOLUTION TEST CHART  
NATIONAL BUREAU OF STANDARDS-1963-A

(12)

Report No. AUE-821

# EVALUATION OF A NONLINEAR FINITE ELEMENT PROGRAM — ABAQUS

T. Y. Chang  
S. M. Wang

Department of Civil Engineering  
The University of Akron  
Akron, Ohio 44325

August 1, 1982  
(Revised on March 15, 1983)

Prepared for  
Office of Naval Research  
Department of the Navy  
Contract N0014-78-C-0691

DTIC  
SELECTE  
JUN 1 1983  
A

AD A 128788



DTIC FILE COPY

This document has been approved  
for public release and sale; its  
distribution is unlimited.

83 06 01 038

00 00 01 088

EVALUATION OF A NONLINEAR  
FINITE ELEMENT PROGRAM - ABAQUS

T. Y. Chang

S. M. Wang

Department of Civil Engineering  
The University of Akron  
Akron, Ohio 44325

August 1, 1982

(Revised on March 15, 1983)



Prepared for

Office of Naval Research  
Department of the Navy

Contract N0014-78-C-0691

An administrative form with several fields. A large handwritten "A" is in the bottom left field. A checkmark is in the top right field. The form has fields for "Approved For", "Date", "Initials", and "Signature".

## TABLE OF CONTENTS

1.	INTRODUCTION . . . . .	1-1
2.	DOCUMENTATION . . . . .	2-1
2.1	User's Manual . . . . .	2-1
2.2	Theoretical Manual . . . . .	2-2
2.3	System Manual . . . . .	2-2
2.4	Example Problem Manual . . . . .	2-3
3.	PROGRAM ORGANIZATION AND DATA BASE DESIGN . . . . .	3-1
3.1	PRE Program . . . . .	3-1
3.2	MAIN Program . . . . .	3-4
3.2.1	Input Step . . . . .	3-5
3.2.2	Procedure Library . . . . .	3-7
3.2.3	Material Library . . . . .	3-10
3.2.4	Element Library . . . . .	3-13
3.2.5	Arithmetic Library . . . . .	3-14
3.3	Data Base Design . . . . .	3-17
4.	FUNCTIONAL DESCRIPTION . . . . .	4-1
4.1	Analysis Procedures . . . . .	4-1
4.1.1	Static Stress Analysis . . . . .	4-1
4.1.2	Dynamic Analysis . . . . .	4-4
4.1.3	Heat Transfer Analysis . . . . .	4-8
4.2	Element Library . . . . .	4-8
4.2.1	Truss Elements . . . . .	4-9
4.2.2	2/D Solid Elements . . . . .	4-9

4.2.3	3/D Solid Elements . . . . .	4-9
4.2.4	Beams . . . . .	4-12
4.2.5	Shell Elements . . . . .	4-13
4.2.6	Elbow Elements . . . . .	4-14
4.2.7	Heat Transfer Elements . . . . .	4-15
4.3	Material Library . . . . .	4-15
4.4	Mesh Generation . . . . .	4-17
4.5	Kinematic Conditions . . . . .	4-18
4.5.1	Equation . . . . .	4-18
4.5.2	Friction . . . . .	4-18
4.5.3	Gap . . . . .	4-19
4.5.4	MPC - Multi Point Constraints . . . . .	4-20
4.6	User Subroutines . . . . .	4-20
4.7	Input and Output . . . . .	4-21
5.	VERIFICATION PROBLEMS . . . . .	5-1
5.1	Elastic-Plastic Deformation of a Cantilever Beam . . . . .	5-2
5.2	A Cantilever Beam Subjected to an End Moment . . . . .	5-4
5.3	Static Analysis of A Pipe Contact Problem . . . . .	5-7
5.4	An Elastic-Plastic Spherical Cap . . . . .	5-11
5.5	Elastic-Plastic Deformation of A Plate . . . . .	5-15
5.6	A Circular Plate With Plasticity . . . . .	5-21
5.7	Large Deformation of a Cylindrical Shell . . . . .	5-23
5.8	Post-Buckling of a Cylindrical Shell Subjected to a Point Load . . . . .	5-26
5.9	Dynamic Response of a Cantilever Beam . . . . .	5-26

6.	ADVANCED EVALUATION . . . . .	6-1
6.1	An Elastica . . . . .	6-1
6.2	An Elastic-Plastic Plate Subjected to Biaxial Loading. . .	6-5
6.3	A Cantilever Beam Subjected to An End Force . . . . .	6-10
6.4	Large Deformation of A Spherical Cap . . . . .	6-19
6.5	Buckling of A Spherical Shell. . . . .	6-21
6.6	A Centrally Cracked Plate. . . . .	6-24
6.7	Dynamic Response of A Spherical Cap. . . . .	6-39
6.8	Dynamic Analysis of A Semi-Spherical Shell . . . . .	6-56
6.9	Longitudinal Pulse in A Prismatic Bar. . . . .	6-60
6.10	Execution Time . . . . .	6-67
7.	SUMMARY AND CONCLUSION . . . . .	7-1
8.	REFERENCES . . . . .	8-1
	APPENDIX A . . . . .	A-1
	APPENDIX B . . . . .	B-1
	APPENDIX C . . . . .	C-1

ACKNOWLEDGEMENT

This work is supported by the Office of Naval Research, Department of the Navy, under the Contract Number N00014-78-C-0691. Assistance received from the project manager, Dr. Nicholas Perrone of ONR, is also appreciated.

The authors wish to acknowledge Mr. E. J. Ni, a graduate student in the Department of Civil Engineering, for helping a portion of this study.



## 1. INTRODUCTION

In recent years there has been an increasing interest in finite element software evaluations due to the widespread availability of such packages. Also recognizing this need, an ISEG (Interagency Software Evaluation Group) associated with the armed forces and other government organizations - such as the National Science Foundation, the Department of Energy, and the Nuclear Regulatory Commission - was formed for continuous coordination of evaluating engineering application software. In this connection, a set of criteria for selecting software, selecting contractors and evaluation procedures were developed by Nickell [1,2]. Subsequently, three general purpose finite element programs for structural mechanics applications were selected and evaluated. These are ADINA, NASTRAN and STAGSC-1 and the evaluation results were reported in references [3,4,5]. A comprehensive summary of evaluation work is given by Nickell [2].

As a part of ISEG's continuing effort, ABAQUS was also included for evaluation. ABAQUS is a general purpose finite element code for nonlinear static and dynamic analysis of structural problems, as well as steady-state and transient analysis of heat transfer problems. The code was a relatively new entry to the nonlinear structural software market; it was developed and released by Hibbitt & Karlsson, Inc., 1979. Although the version 3- ABAQUS\* has limited analysis capabilities (as compared to MARC [6] for example), it has the potential to become a major nonlinear code due to its modern concept software design and strong commitment in coding development by the company.

---

\*It is noted that only the version 3 of ABAQUS was available for the evaluation work. Therefore, whenever ABAQUS is mentioned again in this report, it implies the version 3 of ABAQUS.

By following the procedure outlined in [1], the evaluation work consists of the following:

- i) Review of documentation
- ii) Program organization and data base design
- iii) Functional description
- iv) Benchmark runs for coding verification
- v) Benchmark runs to determine the numerical characteristics of ABAQUS (advanced evaluation).

Since ABAQUS is marketed as a production code, unlike ADINA primarily as a research code, no attempt was made in the review of detailed program architecture. Instead, discussion is focused on the overall coding structure and its data base design. This is in contrast to our previous review work on ADINA [3]. The purpose of functional description is to give a comprehensive overview of the solution methodologies adopted and analysis features available in ABAQUS. The section on verification problems is to demonstrate the operational status of double precision version of ABAQUS on the IBM main frame. Finally, a great deal of effort was devoted to advanced evaluation in which a selected number of benchmark problems were run to determine the operating characteristics of ABAQUS in terms of its solution convergence behavior and computational efficiency (i.e. CPU time).

## 2. Documentation

ABAQUS is supported by four documents:

- User's Manual [7]
- Theoretical Manual [8]
- System Manual [9]
- Example Problem Manual [10]

### 2.1 User's Manual

Obviously, the purpose of user's manual is to provide specific instructions on data input and to give a description of output features. The major importance of this manual is its clarity in instructions.

The user's manual contains ten sections. Sections 1-4 are the reference sections in which input organization and syntax rules, analysis procedures, element and material libraries are described. Sections 6-10 contain data input instructions. Section 5 is not included in the manual; it may have been reserved to cover additional features which will be added into the program. For the most part, the manual was clearly written and easy to follow. To prepare the input data for a problem, the user should be able to find sufficient information from the instruction sections. To input element and material data, some cross-reference in Sections 3 and 4 is often necessary. Although the manual is generally well documented, two points may deserve some future attention:

- i) General shell section (6.5.9) is provided to allow direct input of a shell cross-section with elastic anisotropic, layered or corrugated material. However, the definition of section stiffness matrix D was not clearly specified. Confusion exists in deciding whether the D-matrix

for large deformation analysis has the same meaning as the one for small deformation. An example is needed in order to clarify this point.

ii) Restart (6.8.4) option can be exercised to save and reuse data and analysis results. The manual does not clearly illustrate how to use \*RESTART option to conduct a multi-step analysis. For example, in the case of dynamic analysis it is not clear that whether the analysis time should be accounted from the very beginning of the analysis or from the starting point of each new step? Similar question arises for the definition of new amplitude.

## 2.2 Theoretical Manual

The theoretical manual was written for the advanced user who has had sufficient background in (nonlinear) continuum mechanics and wishes to know the theory behind the code. The manual include the following basic items:

- Review of basic mechanics principles
- Description of analysis procedures
- Element formulations
- Constitutive theories
- General formulations for heat transfer analysis

All basic assumptions are properly stated. Kinematic and kinetic variables are clearly defined. This is a very important point, especially for large deformation analysis.

In the element formulations, considerable details are given for the beam, shell and elbow elements. Discussion on solid elements is rather sketchy; related literature should be cited to compensate this effect.

## 2.3 System Manual

The system manual contains a fairly detailed description on the program design of ABAQUS. The purpose of this manual, as stated in [9], is intended for a user to have access to the source code. The user may be a system

programmer who is charged with installing the program at a computer site, or a person who will make changes or additions to the code in order to solve a particular class of problems. The manual contains the following important information:

- Overall program design concept and decisions
- Brief review of theoretical basis
- Detailed flow of the PRE and MAIN Programs
- Description of data base design and data base managers
- Logic for allocation of workspace
- Description of labelled common blocks in PRE and MAIN
- Definitions of subroutines used
- User interfaces

While the reviewer found that the system manual was helpful to understand certain part of the source code, a good portion of the manual has become outdated. A number of subroutines, which were added to or deleted from the program, are not mentioned. Therefore, the system manual, as the way it stands, can at most be used as a reference material until it is properly updated.

#### 2.4 Example Problem Manual

An example problem manual which contains about sixteen sample problems is also available. The purpose of this manual, as it appears, is to assist the new user in setting up problems, or to verify the code upon installation. Each problem is presented in a standard format: problem statement; description of material, geometry, loading and boundary conditions; results and discussion; listing of input. In general, the example problems are clearly explained in the manual. However, most of the problems are

concentrated on the use of beam or pipe elements with elastic or elasti-plastic materials. There is a lack of representation of different elements or material models. Furthermore, the manual that the reviewer has is in a rough draft form which does not follow a proper sequence order.

### 3. PROGRAM ORGANIZATION AND DATA BASE DESIGN

ABAQUS was designed primarily as a production code for solving nonlinear problems. The program must be run on a fairly big computer (such as a mainframe or a super-mini computer) so that a reasonably large core size can be allocated in order to maintain its efficiency. In terms of its coding structure, ABAQUS is divided distinctively into two sub-programs: namely PRE and MAIN programs. The major functions of PRE are: i) to read the input data and sort the data onto a data structure from which the MAIN will read, and ii) to perform data check analysis. On the other hand, the function of the MAIN program is strictly for engineering analysis. The obvious advantage of this division is that the PRE can be repeatedly run alone for data checking with quick computer turn around time. This feature is extremely helpful for computer systems which assign higher priorities to jobs with short CPU time and/or small central core usage.

In addition, ABAQUS utilizes an extensive data base design concept in the development of its coding. This approach provides three apparent advantages: i) protection for data file over-write, ii) efficient utilization of fast core storage, and iii) ease of future coding extension or modifications. In this section, we will review each of the following three items in ABAQUS; i) PRE program, ii) MAIN program, and iii) data base design.

#### 3.1 PRE Program

The major functions of the PRE, as stated in the ABAQUS system manual [9], are to perform data check and create the data bases for the MAIN. The data bases are written onto a communication data base which are then passed on to the MAIN. If any fatal errors are detected, job execution will be terminated at the end of PRE.

The PRE program consists of 9-modules which are executed sequentially.

These modules are differentiated by step designations:

Step 1. Scan input data - The PRE reads all input data and provides an 'echo' printout of user's input data. All the common blocks are initialized and the locations of the data bases are defined. Each data base has a constant length of 1024 words except that the node point data base has a length of 2048 words (double precision for IBM computer). Also, the buffers of the data bases are initialized.

Step 2. Read bulk data -The input data are read again and they are separated into two different types: a) Bulk data -data associated with elements, nodes, element sets, and node sets, and b ) short list data -data other than a. Mesh and incremental generations, if encountered, are performed. Information such as BEAM SECTION, MATERIAL, STEP, etc. are written onto an input data base, and an input data manager is also created. The buffer space for the input data base manager was set to 1500 words in the program; 3 -words required for each input keyword card. Therefore, a maximum of 500 keyword cards can be read in for the current version of ABAQUS (version 3) unless the buffer space is enlarged. The short list data is separated into different volumes. At the end of this step, volume 1 of short list data base is extracted from a data block in subroutine BELTYP, and then copied onto the buffer area of the short list data base.

Step 3. Read material properties -Material property data are read and written onto volume 2 of the short list data base. Volume 3 of short list data base is also defined.

Step 4. Build element data base - Element data base is created from element data and special elements (springs, dashpots, etc) are inserted at appropriate



points in the data base. All element information (shell sections, beam sections, distributed loads, etc.) are interpreted and resolved onto the element data base and the short list data base (volume 4). Also, the nodes are assigned with internal numbers based on the element ordering.

Step 5. Build node point data base - Node information, such as point loads, boundary conditions, transformations, etc., are interpreted and resolved onto the node point data base and the short list data base (volume 5).

Step 6. Build step- dependent part of short list data base - the step- dependent part of the short list data base (volumes 6 - 9) is created for each analysis step.

Step 7. Space allocations for the MAIN -Based on the global sizing values for the MAIN analysis program, space allocations for the MAIN are made. The parameters for the array pointers (starting addresses of arrays) are stored in common blocks. The maximum sizing is limited by a parameter MCOREM, which is currently set to be 45,000 words. For problems exceeding this capacity, a new value may be assigned to MCOREM in the main driver of PRE.

Step 8. Plot undeformed mesh.

Step 9. Build communication data base - In order to pass all necessary information (values of array pointers, control variables, etc.) from the PRE onto the MAIN, a communication data base is created and copied on disk or tape unit #23. It consists of common blocks, element data base, node point data base, material point data base, and short list data base.

Finally, a driver for the MAIN is written onto a disk or tape unit #28. Two typical drivers are shown as the following:

## a) For Stress Analysis

```

DOUBLE PRECISION SINT
COMMON / CSP / SINT (45000)
CALL EXEC*
STOP
END

```

\*Executive module for stress analysis

## b) For Heat Transfer Analysis

```

DOUBLE PRECISION
COMMON / CSP / SINT (45000)
CALL HEXEC A#
STOP
END

```

# Executive module for heat transfer analysis.

The driver is compiled into an object module and kept on a temporary file. After linking the driver to the object module of the MAIN, the analysis of MAIN Program starts.

## 3.2 MAIN Program.

The MAIN contains a number of modules which perform the actual engineering analysis. In the current version of ABAQUS, there are three major analysis branches:

- Stress/strain analysis
- Offshore analysis (not active in reviewer's version)
- Heat transfer analysis
- Eigenvalue analysis

For a typical analysis branch, several modules are executed in a loop many times over due to the incremental (or time-history) solution approach being used. The main loop consists of three prime calculation stages: i) material calculations, ii) element calculations, and iii) solution of matrix equations. Detailed descriptions of the modules in the MAIN are given in ABAQUS system manual [9]. In this section, we shall review ABAQUS' organization by considering the following:

- Input Step
- Procedure Library
- Material Library
- Element Library
- Equation Solver
- Arithmetic Library

### 3.2.1 Input Step

In accordance with the type of analysis requested, an executive manager is called to read the data on communication data base from disk #23 sequentially. The buffer size of communication data base was set to be 512 in word length. All data in the buffer area of communication data base are then copied to appropriate common blocks and data bases. Tape unit for each data base is also defined as shown in Table 3.1. The core storage arrangement is problem dependent. For a relatively small problem, the buffer area is divided into several segments and a work space. Each segment is occupied exclusively by a data base. On the other hand, for large problems several data bases may share a common segment in the buffer. All the pointers for the buffer division are saved in common blocks. For example, in the material generation

Table 3.1 Tape Arrangement in the MAIN Program

Tape Number	Sequential/ Random	Description
1	S	Eigenvalue data base / half-step residual file
2	S	Decomposed equation file
3	S	Element nickname data base / Quasi Newton data base*
4	S	Temporary file for node point data base
5	S	Read input
6	S	Write input
8	S	FILE output data base
12	S	Restart data base *
19	S	Element operator data base *
20	S	Element operator data base
21	S	Material point data base *
22	S	Material point data base
23	S	Communication data base
24	S	Material stiffness data base / temporary element Output file / solution nickname data base/post plot file
25	S	Element data base *
26	S	Element data base
27	R	Short list data base
28	S	Element nickname data base / Quasi-Newton data base*
29	R	Node point data base
30	S	Element mass matrix data base

\*One for read - one for write

module pointers are stored in the common block called "CMATGI", whereas in the element generation module pointers are in "CELGI". Most of the array pointers are defined in the PRE program although some of the pointers are calculated in the MAIN whenever they are needed. In view of this, two immediate comments can be made: i) If any array allocations are to be redefined in the MAIN, related changes on the definitions of the pointers must also be made in the PRE program, and ii) changes become difficult if the data structure of the data bases is involved.

### 3.2.2 Procedure Library

Currently, there are four executive managers which control the procedure options, namely

- Static Analysis (EXECS)
- Dynamic Analysis (EXECD)
- Natural Frequency Calculations (EXECEV)
- Heat Transfer Analysis (HEXEC)

The relationship of the procedure library for stress analysis, with the input module in the MAIN is shown in Fig. 3.1. Macro flow for each executive manager is almost the same. Typical steps for static stress analysis are outlined as the following (Fig. 3.2):

- i) Initialize step and set-up increment information.
- ii) Calculate material stiffness D (i.e. stress-strain relations) for each material point.
- iii) Calculate element stiffness
- iv) Solve the system of equations by the frontal method
- v) Update the material stiffness for the case of nonlinear materials

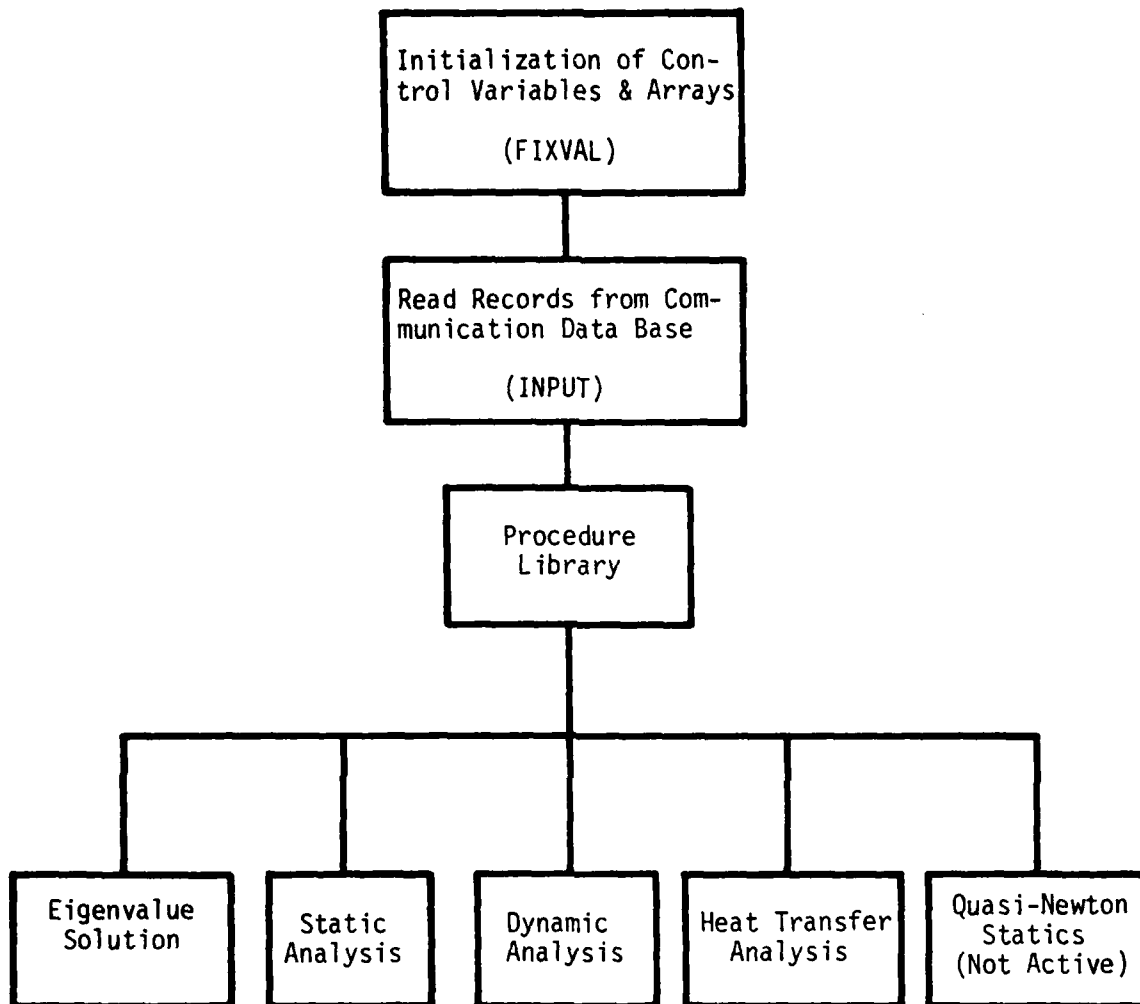


Fig. 3.1. Modules of Procedure Library

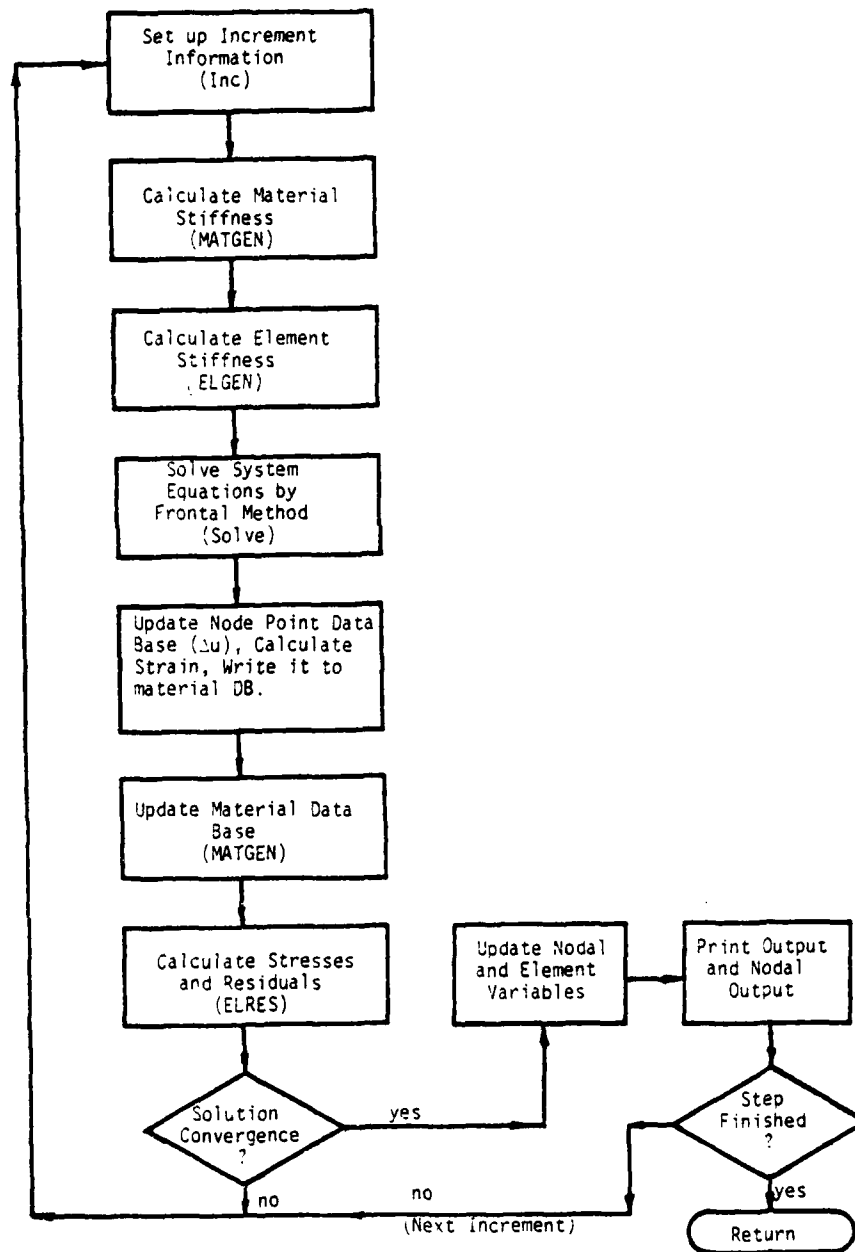


Fig. 3.2 Macro Flow of Static Stress Analysis

- vi) Calculate stresses and residual forces at integration points
- vii) If the solution has converged, update the nodal point data base
- viii) Print output for element and nodal information
- ix) Proceed the analysis for the next time increment.

### 3.2.3 Material Library

The library is controlled by the module driver called MATGEN. The pointers for defining the workspace are stored in the common block 'CMATGI'. The material stiffness data base pointers and other related information to the data bases are initialized in the subroutine MINIT. For every material point (which may differ from the element integration point), material type is checked and the corresponding control variables are defined. Six different types of material models (or routines) can be called to generate the material stiffness matrix D:

- MATELA - Linearly elastic materials with isotropic, orthotropic and anisotropic properties.
- MATEXP - Linearly elastic thermal expansions with isotropic, orthotropic and anisotropic properties.
- MATELG - Linearly elastic materials for general sections (options available for beam and shell elements).
- MATEXG - Linearly elastic thermal expansions for general sections.
- MATCHRP - Creep models (strain-hardening, time-hardening or user input creep law) and irradiation induced swelling.
- MATPLA - Plasticity model (von Mises plasticity with isotropic or kinematic hardening law). The effects of rate- and temperature-dependence are also available.



Also, other material options, such as density, conductivity, specific heat, etc. for heat transfer analysis, are defined in module HEXEC.

Two stages of calculations are involved for material generation:

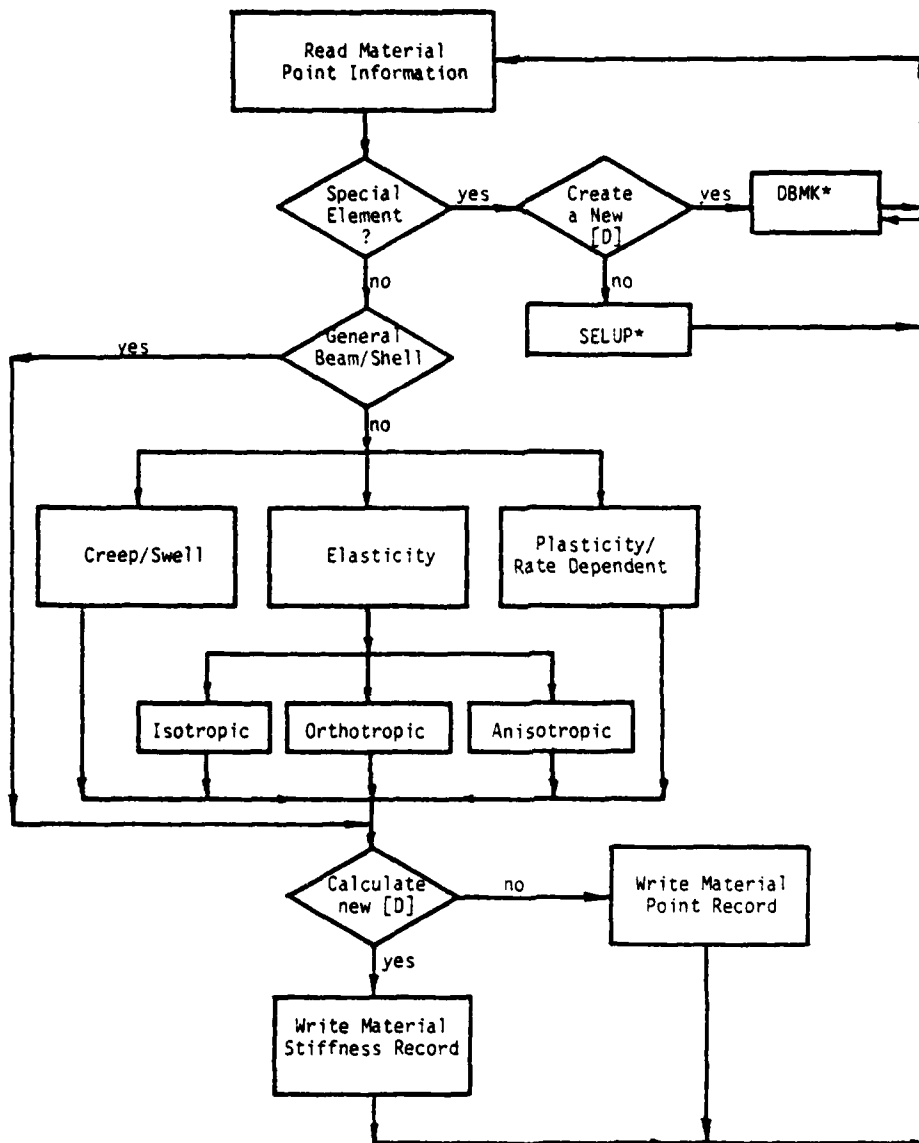
a) Material stiffness calculations, and b) Material data updating. For the material stiffness calculations, the following steps are executed for all material points:

- i) Set up material data
- ii) Calculate the thermal strain, if it is required.
- iii) Calculate initial strain for creep and swelling, whenever appropriate
- iv) Compute tangent modulus.
- v) Write the data on the material stiffness data base.

For the updating stage, executions include:

- i) Compute stress increments.
- ii) Insert new state on material point data base record.
- iii) Write the data on the material point data base.

A flow chart for the material calculations is shown in Fig. 3.3. Both the material stiffness and material point data bases provide necessary communication information between the material library (module MATGEN) and the element library (module ELGEN). It is seen that in ABAQUS the material library is completely independent, in terms of coding organization, from the element library. That is, the material models are uniformly available to all element types. This feature is different from ADINA [11] in which the material library is a sub-module of each element type [2].



DBMK: Material Stiffness Data Base.  
 SETUP: Update Special Element Information.

Fig. 3.3 Flow Chart for Material Generations

### 3.2.4 Element Library

This library is commanded by the routine ELGEN (module driver). Its primary purpose is to calculate element stiffness and other element data and then update the record on the element stiffness data base. Calculations are made in a loop for all elements. The major calculation steps involve the following:

- i) Call ELSET to read element information
- ii) Read data for all material points of the element from material stiffness data base to workspace.
- iii) Initialize element stiffness matrix  $[K]$  and element residual vector  $\{R_e\}$ .
- iv) Form element strain - nodal displacement transformation matrix  $[B]$ .
- v) For dynamic analysis:
  - a. Calculate the mass matrix  $[M]$  for the first time increment
  - b. Add the effect of initial conditions to the right hand side force vector  $\{R_e\}$ .
  - c. Form effective stiffness matrix  $[S]$ .
- vi) Check the value of control variable NREF for appropriate adjustment of stiffness matrix  $[K]$  or  $[S]$ , and force vector  $\{R_e\}$  :
  - a. Additional terms due to distributed loads or foundation stiffness.
  - b. Coordinate transformation from local to global system.
  - c. The effect of boundary condition.
  - d. Equations for multi-point constraints.

- vii) For the first iteration of an increment, write  $\{R_e\}$  to node point data base. Otherwise, read  $\{R_e\}$  from node point data base.
- viii) Write element stiffness data base record consisting of  $[S]$  and  $[R]$ .

### 3.2.5 Arithmetic Library

This library consists of several utility packages which are accessible to all the modules in ABAQUS. These packages are:

- Matrix addition
- Matrix subtraction
- Matrix multiplication
- Element stiffness calculation;  $\int_V [B]^T [D] [B] dv$ .
- Calculation of element residual force vector,

$$\{R_e\} = \{R_e\} - \int_V [B]^T \{\sigma\} dv$$

- Copy a double-precision real array to an integer array.
- Copy an integer array to a double-precision real array.
- Cholesky decomposition of a matrix.
- Q-R algorithm
- Vector normalization, etc.

Obviously, by consolidating all the utility subroutines in a library, ABAQUS has avoided any repetitive coding as it was commonly done in other programs.

Finally, to show the inter-relationship of various modules in the MAIN program, a chart is drawn in Fig. 3.4. The hierarchical level of the modules is that any module can only call other modules inside of its circle. One may

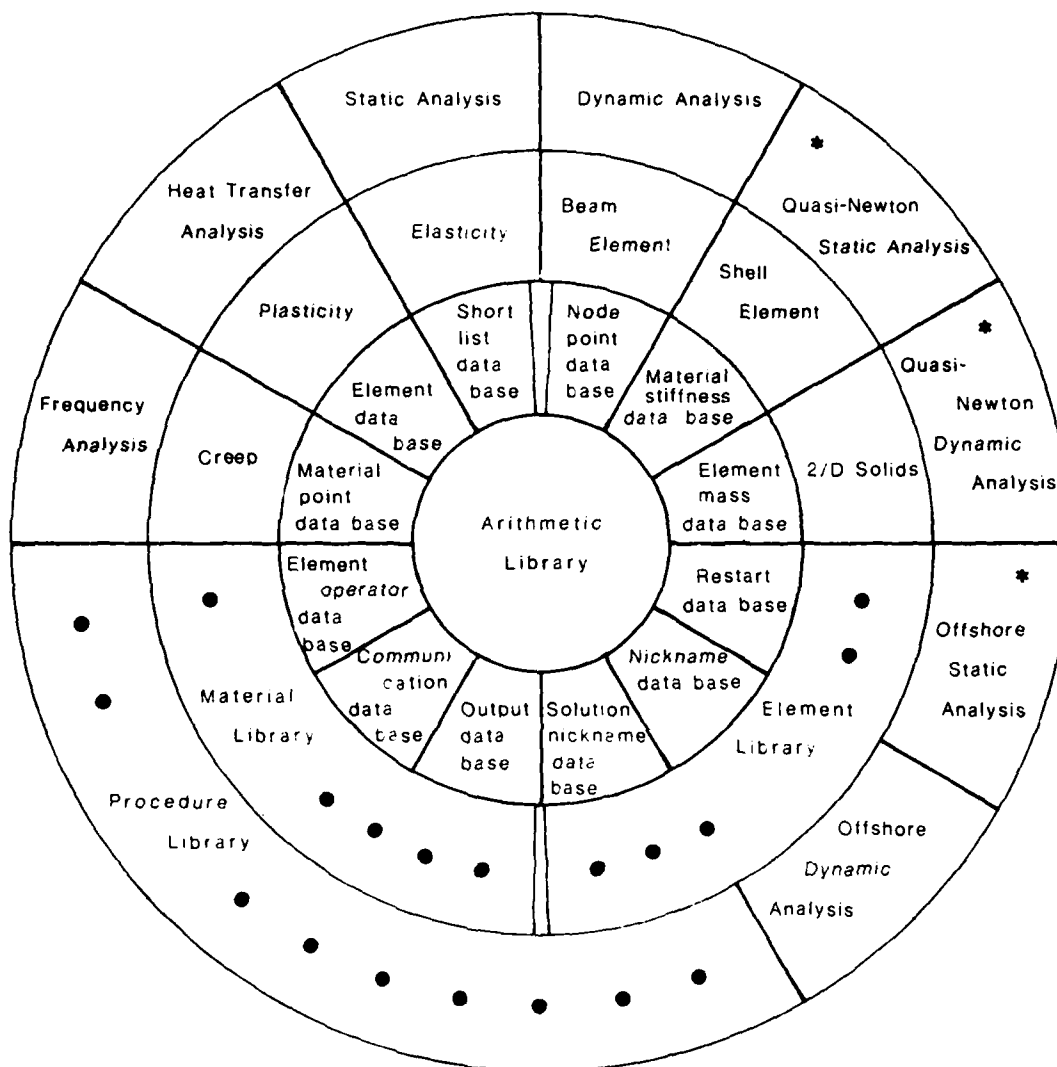


Fig. 3.4. Relationships Between Various Modules  
in the Main Program.

note that the interaction between the element library and the material library is made through material stiffness and material point data bases.

Commentary:

- 1) Separation of the entire program into PRE and MAIN provides apparent advantages:
  - a) Short turn-around time - Running the PRE program only takes a few seconds or a few minutes of CPU time, which has high priority in execution.
  - b) Smaller core requirement - In PRE, all real variables are in single precision and it requires no more than 750 K bytes core size to analyze a fairly sizable finite element problem.The PRE can be run either separately or consecutively with the MAIN.
- 2) The code was very modularly constructed for ease of extension or modification by the developers.
- 3) The codings of ABAQUS are generally difficult to follow by a non-developer since there are very few comment cards in the program for explanation.
- 4) The material library is an independent module from the element library. Therefore any existing material models in ABAQUS are uniformly available to all element types.
- 5) Although ABAQUS was modularly constructed, to add a new material model or element type into the program by a user is by no means obvious. Not only one has to add subroutines corresponding to the new material model or new element, but also changes have to be made in the root subroutines of the main. Moreover, a number of subroutines in the PRE must be modified.

### 3.3 Data Base Design

ABAQUS utilizes the data base concept in both PRE and MAIN programs. In this concept, the data are separated into several files, each file is handled independently. In the program a master array called INTS is allocated and it is divided into data base page pools (or buffer areas) and working-space. All data files are stored in the page pools with pre-assigned sizes. The sizing decision is made in the PRE program. For example, the data base structure used in the PRE is shown in Fig. 3.5. The lengths of the page pools will not remain fixed, they can be redefined during the analysis. All page pools are allocated in the fast core area. If, for a particular data file, the page pool is not large enough, secondary storage device (either sequential or random access file) is utilized.

Access of each data base is controlled by its manager. That is, whenever information needs to be calculated or updated, the data base manager will transfer the data from page pool area to working-space. After the calculations are completed, data are then copied back to the page pool area. Each page pool is a physical record and it is further separated into a number of fields. The field is the smallest unit that can be accessed by the data base manager in ABAQUS. Moreover, each field consists of several pieces of information. The process of transferring data between the page pool area and work-space is shown in Fig. 3.6.

Clearly, the data base manager performs the following important functions:

- i) Transfer data from the data base (page pool) to work space
- ii) After the data has been processed, copy it back to the page pool area.
- iii) If secondary storage device is used, perform necessary I/O operation, then transfer data as i or ii.

## Array INTS

IDREFR		Restart data base (read/write)
IDREFW		Restart data base (write/read)
IDNLFW		Restart data base (write/read)
IDELFW	NGTRC <sup>‡</sup>	Node list file, history data base
(IDMPFW)		
(IDNNFW)	NGTRC	Element list file, Material point data base, etc.
IDNSFW		
(IDCMFW)	NGTRC	Node set file, Communication data base.
IDESFW	NGTRC	Element set file
IDINFW		
(IDNLSB, IDELSB)	NGTRC	Input data base
IDEDFW	NGTRC	Element data base
IDSLFW	NGTRC	Short list data base
IDTPFW	NGTRC	Output file data base
IDNDFW	NGTRC	Output file data base
	2*NGTRC	Node point data base
IDNDF2		
	2*NGTRC	Expanded node point data base
IDIMFW	≤ 1500	Input data base manager
IGFWA		Working space

## Notes:

<sup>‡</sup> NGTRC is defined as 1024.

\* Temporary working area for the arrays indicated.

Fig. 3.5. Buffer Areas of Data Bases in Pre-Program



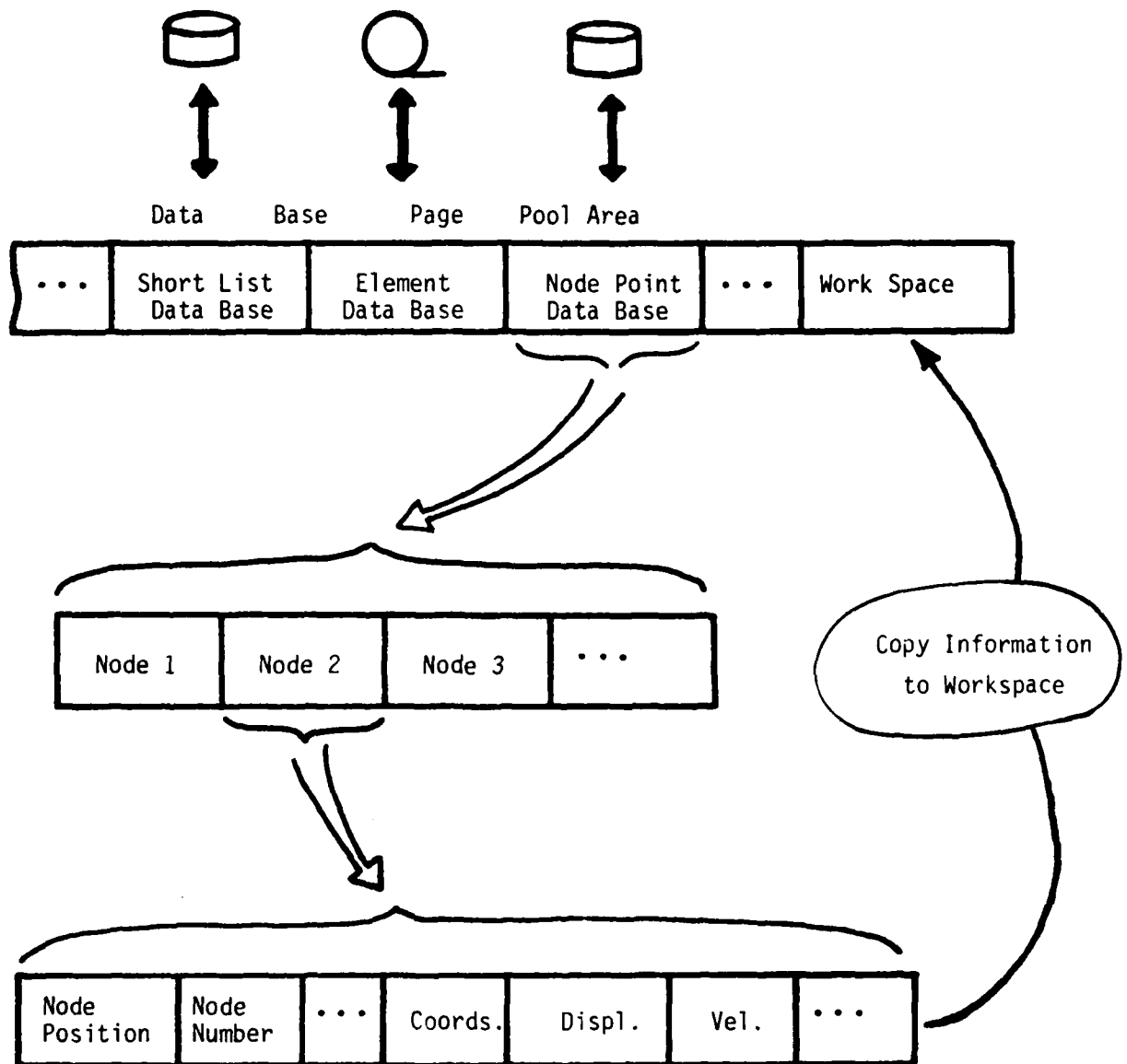


Fig. 3.6. Transfer of Data Between Data Base and Work-Space.

From the above discussion, we may summarize the following characteristics:

- i) By using the data base design concept and separate work-space for processing data, all data are well protected from accidental over-writing or deletion.
- ii) By keeping independent data bases, program modularity can be easily achieved. For example, the material library is an independent module from the element module; interactions between the two modules are made through the material stiffness and material point data bases.
- iii) Data integrity is maintained throughout the analysis; that is, data bases contain only processed data, all calculations or updatings are performed in the workspace.
- iv) The usage of secondary storage devices is kept minimum, it varies with the size of a problem.

Nevertheless, there are two drawbacks which may warrant future improvements:

- i) Pre-defined fixed sizes of data bases may cause unnecessary wasting of storage, which will, in turn, increase I/O swaps. By doing this, some of the data bases (in core) may have been exhausted, whereas others still have excess space or are not being used at all.
- ii) By using separate workspace for data processing, large amounts of data copying are involved and this definitely increases the CPU time significantly.

#### 4. FUNCTIONAL DESCRIPTION

In this section, an overview of the analysis capabilities\* of ABAQUS and a description of solution methodology are given. It is noted again that all discussions are centered on the Version 3 of ABAQUS.

##### 4.1 Analysis Procedures

ABAQUS is designed principally for the nonlinear static and dynamic analysis of structures, and nonlinear steady and transient analysis of heat transfer or conduction problems. Linear analysis for the corresponding problems can also be done as a special case of the nonlinear analysis. The Version 3 of ABAQUS has the following three basic procedures:

- Static stress analysis
- Dynamic analysis
- Heat transfer analysis (both steady state and transient).
- Eigenvalue Analysis

##### 4.1.1 Static Stress Analysis

ABAQUS has fairly extensive nonlinear analysis capabilities. For stress analysis, three major sources of nonlinearity are included:

- i) Material nonlinearity - Possible material models are to be discussed later in the material library.
- ii) Geometric nonlinearity - Only the effect of large rotation but small strain is considered in the current version.
- iii) Boundary nonlinearity - The user may impose gap or no-gap, and friction boundary conditions between two bodies. Classical Coulomb friction is assumed.

The user may request any combinations of the aforementioned nonlinearities.

---

\*Additional analysis capabilities of Version 4 - ABAQUS are listed in Appendix C.

The solution method employed in ABAQUS is an incremental approach with tangent stiffness. For each loading increment, (full) Newton's method is used to solve nonlinear equilibrium equations. The obvious advantage of Newton's method, over the modified Newton or quasi-Newton, is that it has better convergence rate and consequently the method can handle a wider range of nonlinear problems. On the other hand, this procedure is rather expensive since the structural stiffness matrix (or heat conduction matrix for heat transfer analysis) has to be reformed and triangularized for every iteration cycle.

In ABAQUS, the history of a problem is divided into three stages: step, increment, and iteration cycle. A problem may consist of one or several steps; typically each step is simply a change from one load to another (say from static to dynamic load). A step then consists of a number of increments. Within each increment, several iteration cycles are involved. Loading history and solution convergence are controlled by the following input parameters:

- INC - Maximum number of increments in a step
- CYCLE - Maximum number of iteration cycles allowed in an increment
- PTOL - Force tolerance for checking solution convergence during iterations.
- MTOL - Moment tolerance for checking solution convergence during iterations.

The user manual recommends the values of PTOL and MTOL being from 1 to 10% of typical applied forces and reaction forces in a structure. The reason for using such physical quantities for convergence control is based on the assumption that the engineer should know well enough about his model and be able to specify appropriate values for PTOL and MTOL. Contrary to this opinion, the reviewer feels that it is difficult to define a realistic PTOL or MTOL

for a complicated structure since the analyst often does not have any notion as to the order of reaction forces or moments a priori.

For loading increment control, the user has two options to choose from:

- i) Direct step control - user specifies the loading increments .
- ii) Automatic step - The program will choose its own incrementation scheme based on specified tolerance, i.e. PTOL and MTOL.

As explained in the manual, direct step control is suggested in cases where the problem behavior is well understood. Otherwise, automatic step is preferred, especially for start-up of a new nonlinear problem. Generally, automatic step requires much more CPU time than direct step for a given problem.

To exercise the automatic step, two additional input parameters are required:

NUMBER - Suggested number of increments of uniform size needed to complete the solution.

CUTMAX - The maximum number of times current increment size may be subdivided.

The program will proceed the analysis based on a suggested time increment  $\Delta t = (\text{total time})/\text{NUMBER}$ , and monitor the maximum force and moment residuals. Starting at iteration cycle #4, solution convergence is projected at n-th iteration that

$$n = i + \ln (PTOL/R(i)) / \ln(R(i)/R(i-1)) \quad (4-1)$$

where

i = i-th iteration cycle

R(i) = Maximum force or moment residual corresponding to i-th iteration

Once  $n$  is calculated, two possibilities exist:

- a)  $n \leq \text{CYCLE}$ , convergence is expected and hence continue iterations.
- b)  $n > \text{CYCLE}$ , the suggested time increment is too large and cut-back of increment size is made, i.e.

$$\text{New } \Delta t = 0.25 (\text{Old } \Delta t)$$

The solution is then started over again from the end of the previous increment.

On the other hand, if, in two successive increments, convergence is achieved in less than  $\text{CYCLE}/2$  iterations, the increment size is increased by 25% for the next increment, with a minimum number of increments,  $\text{NUMBER}$ .

According to the benchmark problems run by the reviewer (to be shown in Sections 5 and 6), the automatic step control worked quite well in terms of getting a solution successfully. However, in most cases this procedure is extremely time-consuming and it is impractical to solve a large scale nonlinear problem using automatic step exclusively from the beginning to the end.

#### 4.1.2 Dynamic Analysis

With the inclusion of inertia effect, the equilibrium equations corresponding to finite element approximation can be expressed as

$$\bar{M} \ddot{\bar{u}} + \bar{T} - \bar{P} = 0 \quad (4-2)$$

where

$\bar{M}$  = Consistent mass matrix

$\ddot{\bar{u}}$  =  $d^2\bar{u}/dt^2$ ;  $\bar{u}$ , nodal displacement vector

$\bar{T}$  = Internal force vector

$\bar{P}$  = External force vector

For nonlinear problems, internal force vector  $I$  is related to the tangent stiffness matrix of the finite element idealization which may include the effects of geometric as well as material nonlinearities.

To solve Eq. (4-2) numerically, two stages of approximations are involved; Newton's method of iterations as employed in static analysis and direct integration in time. ABAQUS adopted the  $\alpha$  - method due to Hilber and Hughes [12, 13] which is an implicit integration scheme. In this method, the equilibrium equations are written as

$$\bar{M} \ddot{u}_{t+\Delta t} + (1 + \alpha)(T_{t+\Delta t} - P_{t+\Delta t}) - \alpha (T_t - P_t) = 0 \quad (4-3)$$

In addition, Newmark's formulae are used to approximate the displacement and velocity vectors at time  $t+\Delta t$ ,

$$u_{t+\Delta t} = u_t + \Delta t \dot{u}_t + \Delta t^2 \left( \left( \frac{1}{2} - \beta \right) \ddot{u}_t + \beta \ddot{u}_{t+\Delta t} \right) \quad (4-4)$$

$$\dot{u}_{t+\Delta t} = \dot{u}_t + \Delta t \left( (1 - \gamma) \ddot{u}_t + \gamma \ddot{u}_{t+\Delta t} \right) \quad (4-5)$$

with

$$\beta = \frac{1}{4} (1 - \alpha)^2$$

$$\gamma = \frac{1}{2} - \alpha$$

$$-\frac{1}{3} < \alpha <$$

The main characteristics of the  $\alpha$  - operator are:

- i) It is unconditionally stable in linear dynamic analysis
- ii) It offers controllable algorithmic damping by specifying the  $\alpha$ -values
- iii) The operator is more accurate in the lower modes, as compared to the Wilson  $\theta$  - method [14]. For large  $\Delta t/T$  ratio (where  $T$  = period), it ensures strong dissipation in the higher modes.
- iv) For the dynamic effect,  $\alpha = -0.05$  was recommended.

Similar to the static analysis, the user has the options to proceed the time history analysis by using either direct step control or automatic step control. For direct step, solution convergence is determined by comparing the residual force and moment at  $t+\Delta t$  with PTOL and MTOL. On the other hand, for automatic stepping convergence is determined by checking the residual force at the half-step between  $t$  and  $t+\Delta t$ , or called half-step residual  $R_{1/2}$ . This quantity is calculated as follows.

The accelerations  $\ddot{u}$  are assumed to vary linearly over the time interval  $[t, t+\Delta t]$

$$\ddot{u}_\tau = (1 - \tau) \ddot{u}_t + \tau \ddot{u}_{t+\Delta t}, \quad 0 \leq \tau \leq 1 \quad (4-6)$$

Based on the above approximation, by direct integration one can find the expressions for  $u_\tau$ ,  $\dot{u}_\tau$  and  $\ddot{u}_\tau$  in terms of the corresponding quantities at  $t$  and  $t+\Delta t$ . Then from Eq. (4-2), the residual force vector at any  $\tau$  within the step is defined by

$$R(\tau) = M \ddot{u}(\tau) + I(\tau) - P(\tau) \quad (4-7)$$

For convergence check, a half-step residual  $R_{1/2}$  is chosen as a measure against an input tolerance called HAFTOL. The value  $R_{1/2}$  is the magnitude of



the largest entry (absolute value) in the vector  $R$  for  $\tau = 1/2$ . The basis for such a choice is purely empirical.

To specify an appropriate tolerance value for HAFTOL can be a challenging task to the user. According to the manual, the following values for HAFTOL are recommended: If  $P$  is a typical magnitude of real forces in a problem, then

- i) For high accuracy,  $\text{HAFTOL} \sim 10^{-2} P$
- ii) For moderate accuracy,  $\text{HAFTOL} \sim 10^{-1} P$
- iii) For coarse increment size,  $\text{HAFTOL} \sim P$

As will be seen in Section 6, for a given problem the magnitude of  $R_{1/2}$  is rather sensitive to the  $\alpha$ -value. If  $\alpha = 0$ , very large half-step residual was obtained from the analysis and consequently, this results in severe cut-back of increment size in the automatic time stepping. Therefore, when the automatic step control is optioned,  $\alpha = 0$  should not be used for the most cases. Even with  $\alpha = -0.05$  or other nonzero value, some significant oscillations of  $R_{1/2}$  were observed at the initial stage of the dynamic response. In summary, the following commentary can be made:

- i) Automatic time stepping is an extremely useful feature for nonlinear dynamic analysis, particularly for start-up of an analysis. However, the automatic stepping should not be used exclusively for the entire history of a problem, since it usually leads to more CPU time. Some degree of user's intervention or judgment is probably necessary if one is to keep the analysis time within a reasonable limit.
- ii) The magnitude of half-step residual  $R_{1/2}$  is quite sensitive to the  $\alpha$ -value. One should avoid the usage of  $\alpha = 0$  if automatic time step is exercised. As recommended in ABAQUS user manual,  $\alpha = -0.05$  is probably the best damping ratio for practical purposes.

#### 4.1.3 Heat Transfer Analysis

The third general procedure in Version 3 of ABAQUS is the heat transfer analysis. It is primarily for solid body heat conduction with temperature dependent conductivity, internal energy (including latent heat effects), and convection and radiation boundary conditions. Thermo-mechanical coupling was ignored. The heat transfer process can be either steady state or transient.

For time integration of transient heat transfer analysis, a modified Crank-Nicholsen operator (backward difference algorithm) was adopted in conjunction with Newton's method of iterations.

In terms of coding organization, the heat transfer part is an independent module, parallel to the stress analysis module. This module has its own element library and material library. The output of heat transfer analysis are the nodal temperatures, which can be directly used for thermal stress analysis.

#### 4.2 Element Library

In ABAQUS, there are two major categories of elements: Elements for stress analysis and elements for heat transfer analysis.

##### Stress Analysis:

- Truss elements
- 2/3 Solid elements
- 3/D Solid elements
- Beams
- Shell elements
- Elbows

### Heat Transfer Analysis:

- Link elements
- Plane and axisymmetric solids
- 3/D Solid elements

A brief summary of the above elements is given in Table 4.1. Each of the element types is outlined as below.

#### 4.2.1 Truss Elements

These are one-dimensional bar elements which can have axial deformation only. Two different truss elements are available: 2-node truss with linear displacement and 3-node truss with quadratic displacement. In 3/D space, each node has three translational degrees of freedom,  $u_x$ ,  $u_y$ ,  $u_z$ .

#### 4.2.2 2/D Solid Elements

These are first order (4-node quadrilateral) and second order (8-node quadrilateral) isoparametric elements. Moreover, the elements are divided into three sub-classes in accordance with the state of deformations: a) plane stress, b) plane strain, and c) axisymmetric deformation. For each element, the orders of numerical integration for evaluating element stiffness, stress/strain output, consistent mass matrix, etc., are fixed in the program. Reduced integration scheme is available for 8-node elements which are useful for such cases where near incompressible materials or significant plastic deformations are encountered.

#### 4.2.3 3/D Solid Elements

These are equivalent to 2/D solid elements except that they are defined in three-dimensional space. The elements include 8-node brick with linear displacement, 20-node brick with quadratic displacement, and 20-node brick with quadratic displacement and reduced integration.

Table 4.1 Element Library Summary

<u>Element Type</u>	<u>No. of Nodes per Element</u>	<u>DOF per node</u>	<u>No. of Integration Points</u>	
			<u>Stiffness and Stress/Strain</u>	<u>Mass and Forces *</u>
<u>Truss:</u>				
Linear Displacement	2	3	1	2
Quadratic Displace.	3	3	2	3
<u>2/D Solid:</u>				
(Plane stress, plane strain, axisymmetric)				
Bilinear Displacement	4	2	2x2	2x2
Biquadratic Displace.	8	2	3x3	3x3
Biquadratic with Reduced Integration	8	2	2x2	3x3
<u>3/D Solid:</u>				
Linear Displacement	8	3	2 x 2 x 2	2 x 2 x 3
Quadratic Displace.	20	3	3 x 3 x 3	3 x 3 x 3
Quadratic with Reduced Integration	20	3	2 x 2 x 2	3 x 3 x 3
<u>Beam:</u>				
Planar Beam				
Straight Linear	2	3	1 <sup>+</sup>	2
Curved Quadratic	3	3	2	3
Curved Cubic	2	3	3	3
<u>Space Beam:</u>				
Straight Linear	2	6	1 <sup>+</sup>	2
Quadratic Linear	3	6	2	3
Cubic-Curved	2	6	3	3
Cubic-Straight	2	6	3	3
<u>Shell Elementst:</u>				
Linear Displacement	4	6	1	2 x 2
Quadratic Displace.	8	6	2 x 2	3 x 3

Table 4.1 Element Library Summary (continued)

<u>Element Type</u>	<u>No. of Nodes per Element</u>	<u>DOF per node</u>	<u>No. of Integration Points</u> <u>Stiffness and</u> <u>Stress/Strain</u>	<u>Mass and</u> <u>Forces *</u>
<u>Elbow:</u>				
Linear Displacement	2	6	1 <sup>†</sup>	2
Linear with Ovalization	2	6	1	2
Quadratic Displace.	3	6	2	3
Quadratic with Ovalization	3	6	2	3
<u>Heat Transfer Elements</u>			<u>Conductivity</u>	<u>Specific Heat and Flux</u>
<u>Link Elements:</u>				
2-Node Link	2	1	2	2
3-Node Link	3	1	3	3
<u>Plane and Axisymmetric</u>				
4-Node Element	4	1	2 x 2	2 x 2
8-Node Element	8	1	3 x 3	3 x 3
<u>3/D Elements</u>				
8-Node Element	8	1	2 x 2 x 2	2 x 2 x 2
20-Node Element	20	1	3 x 3 x 3	3 x 3 x 3

Notes:

- \* Integrations including consistent mass matrix, body forces, specific heat and flux, surface pressure or flux, etc.
- + For planar beam, space beam and elbow elements, the indicated integration points are along the axis of the element. Integration scheme over the cross section of the beam or elbow is specified separately in the user manual.
- † For shell elements, reduced integration scheme is mandatorily enforced in the program.

#### 4.2.4 Beams

Several beam elements with a wide variety of cross-sectional shapes are available in ABAQUS. Cross sections include

- General section - User defines section properties
- Pipe section
- Box section
- Circular solid section
- I - section
- Rectangular solid section
- Hexagonal box section

The beam elements are further divided into two different types according to their spacial configurations.

##### A. Planar Beams

- 2 node straight beam - linear interpolation function and elastic transverse shear deformation
- 3 node curved beam - quadratic interpolation function and elastic transverse shear deformation
- 2 node curved beam - cubic interpolation function and elementary beam theory

##### B. Space Beams

In addition to those equivalent to the planar beams, the fourth entry is

- 2 node straight beam - cubic interpolation function and elementary beam theory

Numerical integration for evaluating element properties is performed somewhat differently from other element types: Along the beam axis, Gauss integration scheme is used. Over the cross section, however, default integration is the Newton-Cotes method whereas Gauss integration is optional for some of the cross sections. The Newton-Cotes method is preferred for maximum (or minimum) bending stresses occurred near the outer fibers of the beam.

#### 4.2.5 Shell Elements

ABAQUS has fairly sophisticated shell elements for conducting three-dimensional thin shell analysis. Two different elements of the same type are available for use: 4-node and 8-node elements; each node has 6 - degrees of freedom, i.e. 3 - translations and 3 - rotations referring to a global Cartesian coordinates. The shell equations were derived from a two-dimensional classical shell theory [15], differing from the so-called degenerated 3/D continuum theory [16].

The shell is defined by its middle surface which, in turn, is approximated by the nodal coordinates and isoparametric functions. All displacement components and rotations, and the geometry of the middle surface are interpolated by the same 'serendipity' functions. The direct strain in the thickness direction of the shell is assumed to be zero. Since the element is specifically intended for thin shell analysis, Kirchhoff assumption with no transverse shear deformation was imposed; i.e. normal vectors to the middle surface of the shell always remain normal during deformation. This assumption is enforced by using a penalty function at a set of (uniformly) reduced integration points.

Based on its formulations and sample problems tested, it appears that the shell elements in ABAQUS have the following characteristics:

- i) The elements are very reliable for solving a wide range of thin shell structures.
- ii) It gave better numerical behavior for shells of small thickness, as compared to the serendipity element with reduced integration.
- iii) The shell must have uniform thickness within the element.

#### 4.2.6 Elbow Elements

Elbows are often used in the design of piping systems for nuclear power plants, petro-chemical facilities, etc. It is known that elbows achieve their flexibility through a shell-like behavior, resisting bending actions with significant cross-sectional ovalizations. For elastic elbows, stiffness matrix based on the 3/D straight beam theory is used in conjunction with flexibility factors and the stresses are corrected by using appropriate intensity factors [17]. However, for inelastic elbows no such simple approach is available and one has to resort to other numerical means. In this connection, a number of elbow elements have been proposed [18-21] and they generally suffer two drawbacks:

- i) Element formulations were made on the over-simplified theory and consequently its applications become restrictive.
- ii) Computational cost is very high.

From its theoretical considerations, the elbow elements in ABAQUS probably represent one of the most attractive types for nonlinear (material) analysis. The element formulations were derived on the basis of the following assumptions:



- Only small deformations are considered.
- Ovalization of the pipe cross section is allowed and the effect of warping may also be included.
- The total deformation of the pipe section is considered to be the linear superposition of strains caused by beam actions and strains by ovalization and uniform radial expansion of the pipe section.
- Interpolation functions for beam deformation are similar to the elementary beam elements.
- Interpolation for cross-section deformation in the axial direction can be either linear or quadratic polynomial function. Up to six Fourier modes (sine and cosine functions) can be specified for deformation associated with ovalization of the pipe section.

#### 4.2.6 Heat Transfer Elements

As mentioned previously, only solid body is considered for heat transfer analysis in ABAQUS. This is sufficiently general for the geometric description of most application problems. Therefore, the elements include:

- 1/D link (bar) elements - 2 nodes or 3 nodes
- 2/D plane and axisymmetric elements - 4 nodes or 8 nodes
- 3/D solid elements - 8 nodes or 20 nodes

#### 4.3 Material Library

In the present version of ABAQUS, analysis is limited to large rotations but small strains for which case the second Piola-Kirchhoff stress and Green's strain are used for stress and strain measures, respectively. In this way, any rotational effects of constitutive properties due to the deformation of material coordinates are already accounted for.

Basically, there are four different types of material models for stress analysis in conjunction with heat transfer models:

### Stress Analysis

- a) Elastic models - Isotropic, orthotropic or fully anisotropic materials
- b) von Mises Plasticity - Isotropic or Hill's anisotropic materials with plastic incompressibility
  - Isotropic strain - hardening
  - Kinematic strain - hardening
- c) Creep models - Isotropic or Hill's anisotropic materials.

uniaxial creep equation :

$$\dot{\epsilon}^C = A \sigma^n t^m$$

where

$$\dot{\epsilon}^C = \text{creep strain rate}$$

$$\sigma = \text{equivalent stress}$$

$$t = \text{time}$$

and A, n, m are material constants which may be functions of temperature. Or, user may specify his own creep equation through user subroutine. Creep hardening options include

- Time hardening law
- Strain hardening law

#### d) Volumetric swelling

This model was prepared primarily for the stress analysis of fuel elements in reactor core where irradiation induced strain (swelling) occurs in flux fields. The rate of swelling is defined as a function of temperature and other field variables, such as time and/or radiation

flux. The user has the option to input the swelling data in tabular form or specify the swelling law by a user subroutine.

It is noted that all material constants involved in the above models can vary with temperature. Moreover, thermal stresses can be analyzed through the option 'EXPANSION'.

#### Heat Transfer Analysis

- a) Conductivity - Isotropic, orthotropic or fully anisotropic
- b) Specific heat - This option is needed for transient heat transfer analysis. Specific heat is defined as a function of temperature.

As it has been discussed before, each material model is uniformly available to all element types in ABAQUS.

#### 4.4 Mesh Generation

ABAQUS has a simple version mesh generation, i.e., generating a mesh of uniform grid. The mesh generation option is provided in nodal point data and element data input, led by two keyword cards:

- \* NGEN - Incremental node generation
- \* ELGEN - Incremental element generation

The program can generate all the intermediate nodes along a straight line or curved line (parabolic or circular) by specifying the nodal numbers and coordinates of two end nodes. If a parabola is chosen, the user must supply the coordinates of the mid-point on the curve between the two end points. On the other hand, if a circular arc is used, the user must define the coordinates of the center of the circle or the number of center as one node. In addition, the option ELGEN is used to generate a series of elements with uniform element and nodal number increments. For this purpose, first the user has to specify a master element and associated nodal numbers.

Then the program will use the master element to generate successive elements of the same type with constant element and nodal increments.

Therefore, it is clear that the version 3-ABAQUS does not yet have any sophisticated mesh generation features beyond the uniform grid.

#### 4.5 Kinematic Conditions

In addition to the fixed or prescribed displacement boundary conditions, four kinematic constraining features are available in ABAQUS:

- EQUATION - User defined multi-point constraint by a linear equation.
- FRICTION - Friction between node pairs.
- GAP - Possible contact and gap conditions between node pairs.
- MPC - General multi-point constraints.

Each option is defined by a leading keyword card with additional input data. These features are briefly discussed as follows.

##### 4.5.1 EQUATION

This feature provides an option to specify multi-point constraints in a linear equation form

$$A_1 u_1 + A_2 u_2 + \dots + A_n u_n = 0 \quad (4-8)$$

where  $A_1, A_2, \dots, A_n$  are user defined values;  $u_1, u_2, \dots, u_n$  are nodal degrees of freedom, which are specified by node numbers and their degrees of freedom. This option is an alternative to the MPC option with more flexibility in the manner of constraining the nodal degrees of freedom.

##### 4.5.2 FRICTION

This is an option to define the interaction effect, namely friction, between the contacting surfaces of two bodies and it is usually used in

conjunction with GAP option. The friction action is represented by the Coulomb model for which the friction property is a function of the normal force acting at the interface of contact. For this option, the user must supply the following data

- The pair of node number in contact
- Coefficient of friction
- Stiffness in Stick Condition
- Closure distance (if there is a gap)
- Normal force (if gap is always closed).
- Direction cosines of closure distance
- Direction cosines of first friction direction.

Although the program considers the friction effect, it does not print out slip deformation between two nodes. Moreover, the friction relationship is limited to small deformation.

#### 4.5.3 GAP

This condition allows pairs of nodes to be in contact or separated; it is equivalent to a bar - contact - element. The user specifies the direction and closure  $d$  of two nodes, which represents the initial gap between two bodies. Then the program monitors the relative displacement of the two gap nodes. When the relative displacement reaches the value  $d$ , the gap is closed and subsequently a constraint is imposed.

The program handles both static and dynamic contact problems. For dynamic contact, a set of impact equations are solved to obtain the velocity and acceleration jumps of those nodes in contact during the instant before and after the contact has occurred. Then, the initial velocities and acceleration of the contacting nodes can be calculated and the usual time stepping integration proceeds.

#### 4.5.4 MPC - Multi Point Constraints

This option is useful for the transition region between a fine mesh and coarse mesh of a finite element model layout. As seen in Fig. 4.1, the mesh is refined from coarse to fine with two different cases: i) linear displacement elements ii) quadratic displacement elements. In either case, the node P on ab line or nodes  $P_1$  and  $P_2$  on abc lines must be constrained to have compatible displacement field for the elements on both side of the node. If these nodes are not constrained, significant solution errors could occur, especially when plasticity is spread in the transition zone [22]. In ABAQUS, the MPC option is available for both 2/D and 3/D solid elements

#### 4.6 User Subroutines

In addition to the standard data input, certain data can be specified through user subroutines. This option provides added flexibility and convenience for the program to generate data which follow specialized equation or patterns. The user subroutines available are:

- CREEP - To calculate creep rate from a specific creep law.
- DFLUX - To define a non-uniform distributed flux in heat transfer analysis.
- DISP - To specify the magnitude of displacement for all degrees of freedom of the nodes where the boundary conditions are defined.
- DLOAD - To define non-uniform distributed loads in an element.
- FILM - To define non-uniform film coefficient and associated sink temperatures for heat transfer analysis.
- MPC - To define a multi-point constraint similar to but more general than the option in Section 4.5.4.

SWELL - To define a time dependent volumetric swelling law.

Although the usage of some of the subroutines is fairly obvious, specific examples for each option should be given in the manual to provide better clarity on the parameters involved in the subroutines.

#### 4.7 Input and Output

Data input in ABAQUS is organized in two major sections:

Model input - specifying geometric definitions of finite element model such as: nodal number, coordinates of nodes, element-node connectivity, constraint conditions, etc.; material model information; and plotting of undeformed geometry.

History Input-These include data related to analysis procedure, loading history, output control and solution control (e.g. direct or automatic stepping method), etc.

Input data are divided into distinct sections and each section has a leading keyword card. A keyword card begins with a '\*' notation (e.g. \* ELEMENT), also contains optional parameters. Following the keyword card are the data cards. On any data card, free or fixed format may be used. It is the reviewer's opinion that ABAQUS input has the following merits:

- i) Input sequence was logically laid out and therefore it is easy for the user to follow the input manual.
- ii) Separation of data sections by keyword cards enhances the user's ability to scan input data quickly and spot possible errors.
- iii) Free format input is most convenient to use.

With respect to the output of ABAQUS, four types of output are available:

- Printed output
- Plotting
- File output for post-processing analysis
- Restart file output

Our discussion is focused on the printed output.

In ABAQUS, the printed output is divided into two sections; namely, in the PRE and the MAIN.

In PRE:

- Input echo (or input card image)
- A summary of various options processed by the program
- Processed input data - element definitions, material description, node definitions, analysis step information, loads, mesh plotting, etc.
- Work space allocation

In MAIN:

- Element stresses and strains
- Total nodal displacements, velocities and accelerations (for the case of dynamic analysis).
- Nodal residual or reaction forces
- Information about iteration and solution convergence

The user has the option to suppress some of the printout through the input section '\*PRINT'. Among various options, for example, the user may choose:

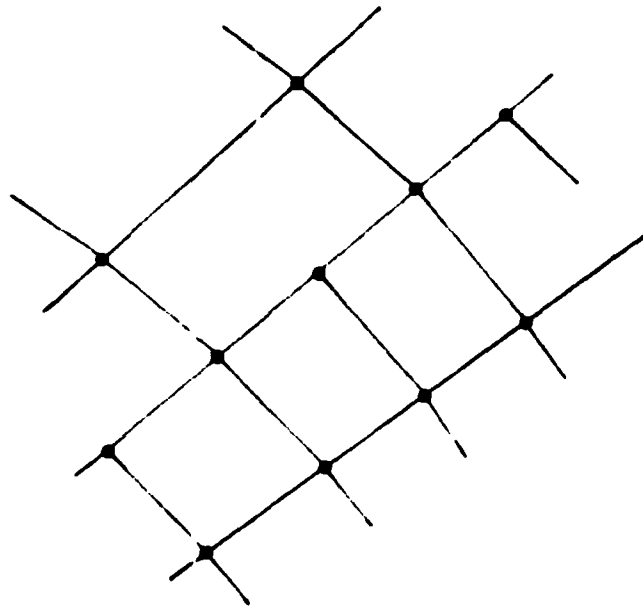
- i) Printout can be requested at every k-th interval.



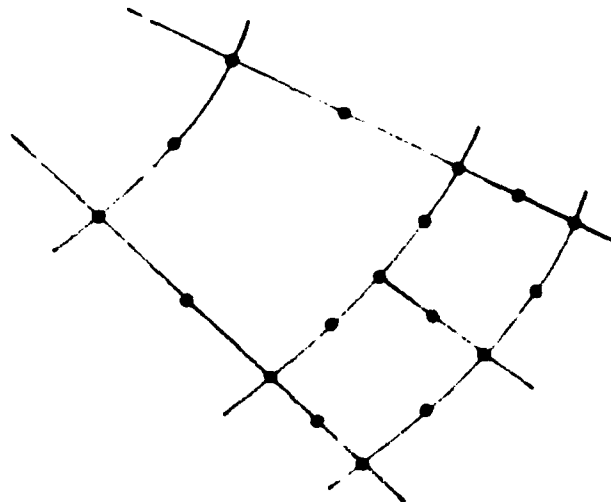
- ii) The user has the option to print out the element data for a specific number of elements which are designated in one ELSET.
- iii) The printout of element variables, such as stress components, stress variants, total strain components, creep strains, etc, can be specified.
- iv) Printout of node set, total displacements, velocities, accelerations, etc. may also be optioned.

It is apparent that ABAQUS provides a very flexible printout option to the user, which represents one of the friendly features of the code. Nevertheless, two negative points about its printed output are mentioned for consideration of future improvement:

- i) Printout of real numbers are in P-format which is the mixture of F- and E- format. Although the use of such format is well intentioned, it does not have a good appearance for report purpose. The reviewer still prefers the use of E- format for printing real numbers.
- ii) Stress and strain components are not defined in the printout. Consequently, it is not convenient for the user to identify their meanings unless the input manual is referenced.



(a) Linear Displacement Elements



(b) Quadratic Displacements

Fig. 4.1. Use of MPC for Transition Region

## 5. Verification Problems

Eleven verification problems were run to check the execution status of ABAQUS. The purpose of such verification exercises is purely to ensure the program, which was developed on a CDC Cybernet System, is functioning properly on the IBM 370-158 computer with double precision arithmetic on floating point numbers. The verification problems represent different types of nonlinearities, but are of routine nature in that they do not present any numerical difficulty in obtaining convergent solutions. Each problem is presented in a standardized format including:

- i) Problem statement
- ii) Geometry
- iii) Nonlinearity
- iv) Material properties
- v) Loading
- vi) Finite element model
- vii) Analysis procedure
- viii) Results

For later discussion, several parameters being used in ABAQUS are defined as the following:

- R = Maximum reaction force
- E = Young's modulus
- $\nu$  = Poisson's ratio
- $\sigma_0$  = Initial yield stress
- $E_p$  = Plastic modulus
- $\rho$  = Density

### 5.1 Elastic-plastic Deformation of a Cantilever Beam

Geometry: A short cantilever beam with a rectangular cross section.

Length = 91.4 cm. Height = 30.5 cm, Width = 2.54 cm.

Nonlinearity: Material nonlinearity with small deformation

Material properties: Elastic-perfectly plastic material

$E = 68.95 \text{ mpa}, \quad \nu = 0$

$\sigma_0 = 0.69 \text{ mpa}$

Loading: A concentrated transverse load  $P$  applied at the free end.

Model: Two different models were used.

A. 10-beam (B22) elements

B. 20-eight node plane stress (CPS8) elements.

Procedure: Automatic load incrementing

Results: The load deflection response at the free end is plotted in Fig.

5.1 for both models A and B in conjunction with an independent solution by Felippa [23]. It is seen that the elastic responses of model A and model B agree with that of Felippa. However, the results obtained from beam elements show some discrepancy near the transition zone between elastic and plastic deformations. This is probably due to insufficient integration order being used in the code for this problem. Nevertheless, the limit loads from models A and B, and reference [23] are about the same.

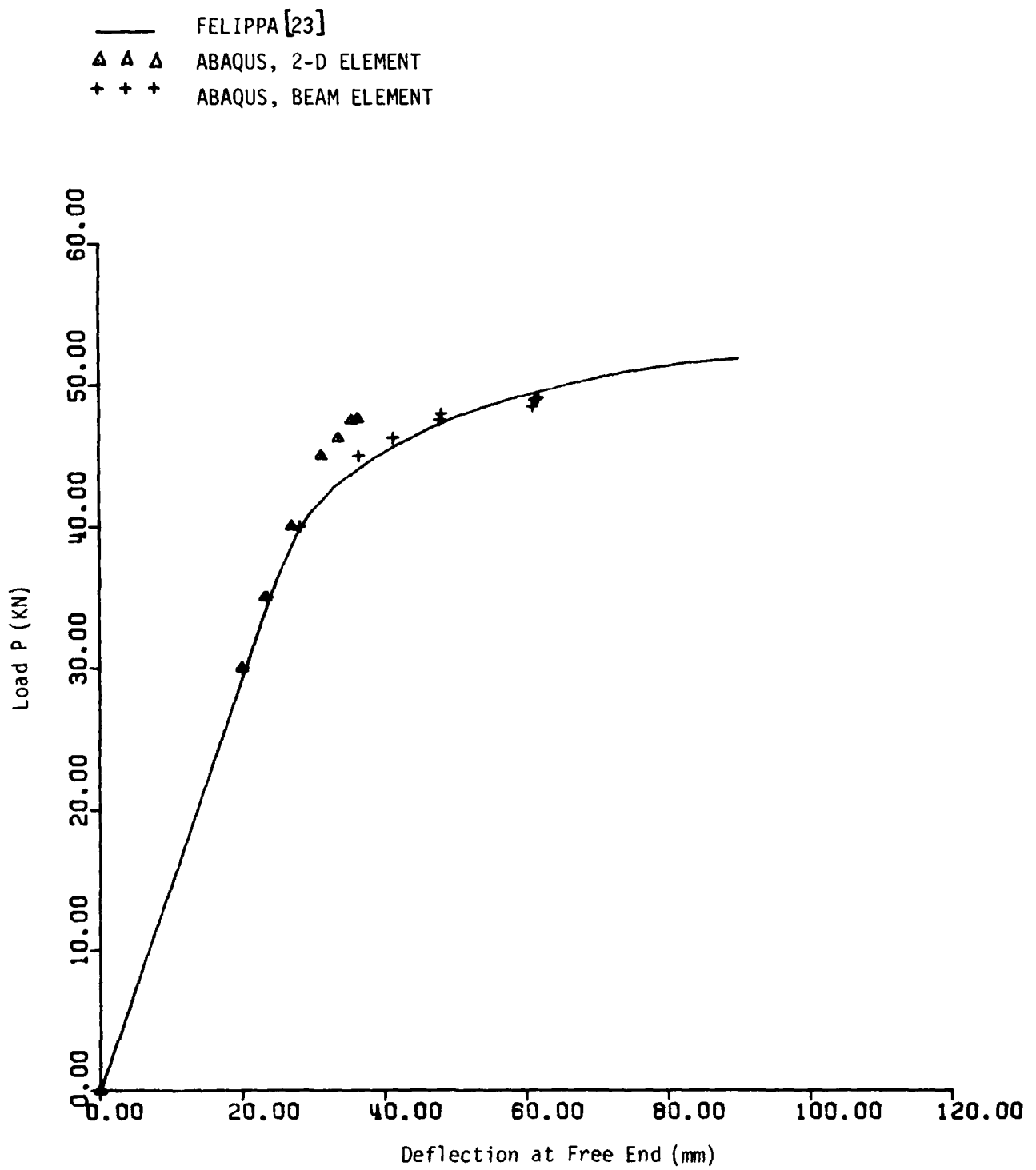


Fig. 5.1. Load-Deflection Response of a Cantilever Beam with Plastic Deformation

## 5.2 A Cantilever Beam Subjected to An End Moment.

Geometry: A slender cantilever beam with a rectangular cross section

(Fig. 5.2)

Length = 10m, Height = 0.1m, Width = 1 m.

Nonlinearity: Large rotation and linear material

Material Properties: Linearly elastic material,  $E = 1.2 \times 10^5 \text{ KN/m}^2$

Loading: A moment applied at the free end

Model: 8-beam (B21) elements

Procedure: Automatic load incrementing

Results:

After a few trial runs, it was found that a model consisting of 8 beam elements is sufficient to represent the bending action of the beam, including large deformation response. The moment was applied in such a manner that the beam was deformed from its straight shape to a complete circle. Three different sets of solution parameters were specified to determine the solution sensitivity:

<u>Case</u>	<u>PTOL</u>	<u>MTOL</u>	<u>NUM</u>
1	0.3 lb	0.3(in-lb)	10
2	0.3	0.3	30
3	0.03	0.3	10
4	0.1	0.1	10

The moment vs. vertical and horizontal deflections are shown in Figs. 5.2 and 5.3, respectively. All results correlate with those obtained by Horrigmoe [24] quite well except the Case 1 in which some localized numerical instability was indicated for the horizontal deflection (see dotted line in Fig. 5.3).

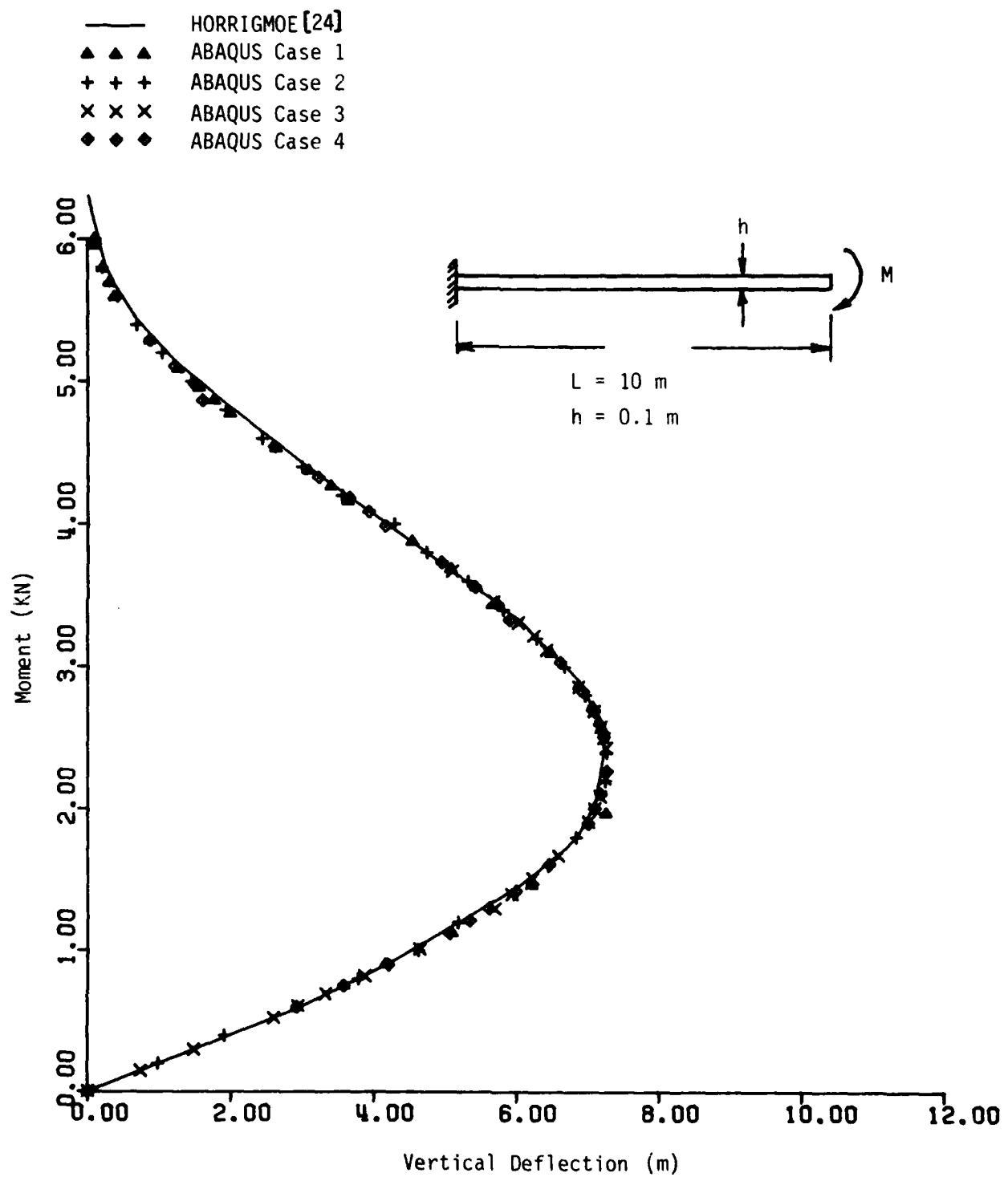


Fig. 5.2. Moment vs. Vertical Deflection of a Cantilever Beam

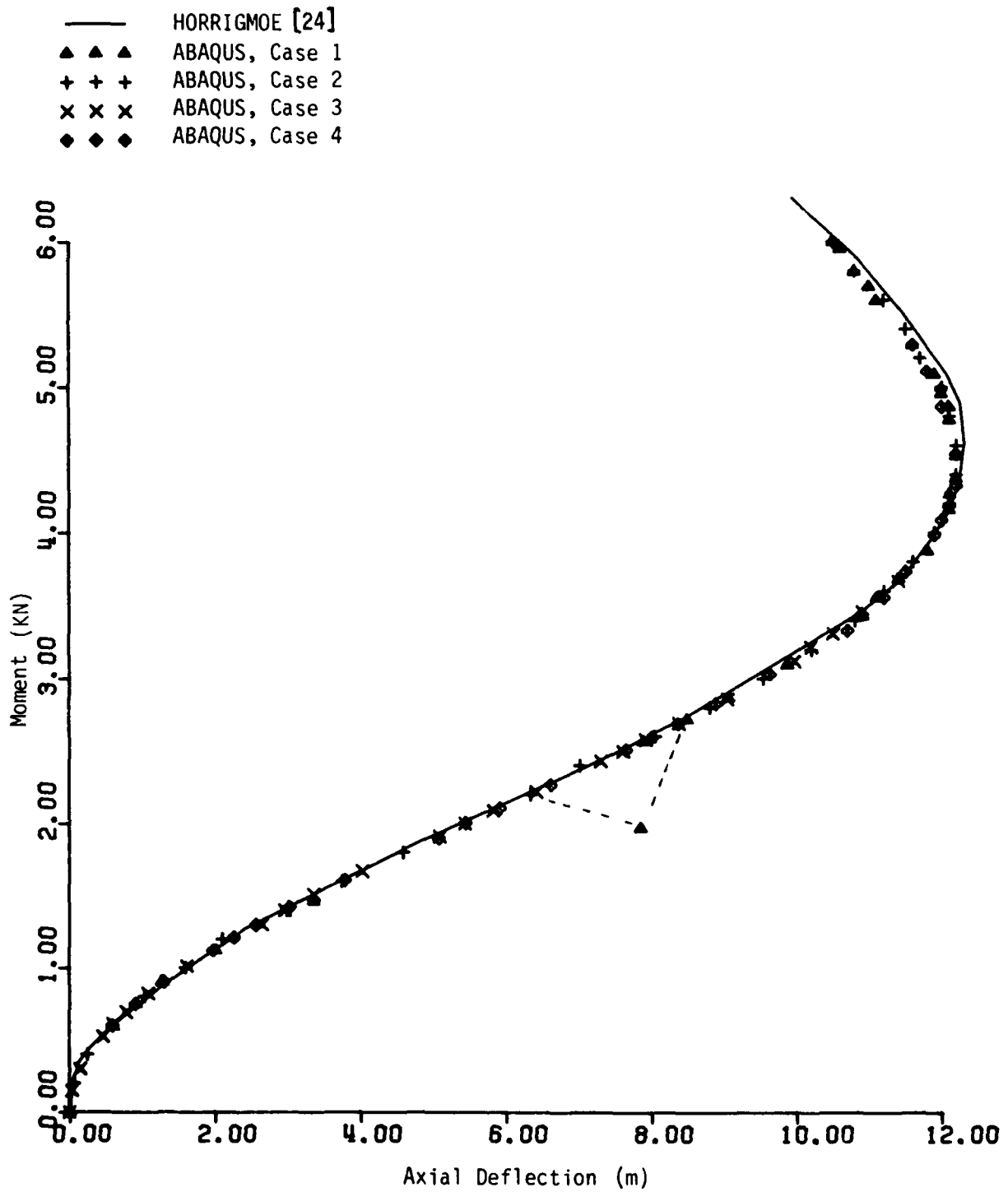


Fig. 5.3. Moment vs. Horizontal Deflection of a Cantilever Beam



Fig. 5.3). This instability was removed by either reducing the force tolerance or increasing the maximum number of iterations. Fig. 5.4 shows the deflection curves of the beam corresponding to different values of applied moment.

### 5.3 Static Analysis of A Pipe Contact Problem

Geometry: (see Fig. 5.5)

Pipe:	$L_1 = 300 \text{ in.}$	$L_2 = 100 \text{ in.}$	
	$L_3 = 50 \text{ in.}$	$L_4 = 120 \text{ in.}$	
	$R = 45 \text{ in.}$	$r = 15 \text{ in.}$	$t = 1 \frac{1}{8} \text{ in.}$

Restraint  $L_5 = 27 \text{ in}$       Area =  $26 \text{ in}^2$  .

Gap  $h = 3 \text{ in.}$

Nonlinearity: Nonlinear boundary condition (gap and contact) and elastic-plastic material

Material Properties:

Pipe -  $E = 27 \times 10^3 \text{ ksi}$        $\sigma_0 = 28 \text{ ksi}$

Restraints -  $E = 30 \times 10^3 \text{ ksi}$        $\sigma_0 = 38 \text{ ksi}$

Loading: A vertical concentrated force  $P = -50\text{K}$  was applied at the free end.

Model: The model consists of (see Fig. 5.6)

Pipe - 7 straight beam (B21) elements

1 curved beam (B22) element

All elements have pipe cross sections.

Restraints - 2 truss (C102) elements.

Procedure: Automatic load incrementing.

This problem was selected from the ABAQUS example problem manual [10] to test the analysis capability of gap elements. Three different cases of solution parameters were specified:

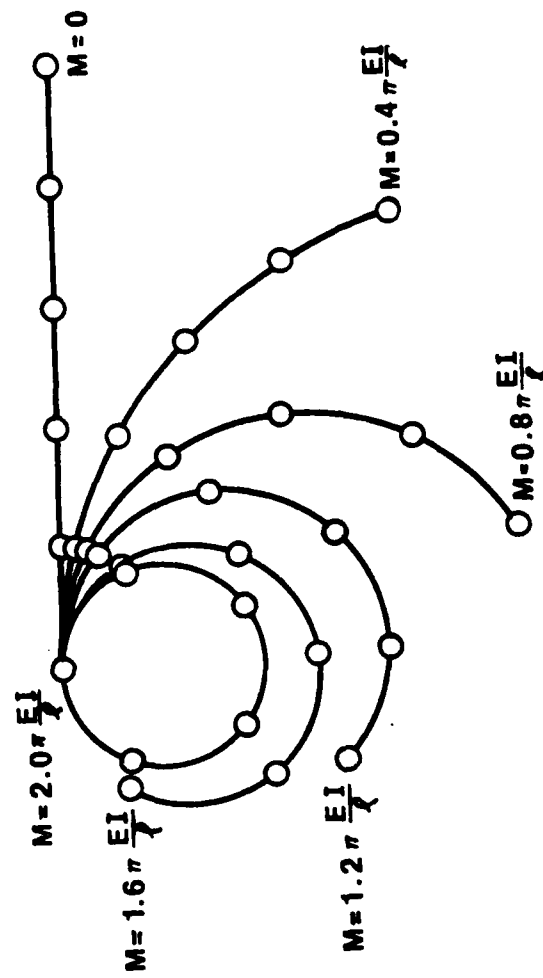


Fig. 5.4 Deflected Shapes of a Cantilever.

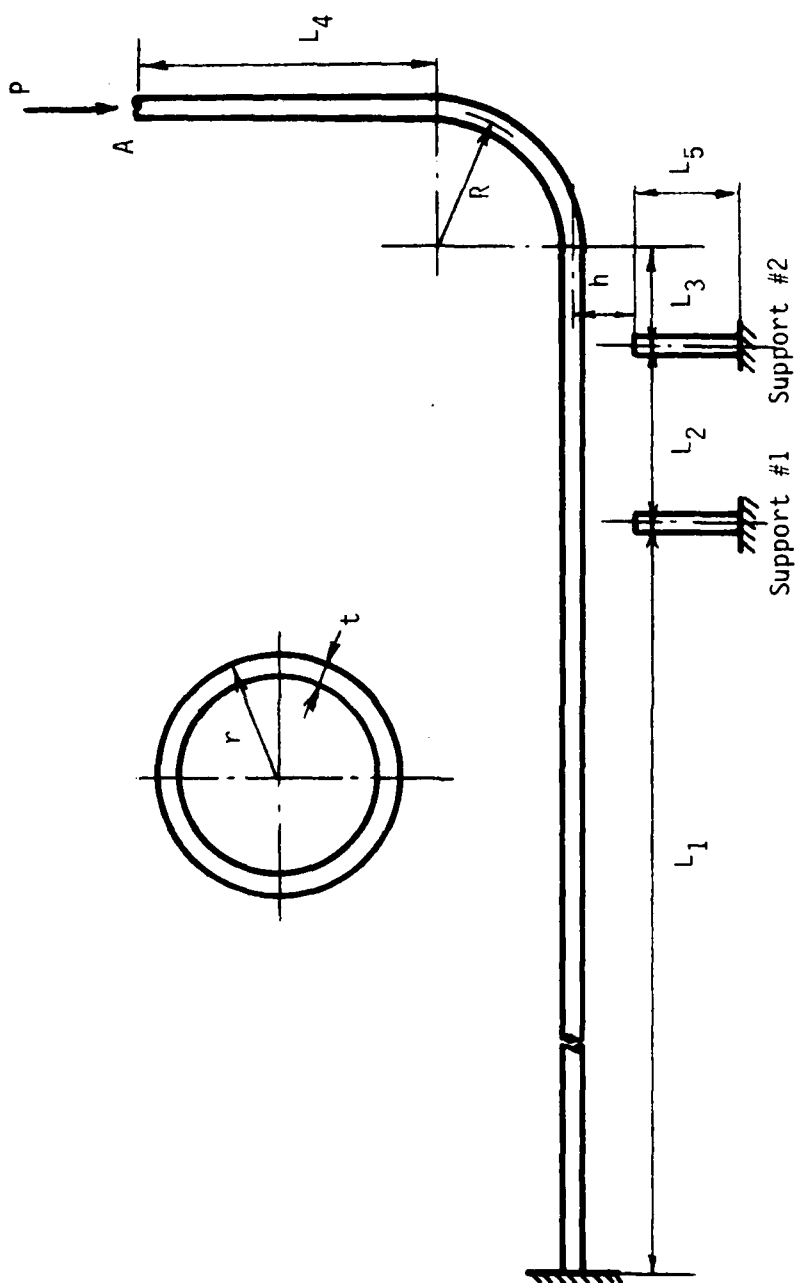


Fig. 5.5. A Pipe Contact Problem

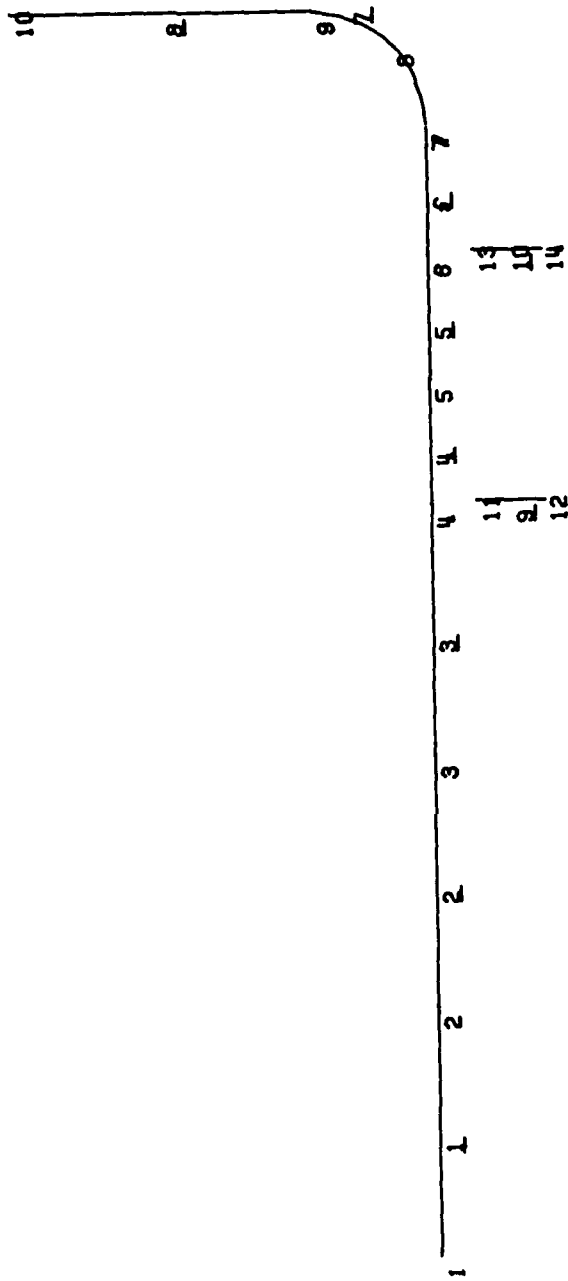


Fig. 5.6. Finite Element Model for the Pipe Contact Problem

<u>Case</u>	<u>PTOL</u>	<u>NUM</u>
1	0.1K (.2%)*	20
2	0.1K (.2%)	2
3	50K (100%)	5

---

\* Percentage of the total applied load or maximum reaction force.

The change of gap size and the development of contact force in the supports were plotted against the applied load shown in Figs. 5.7 and 5.8, respectively. It is seen that the results for all cases are almost identical. The only difference was the CPU time, i.e. Case 1 = 2 min.-32 sec. Cases 2 & 3 = 10 sec. For this problem, the source of nonlinearity is primarily due to the contact action between the pipe and supports. Ideally, two load increments would be sufficient to complete the analysis; namely, load up to the point of initial contact and the remaining total load. In all cases, the residual force calculated for each loading increment was very small, well below the smallest tolerance specified.

#### 5.4 An Elastic-Plastic Spherical Cap

Geometry: A spherical shell with initial imperfection (axisymmetric) as shown in Fig. 5.9.

Two different cases of dimensions were considered.

Case A:	R = 0.8177 in.	R <sub>1</sub> = 1.1432 in.	$\phi$ = 30°
	h = 0.0104 in.	a = 0.297 in.	
Case B:	R = 0.825 in.	R <sub>1</sub> = 1.1511 in.	$\phi$ = 20°
	h = 0.025 in.	a = 0.267 in.	

The cap was fixed along its edge.

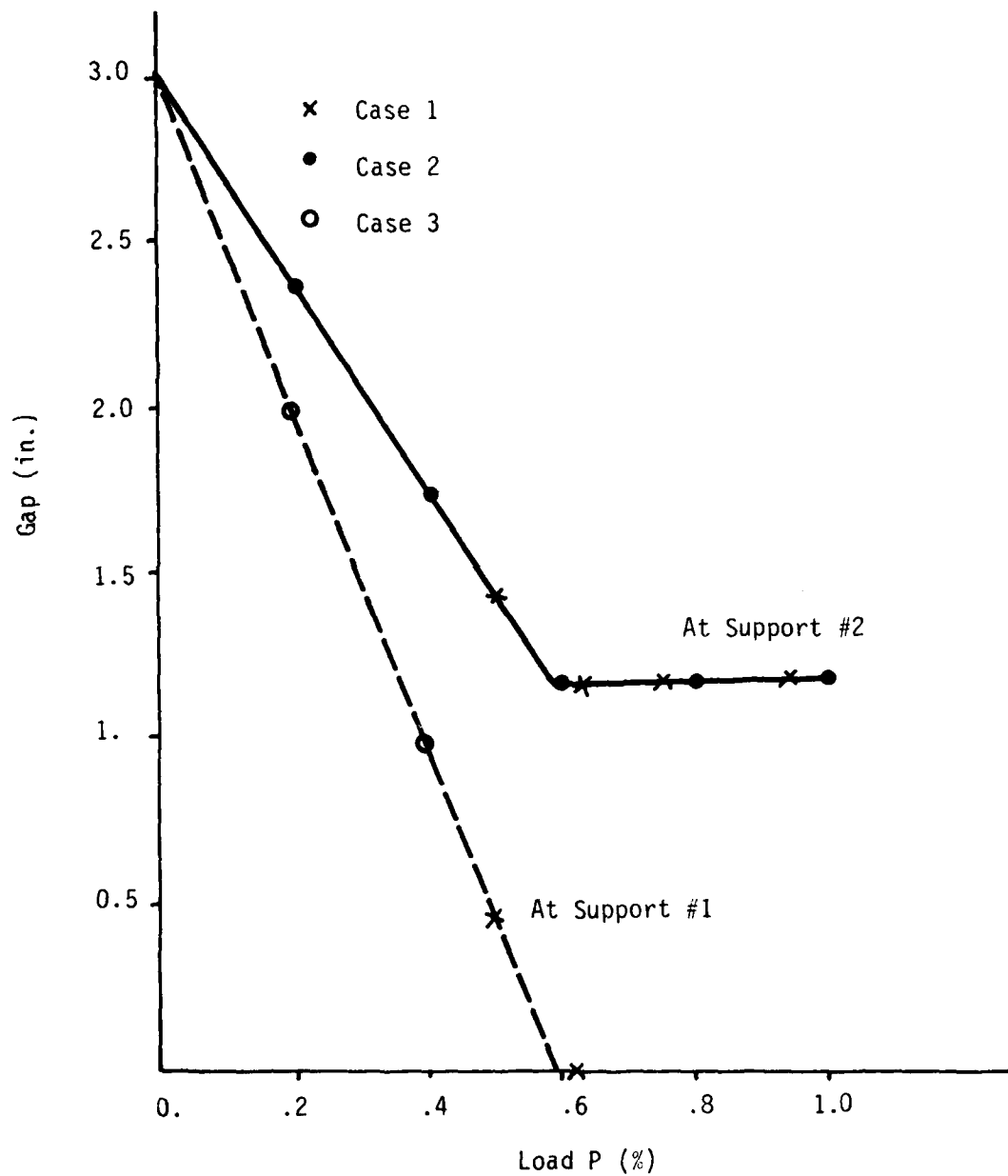


Fig. 5.7. Change of Gap Size vs. Applied Load

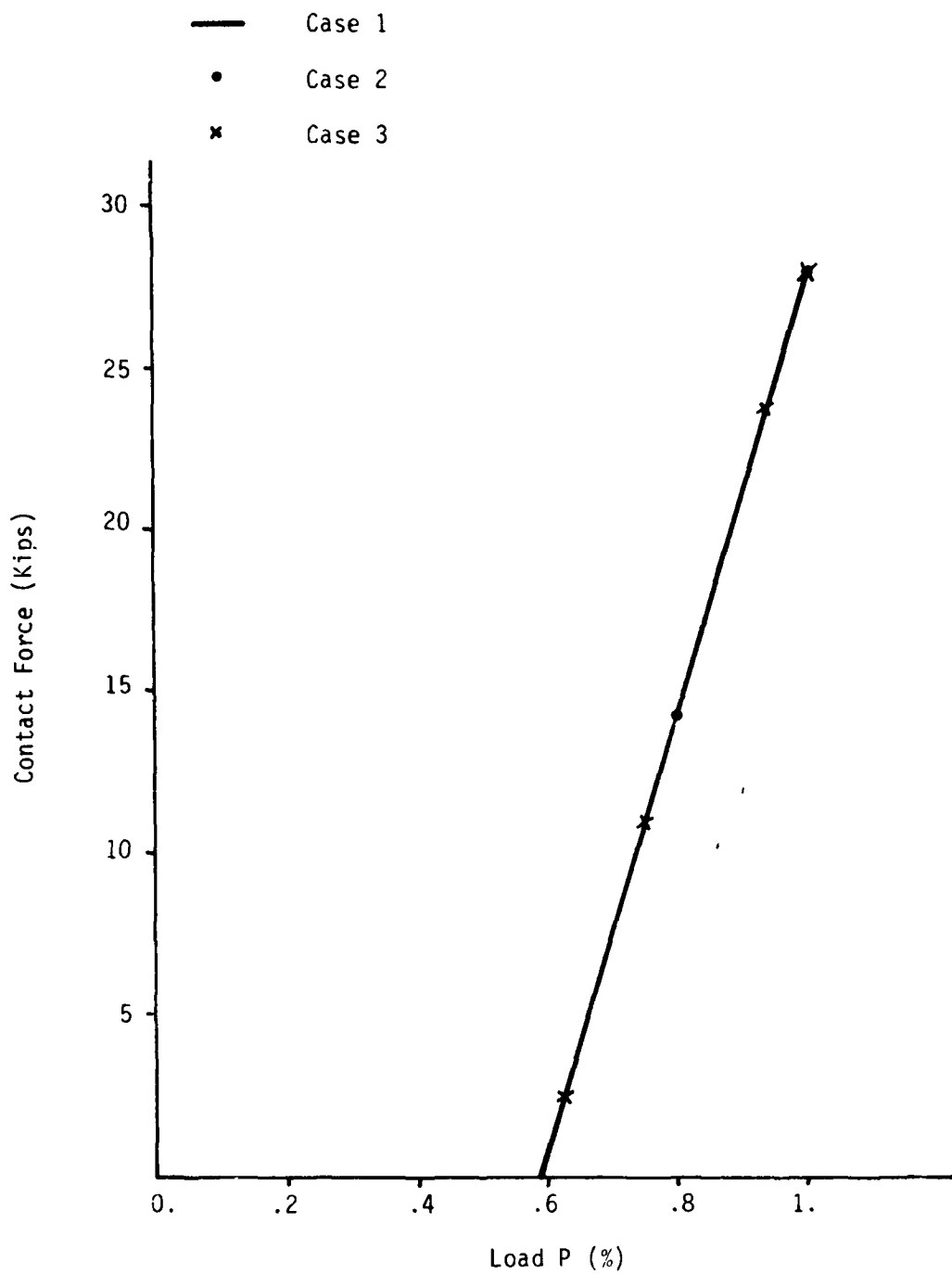


Fig. 5.8. Development of Contact Force at Support #1 vs. Applied Load

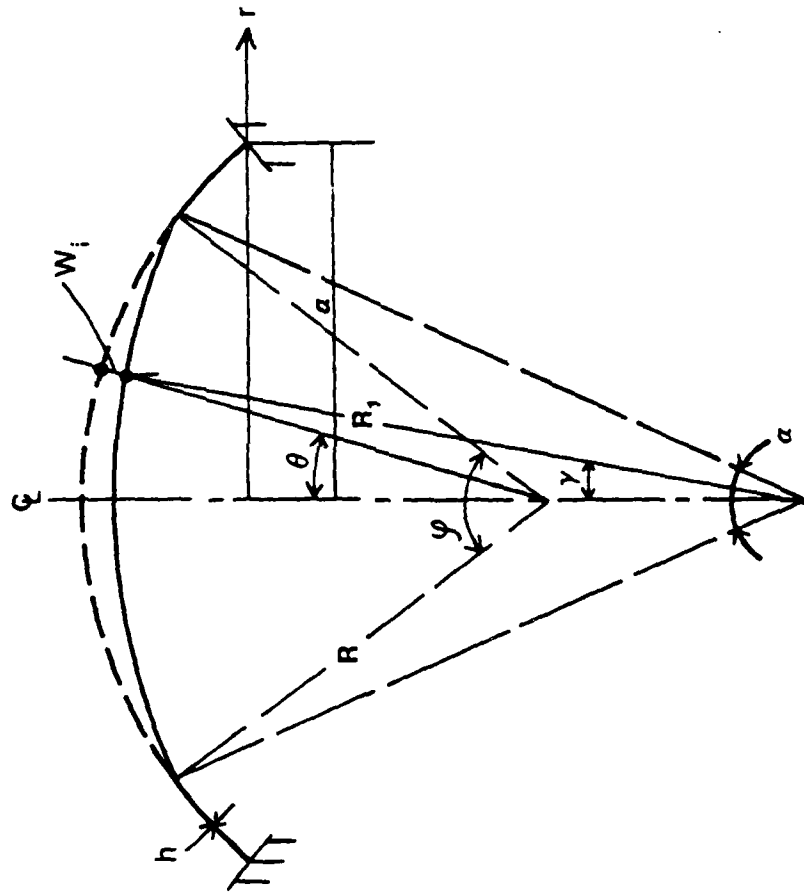


Fig. 5.9. A Spherical Cap with Initial Imperfection



Nonlinearity: Elastic-plastic material and small deformation.

Material properties: Bi-linear elastic-plastic material

$$E = 1.8 \times 10^3 \text{ ksi}$$

$$\nu = 0.3$$

$$\sigma_0 = 78 \text{ ksi}$$

$$E_p = 1.1 \times 10^3 \text{ ksi}$$

Loading: Uniform normal pressure P

Model: 10 - axisymmetric 2/D eight-node (CAX8R) elements with reduced integration.

Procedure: Automatic load incrementing

$$PTOL = 10 \text{ lb.}, \quad NUM = 5$$

Results:

This problem was previously analyzed by Kao [25] using the finite difference method for axisymmetric shells. The cap has an initial imperfection which is also axisymmetric. The load vs. deflections at the crown for Case A and Case B are shown in Figs. 5.10 and 5.11, respectively. In general, ABAQUS results agree with those in [25], except that a small discrepancy is seen for Case B.

### 5.5 Elastic-Plastic Deformation of A Plate

Geometry: A square plate with a span of 40 in and uniform thickness of 0.4 in.

Two different support conditions were considered:

A. Clamped along all edges

B. Simply supported

Nonlinearity: Elastic-plastic material and small deformation

Material properties: Perfectly elastic-plastic material

$$E = 30 \times 10^3 \text{ Ksi}$$

$$\nu = 0.3$$

$$\sigma_0 = 30 \text{ ksi}$$

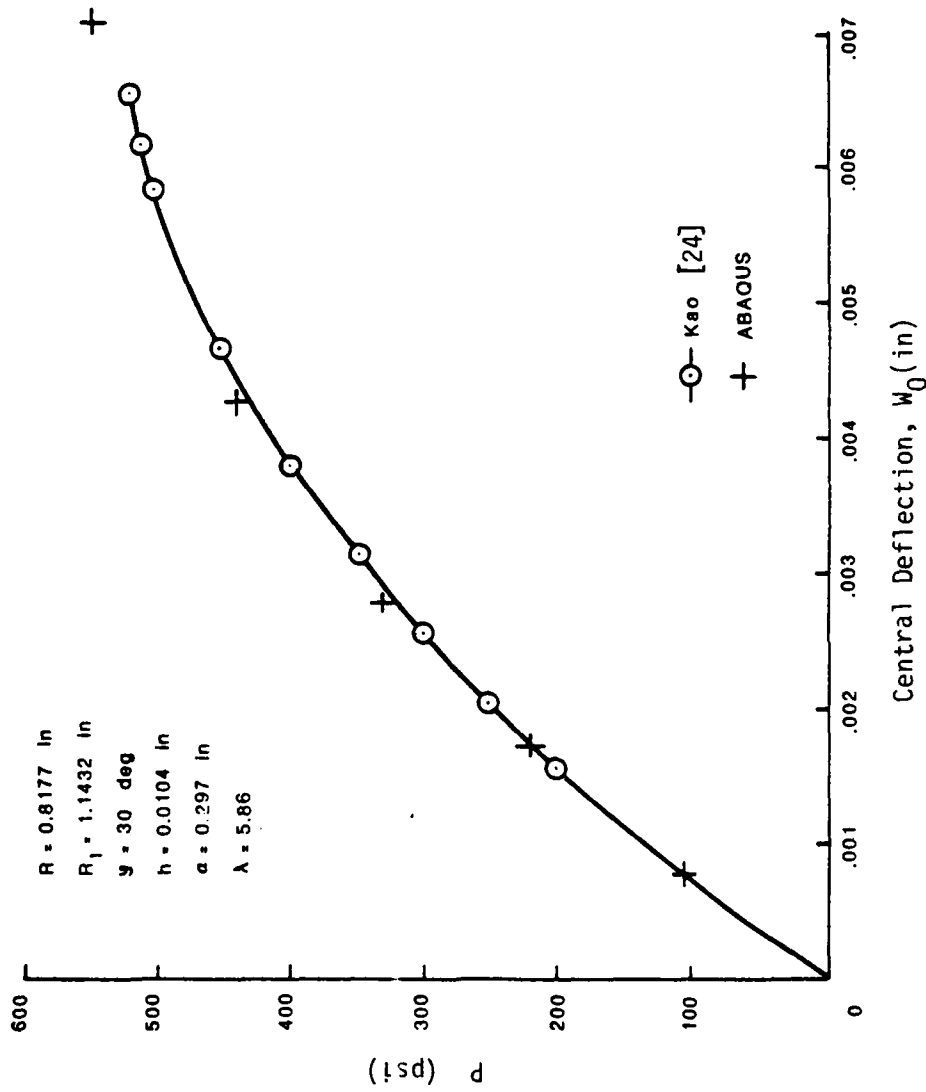


Fig. 5.10. Load-Deflection Response of Spherical Cap A

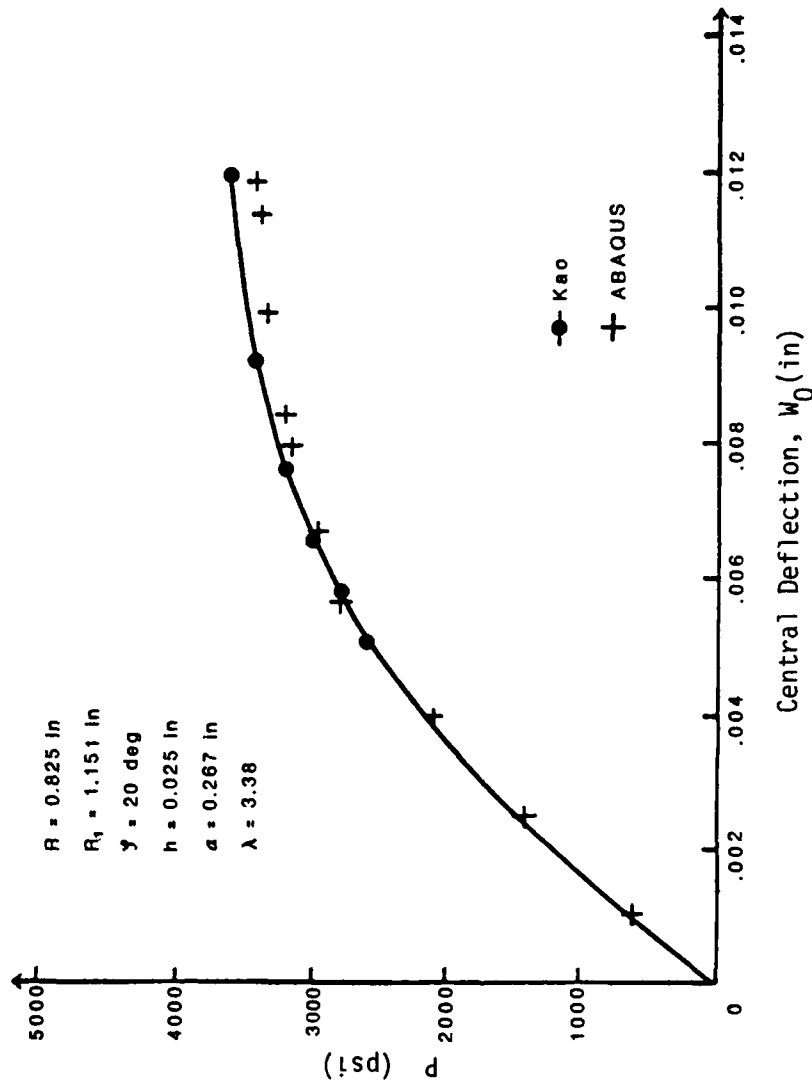


Fig. 5.11. Load-Deflection Response of Spherical Cap B.

Loading: Uniform pressure  $p$

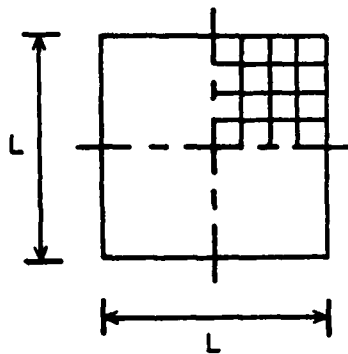
Model: A 4 x 4 mesh consisting of 16 shell (S8R) elements with reduced integration

Procedure: Both automatic and direct load incrementing procedures were used.

Results:

For the clamped boundary conditions, the non-dimensionalized load vs. maximum deflection of the plate obtained from ABAQUS was plotted in Fig. 4.12 as compared with existing solutions. ABAQUS result agrees closely with that of Horrigmoe and Eidsheim [26], and the ultimate load of the plate coincides with upper bound obtained by Hodge and Belytschko [27].

For the simply supported plate, ABAQUS solution correlates with that in [26] quite well until the load reaches the ultimate value. Some numerical disparity is clearly seen in Fig. 5.13. It is noted that the analysis was performed using automatic load incrementing with the solution parameters: PTOL = 25 lb, (2% of the maximum reaction force), NUM = 10. Initially, ABAQUS solution followed that of Horrigmoe and Eidsheim quite closely all the way near the ultimate load. Then, convergence became difficult and ABAQUS cut back the load increments in order to achieve solution convergence. As a result, gradual stiffening of the plate can be seen in Fig. 5.13 until the load approaches the upper bound solution, analysis was interrupted due to numerical instability of the plate (or reaching ultimate load). Similar stiffening behavior occurred even when PTOL was reduced with greater iteration allowance. It is believed that the stiffening effect was caused by some unknown numerical difficulty in ABAQUS.



$L = 40$  in

$t =$  thickness 0.4 in

$W_c =$  central deflection

$p =$  uniform load

$M_p = \sigma_y t^2 / 4$

$D = Et^3 / 12(1-\nu^2)$

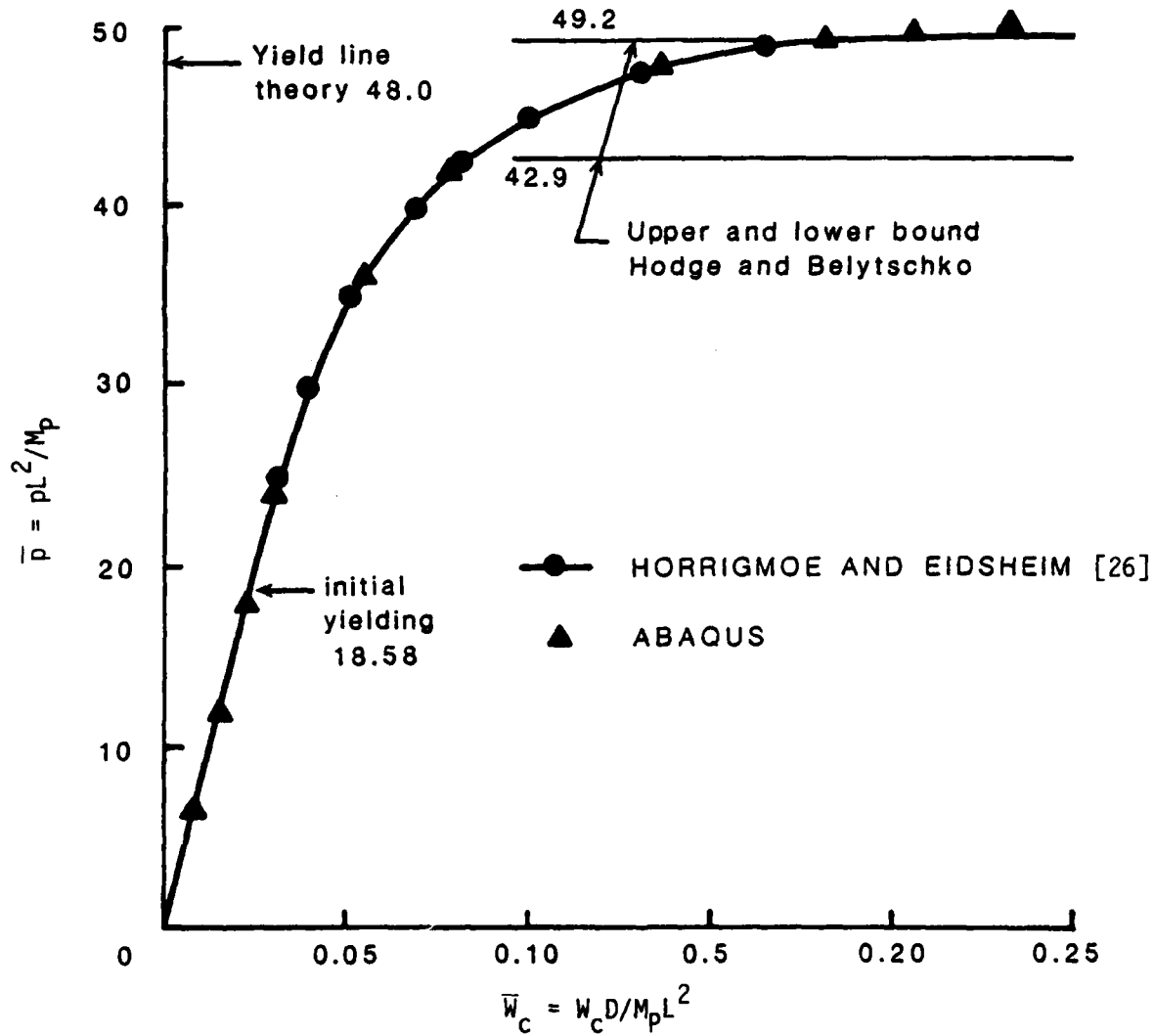


Fig. 5.12. Load-Deflection Curve of an Elastic Plastic Clamped Plate.

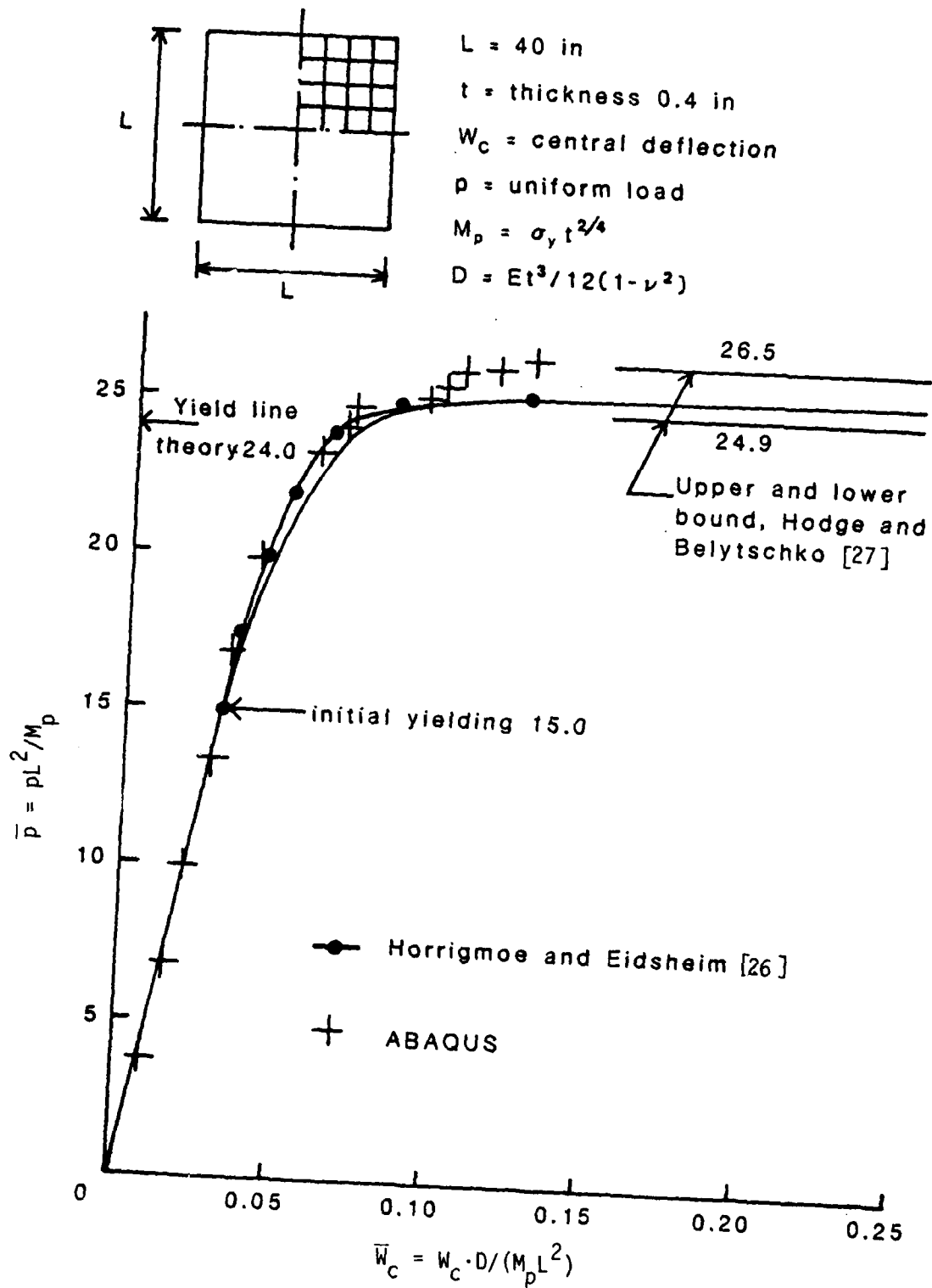


Fig. 5.13. Load-Deflection Curve of an Elastic-Plastic Simply Supported Plate

## 5.6 A Circular Plate with Plasticity

Geometry: A clamped circular plate with dimensions

Radius  $a = 10$  in. , thickness  $t = 1$  in.

Nonlinearity: Elastic-plastic material and small deformation

Material Properties: A Ramberg-Osgood stress-strain curve was assumed to represent the strain-hardening behavior of the material,

$$\epsilon = \frac{\sigma}{E} + \frac{3\sigma}{7E} \left( \frac{\sigma}{\bar{\sigma}} \right)^{n-1}$$

where

$\epsilon$  = Total effective strain

$\sigma$  = Total effective stress

$\bar{\sigma} = 24$  ksi

$n = 6.67$

Also  $E = 10^4$  ksi,  $\nu = 0.33$  ,  $\sigma_0 = 16$  ksi

Loading: Uniform pressure  $p$

Model: From symmetry, one quarter of the plate was modeled by 12- shell (S3R) elements as shown in Fig. 5.14.

Procedure: Direct load incrementing.

Results:

Several runs were made by specifying different solution tolerances, i.e. PTOL and MTOL, ranging from 0.7 to 20% of the maximum reaction forces. It was found that the solution corresponding to the maximum tolerance differs from that of the minimum tolerance by about 8% at the highest loading level. On the other hand, when PTOL and MTOL  $\leq$  5% of the maximum reaction force, the solutions can hardly be distinguishable.

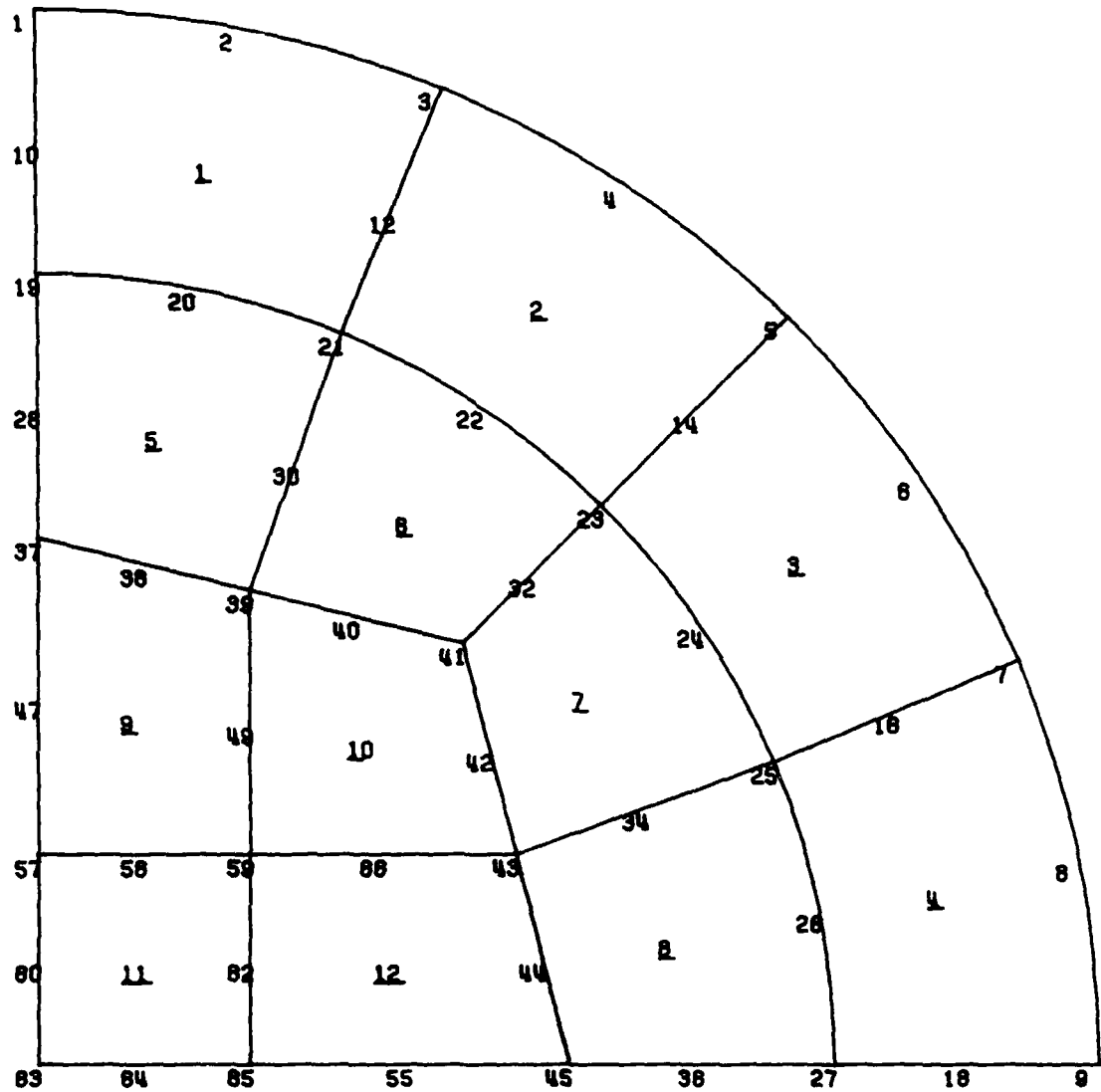


Fig. 5.14. Finite Element Model for One Quarter of a Circular Plate



Results obtained from ABAQUS are compared with those from Kao [25] and Popov et al [28] in Fig. 5.5 and good agreement can be seen.

### 5.7 Large Deformation of a Cylindrical Shell

Geometry: A cylindrical shell (shown in Fig. 5.16) has the dimensions

$$R = 2540 \text{ mm}$$

$$L = 2540 \text{ mm}$$

$$h = 3.175 \text{ mm}$$

$$\theta = 0.1 \text{ rad.}$$

All edges are clamped.

Nonlinearity: Large rotation and linearly elastic material

Material Properties:  $E = 3.1 \text{ KN/mm}^2$ ,  $\nu = 0.3$

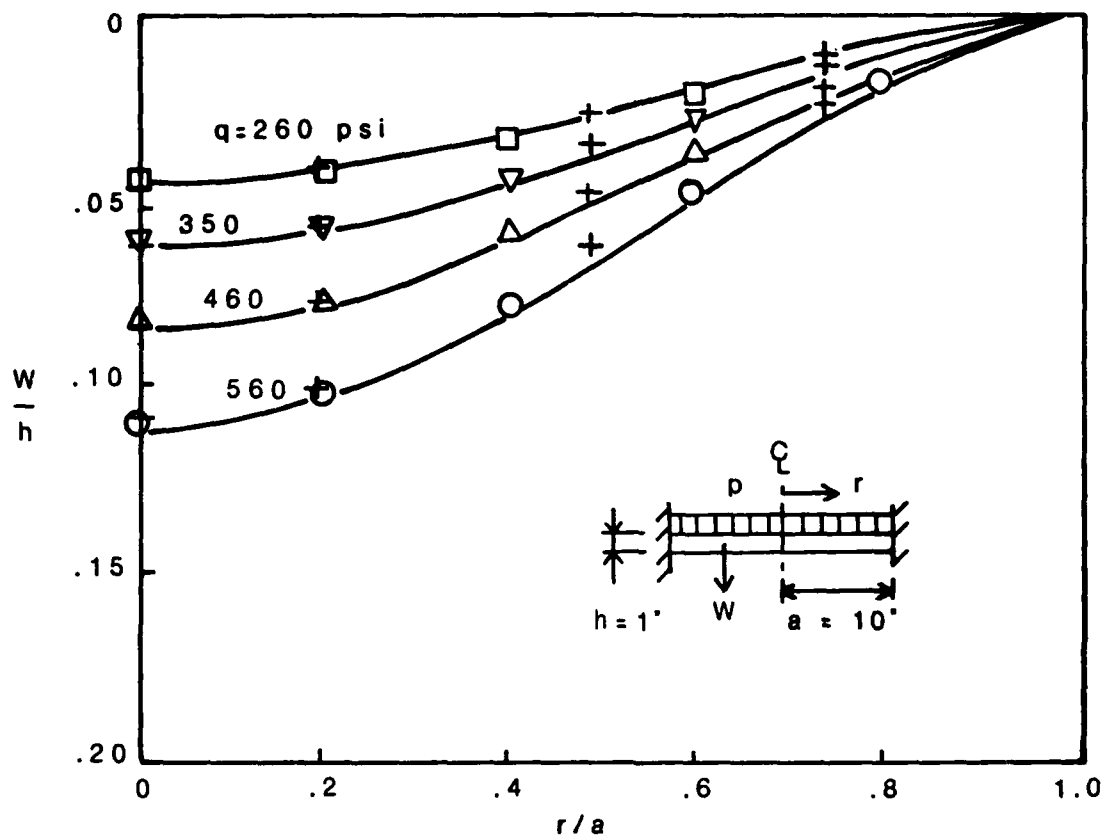
Loading: Uniform pressure normal to the surface of the shell.

Model: A  $4 \times 4$  mesh consisting of 16 shell (S8R) elements.

Procedure: Direct loads incrementing, PTOL = 10N (3% R), MTOL = 25 N.M.,

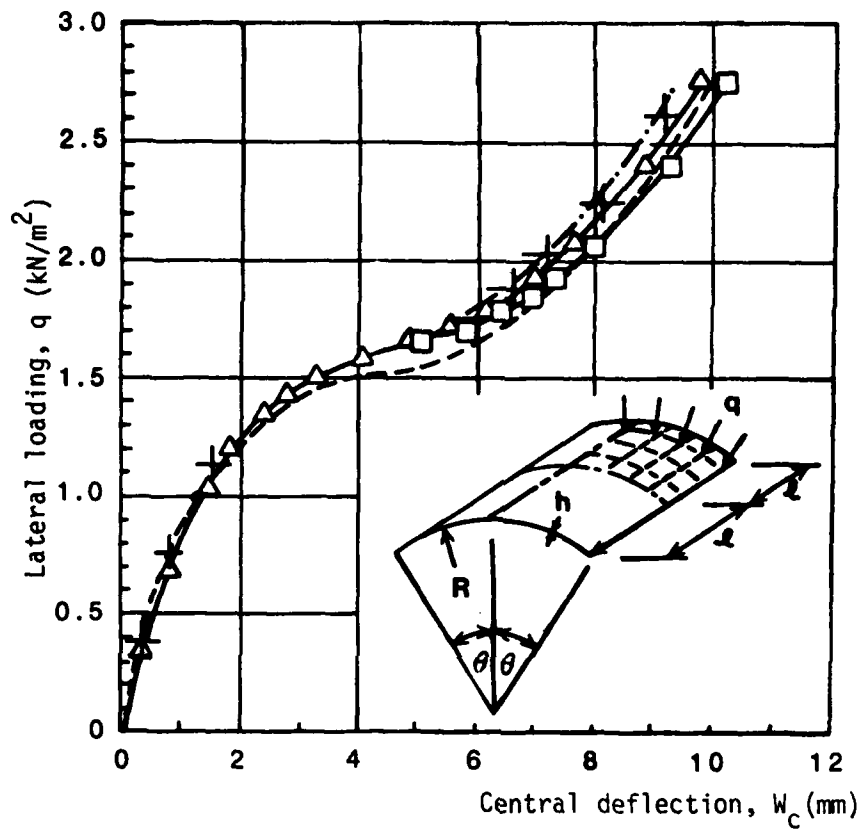
Results:

The purpose of this problem is to test the large deformation feature of the shell element in ABAQUS, including both the pre- and post-buckling responses. This shell has been a rather popular choice by several investigators [24, 29 and 30] due to its stable behavior during the buckling stage so that no numerical difficulty was encountered. As seen in Fig. 5.16, the post-buckling response shows some noticeable differences among various investigators. One possible explanation is the inclusion of deformation - dependent pressure, which was considered in our ABAQUS run.



- |   |   |                   |
|---|---|-------------------|
| + | + | ABAQUS            |
| — |   | Kao [25]          |
| □ | ▽ | Popov et al. [28] |

Fig. 5.15. Deflection Curves of a Circular Plate



- $\square$  } Horrigmoe, Different Elements [24]  
 $\Delta$  }  
 --- Dhatt [30]  
 - · - Sabir & Lock [29]  
 + ABAQUS

Fig. 5.16. Load-Deflection of a Cylindrical Shell.

### 5.8 Post-Buckling of a Cylindrical Shell Subjected to a Point Load

Geometry: The dimensions are

$$\begin{array}{ll} R = 2540 \text{ mm} & \ell = 2540 \text{ mm} \\ h = 12.7 \text{ mm} & \theta = 0.1 \text{ rad} \end{array}$$

The two longitudinal edges were hinged and immovable, whereas the curved ends were free.

Nonlinearity: Large rotation and linearly elastic material.

Material Properties:  $E = 3.1 \text{ KN/mm}^2$ ,  $\nu = 0.3$

Loading: A concentrated vertical force applied at the center.

Model: A  $4 \times 4$  mesh consisting of 16-shell (S8R) elements.

Procedure: Automatic load incrementing

Results:

Although the geometry of this problem is very similar to the preceding benchmark, its post-buckling behavior is quite different due to the simply supported boundaries and concentrated load. In order to carry on the analysis beyond the buckling point of the shell, a displacement boundary condition, instead of load control, must be specified at the center of the shell. The load vs. deflection response is shown in Fig. 5.17. The solution from ABAQUS is almost identical to that of Horrigmoe [24].

### 5.9 Dynamic Response of a Cantilever Beam

Geometry: A cantilever beam with a rectangular cross section

$$\text{length} = 10 \text{ in.}, \quad \text{height} = 1 \text{ in.}, \quad \text{width} = 1 \text{ in.}$$

Nonlinearity: Two cases were analyzed.

- A. Small deformation
- B. Large deformation

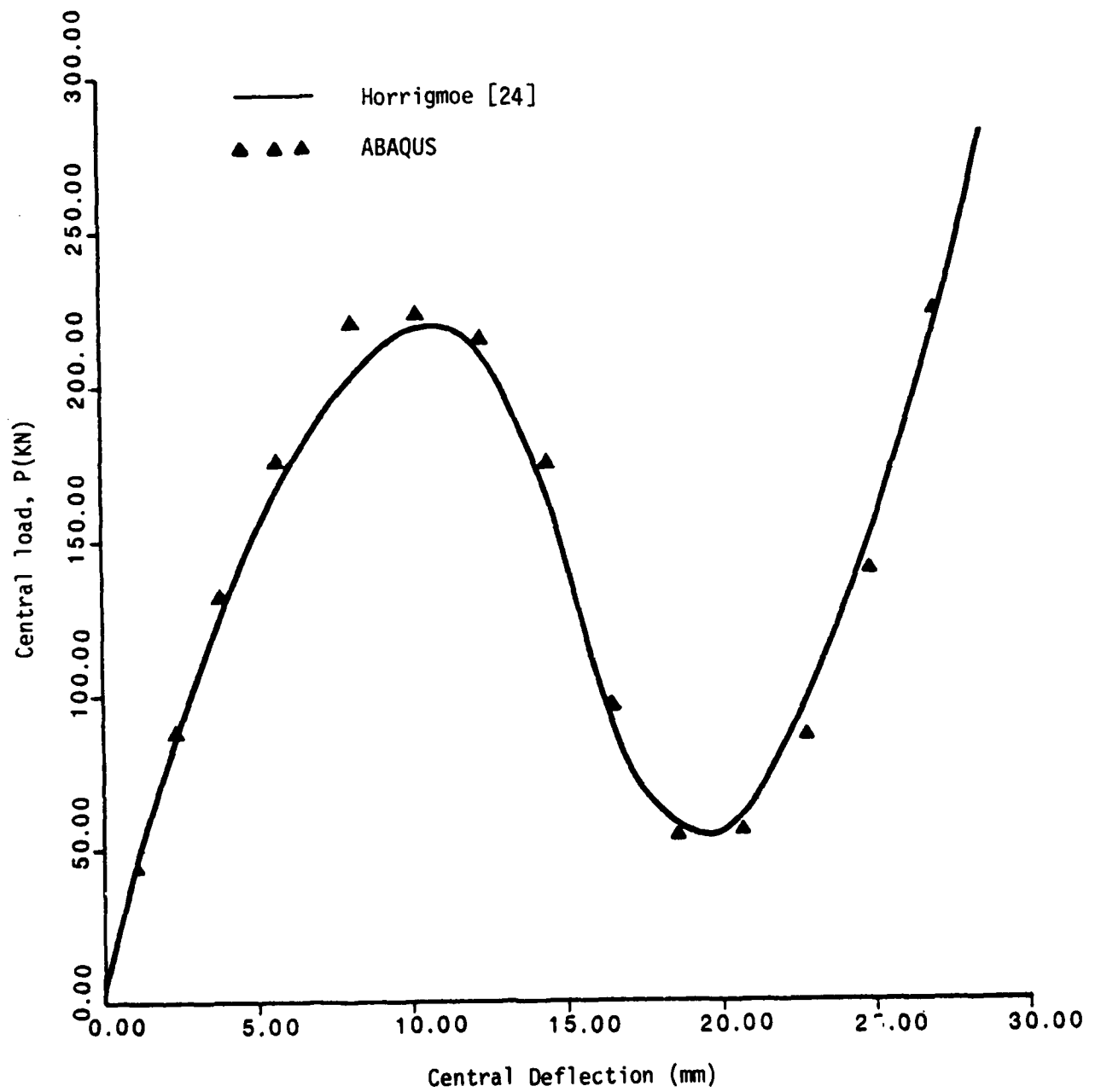


Fig. 5.17. Post-Buckling Behavior of a Cylindrical Shell

Material properties: Linearly elastic material was assumed for both cases,

i.e.  $E = 1.2 \times 10^4$  psi,  $\nu = 0.2$

$\rho = 10^{-6}$  lb-sec<sup>2</sup>/in<sup>4</sup>.

Loading: The beam is subjected to a step-loading uniform pressure of 2.85 psi, the pressure was equally distributed on the top and bottom surfaces of the beam as shown in Fig. 5.18.

Model: The cantilever was modeled by 5 beam (B21) elements.

Procedure: Two different time increments were analyzed, namely  $\Delta t_1 =$

$4.5 \times 10^{-5}$  sec and  $\Delta t_2 = 9 \times 10^{-5}$  sec.

Results:

The purpose of this problem was to test the dynamic algorithms of ABAQUS. The same problem was previously analyzed by ADINA [11]. The maximum deflection histories for small and large deformation cases are shown in Figs. 5.19 and 5.20, respectively. It is seen that ABAQUS results agree with those of ADINA.

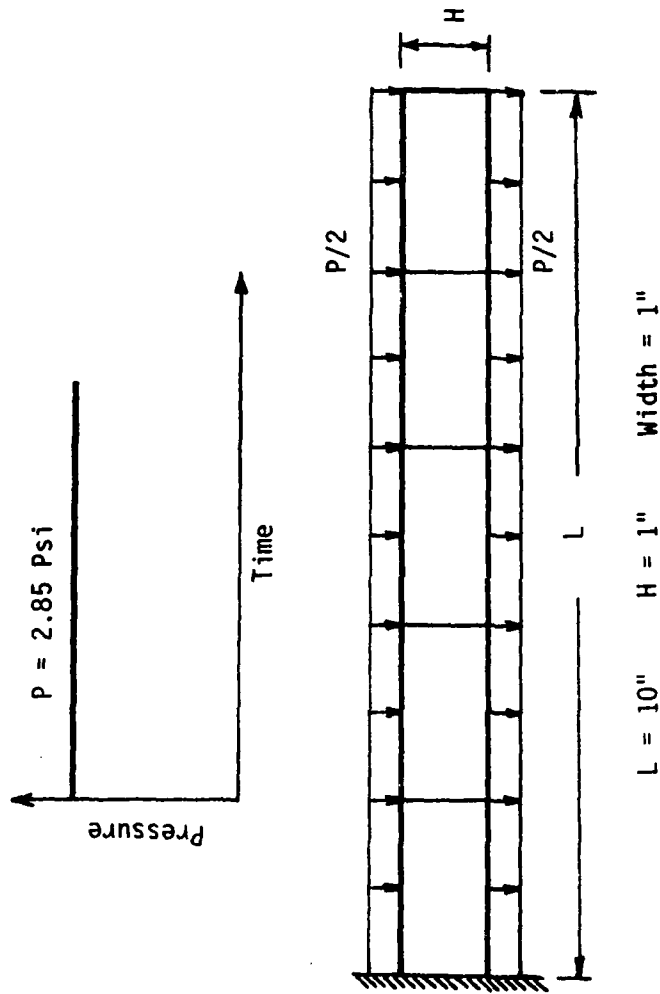


Fig. 5.18. A Cantilever Beam.

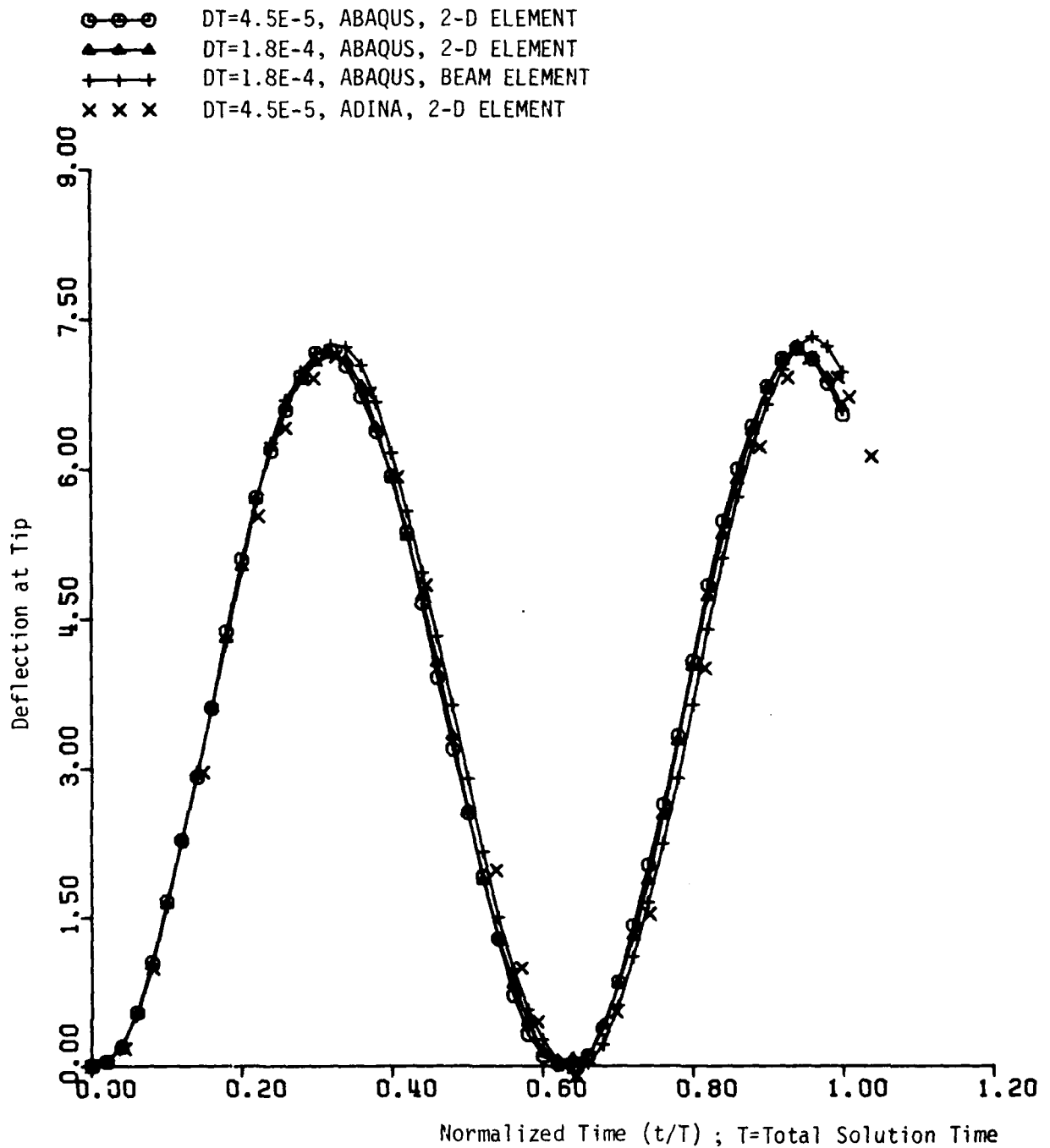


Fig. 5.19. Deflection History of a Cantilever Beam With Small Deformation



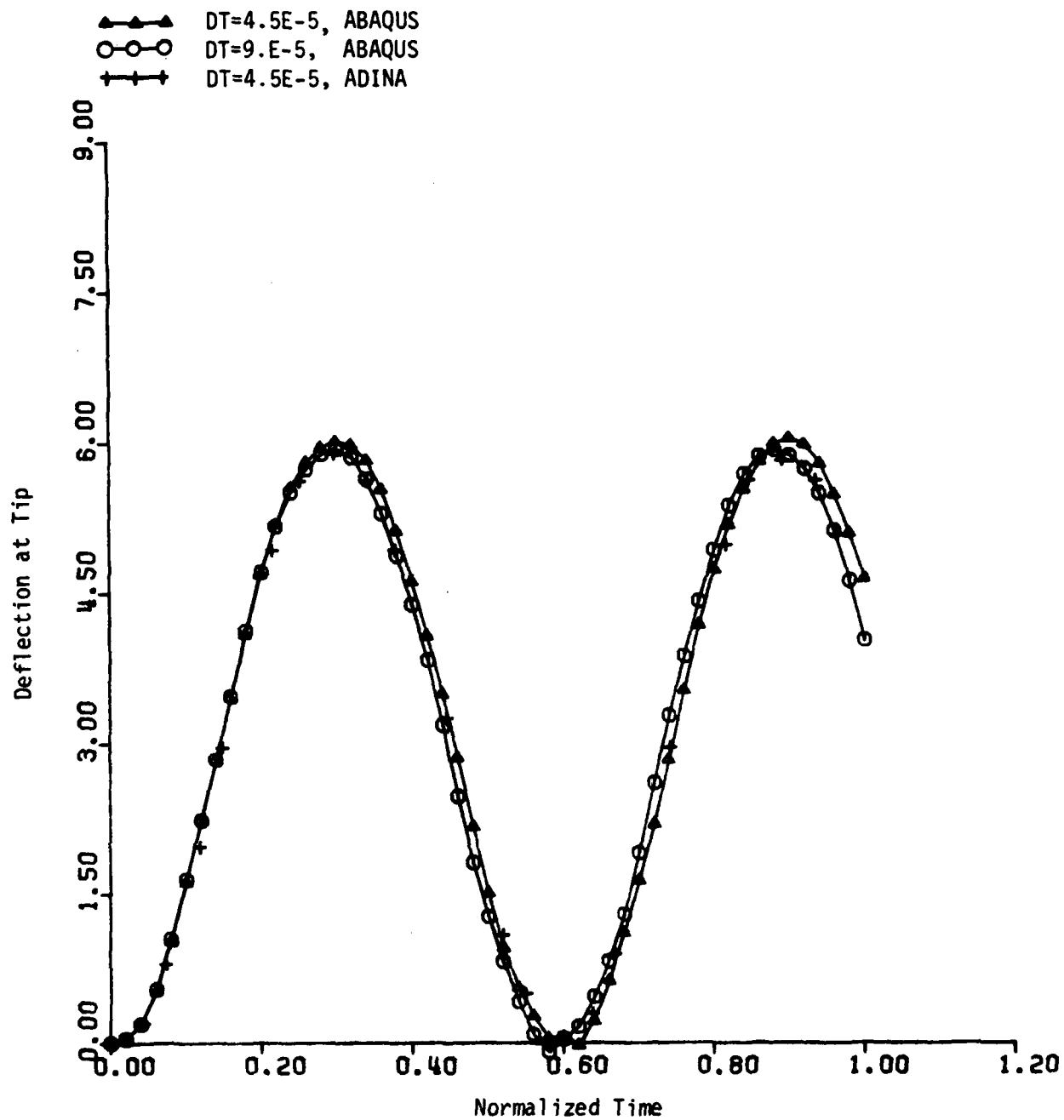


Fig. 5.20. Deflection History of a Cantilever Beam With Large Deformation

## 6. ADVANCED EVALUATION

Several advanced benchmark problems were selected to test the numerical characteristics of ABAQUS. These include

- i) Selection of solution parameters, such as PTOL or HAFTOL, etc.
- ii) Sensitivity of solution to convergence control.
- iii) Analysis time vs. procedure option and the range of convergence tolerance specified.
- iv) Execution time of ABAQUS vs. ADINA.

The benchmarks selected are those with simple geometries so that data preparation effort was kept at a minimum. These problems are relatively complex in terms of their numerical natures.

### 6.1 An Elastica

Elastica is a well-known, classical problem, for which the closed-form solution is available in reference [31]. Several investigators have taken this problem as a benchmark to verify the large deformation algorithm of their finite element programs [24, 32]. Although successful finite element solutions were obtained by previous authors, caution must be given to this problem from the numerical standpoint.

A bar of rectangular cross-section is subjected to uniaxial load as shown in Fig. 6.1. Material was assumed to be linearly elastic; Young's modulus  $E = 30,000$  ksi, Poisson's ratio  $\nu = 0.3$ . A beam element B22 was chosen to represent the bending action of the bar and the corresponding finite element model is given in Fig. 6.1. In order to activate the buckling of the bar, an initial imperfection in the y-ordinates of the nodes was introduced according to  $y = \delta \cdot \cos(\pi x/2L)$ ,  $\delta = 0.1$ .

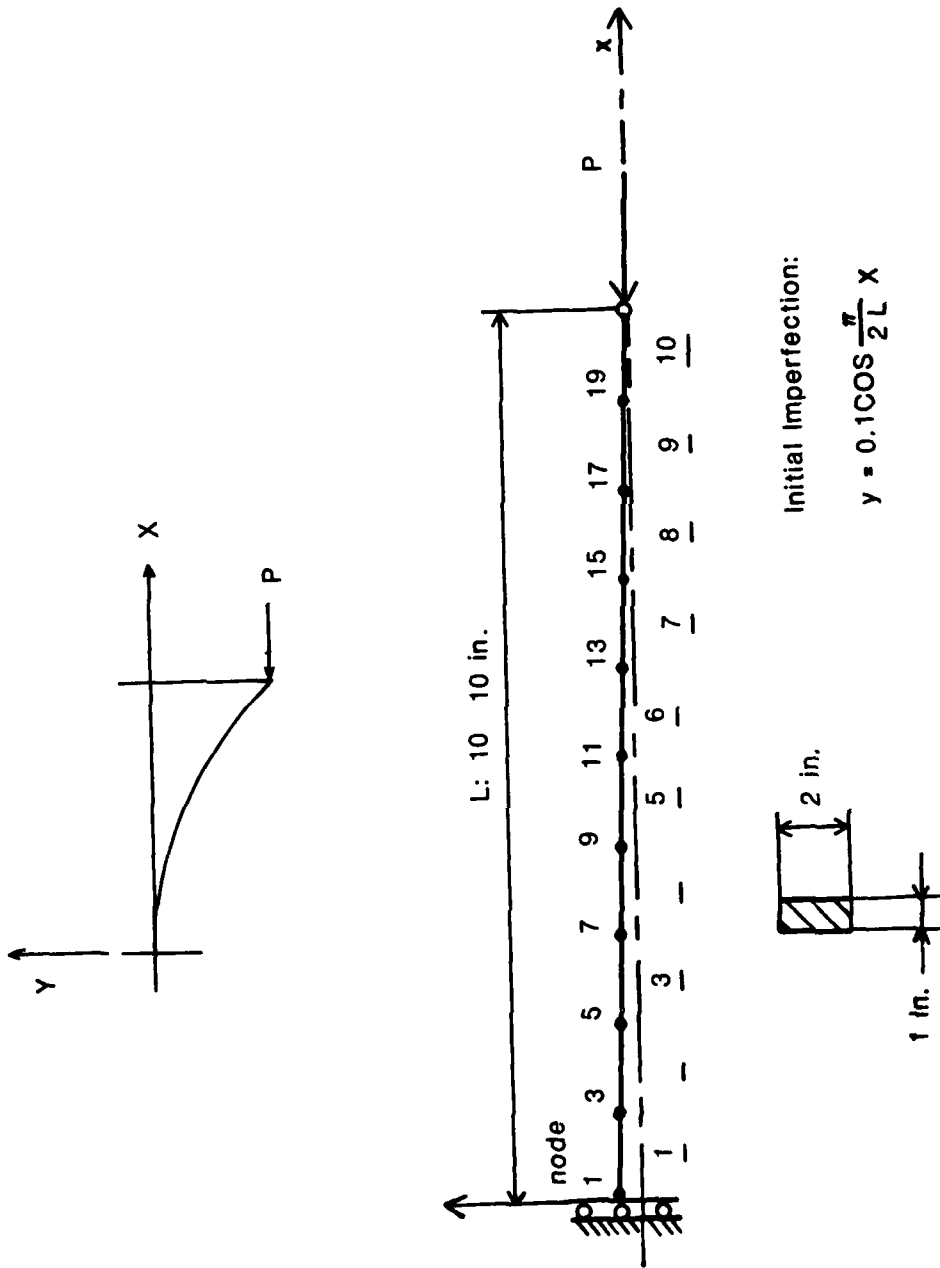


Fig. 6.1. An Elastica.





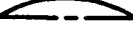

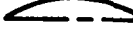

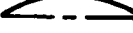
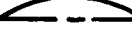


Several computer runs were made using ABAQUS and it was found that the solution of this problem was rather sensitive to three parameters tested:

a) mesh size, b) increment size, and c) convergence tolerance for iterations.

Initially, a relatively coarse mesh consisting of 5 B22 beam elements was used to model the beam. This model appeared to be satisfactory when compared with elementary beam theory within the small deformation range. In running ABAQUS, a prescribed nodal displacement of 150" at the right end of the bar and automatic incrementing procedure were specified. The deflection shapes for several runs by varying the number of solution increments (NUM) and convergence tolerance (i.e. PTOL and MTOL) are tabulated in Table 6.1. It is seen that when  $PTOL = MTOL = 1$ , and  $NUM = 1$ , pure compressive mode of deformation was obtained from the analysis. While for  $PTOL = MTOL = 10$ , and  $NUM = 5$  and 20, respectively, the corresponding deformation mode was switched to a direction opposite to that of the induced initial imperfection. Whereas, for other cases the results were close to the analytical solution for the nodal displacement greater than 100", but considerable differences were found for smaller values of nodal displacement.

In order to obtain an improved solution for the elastica problem, the finite element mesh was revised to consist of 10 B22 elements. Due to numerical sensitivity of this problem, the analysis was carried out in two stages; namely, pre-buckling and post-buckling stages. For the pre-buckling stage, the load control option with direct incrementing procedure was exercised. The load was increased from 0 to a critical value  $P_{Cr} = -4.8$  lb. For the post-buckling stage, the analysis was switched to displacement control with an automatic incrementing procedure. In both cases, a tight tolerance, i.e.  $PTOL = MTOL = .05$  was specified.

Table 6.1. Deformation Modes of Elastica vs. Solution Parameters.

NUM(*) PTOL(lb) MTOL(ft-lb)	1	5	10	20
1				
10				
100				

(\*) NUM: User suggested number of increments

MTOL } User defined moment and force tolerances for  
 PTOL } accuracy control (notice that the max. value of end  
 force for this problem is about 35 lb.)

The load-deflection response obtained from ABAQUS is compared with the closed form solution [31] as shown in Fig. 6.2. Obviously, excellent agreement was found. The deflected shapes of the elastica corresponding to different loads were plotted in Fig. 6.3. These shapes appear to be in reasonable agreement with those in reference [31].

## 6.2 An Elastic-Plastic Plate Subjected to Biaxial Loading.

A square plate subjected to biaxial stresses was considered. The primary objective of this benchmark is to test the numerical stability of ABAQUS under elastic-plastic loading, unloading and neutral loading. The material was assumed to bilinearly elastic-plastic with kinematic strain hardening. The material constants are:

Young's modulus:  $E = 30 \times 10^3$  Ksi

Poisson's ratio:  $\nu = 0.3$

Initial yield stress:  $\sigma_0 = 30$  ksi

Plastic modulus:  $E_p = 1.5 \times 10^3$  ksi

The loading path was specified in 3 successive steps:

Step 1.  $0 < \sigma_x \leq 40.5$  ksi

$$\sigma_y = 0$$

Step 2.  $\sigma_x$  was reduced from 40.5 ksi to  $\sigma_0$  (unloading)

$$\sigma_y = 0$$

Step 3.  $\sigma_x$  and  $\sigma_y$  were varied according to

$$\sigma_x^2 + \sigma_y^2 - \sigma_x \sigma_y = (40 \text{ ksi})^2$$

Until  $\sigma_y = 0$  and  $\sigma_x = -40$  ksi

The above loading path is depicted in Figs. 6.4. and 6.5.

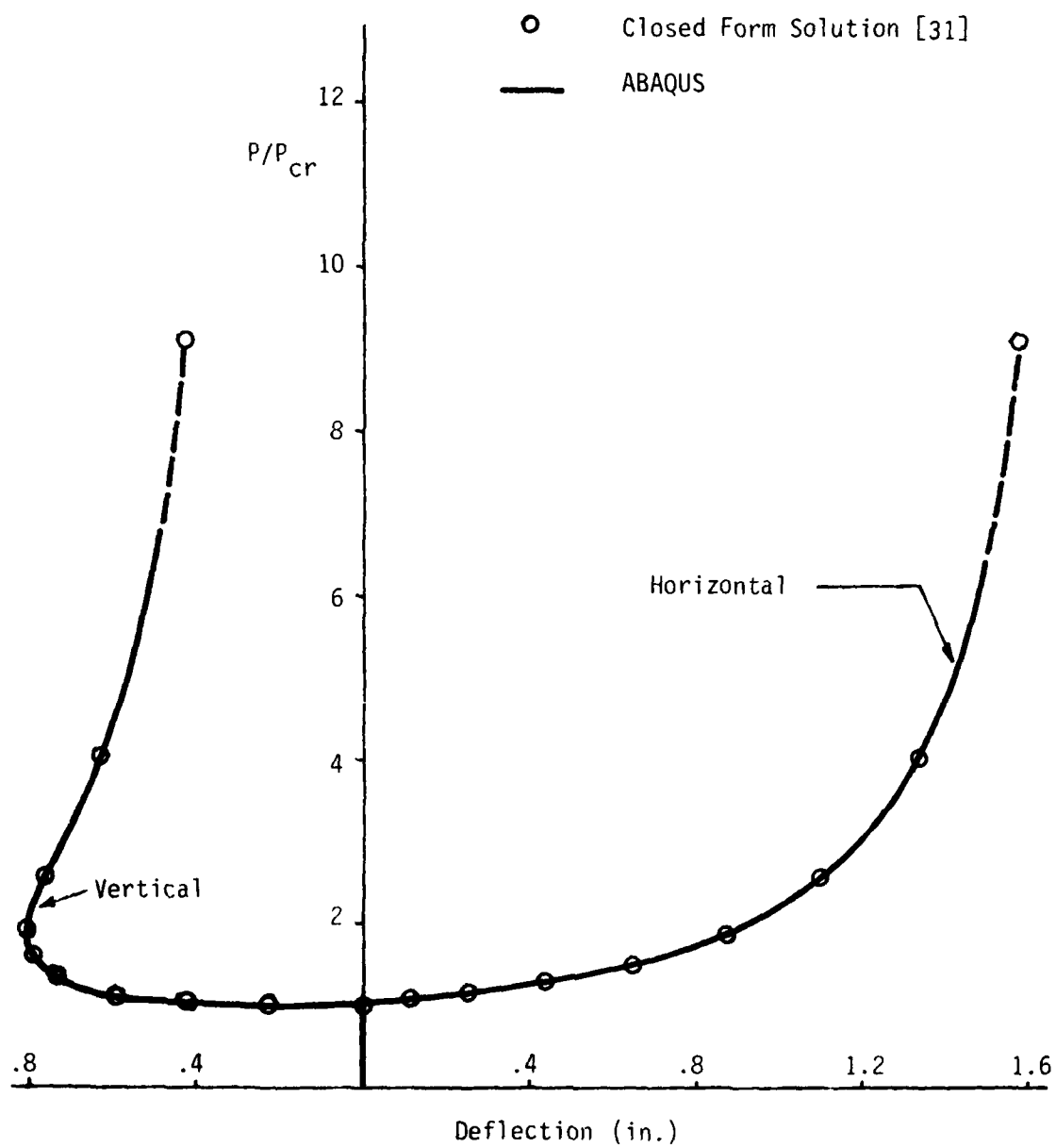


Fig. 6.2. Load - Deflection Response of An Elastica

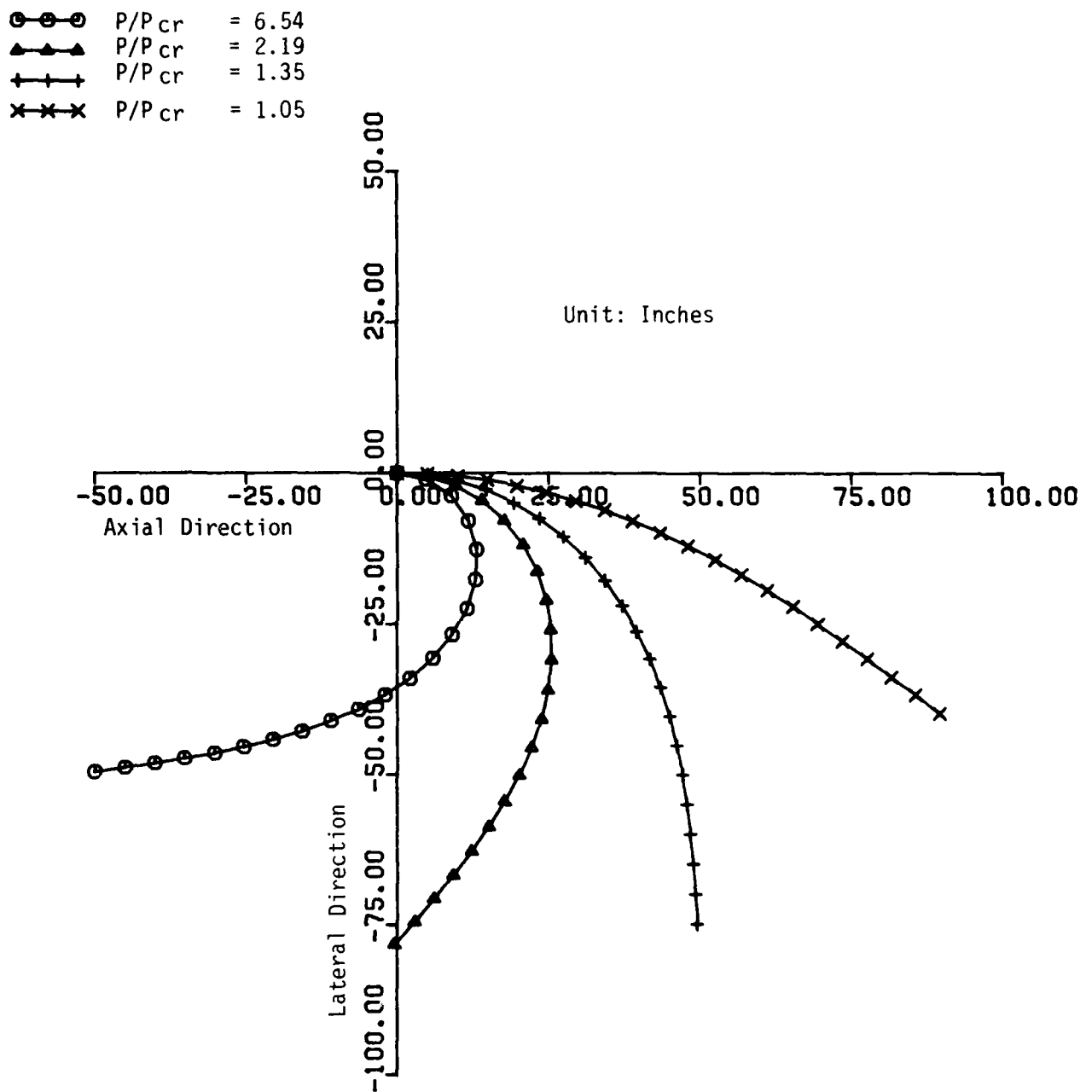


Fig. 6.3. Deformed Curves of the Elastica



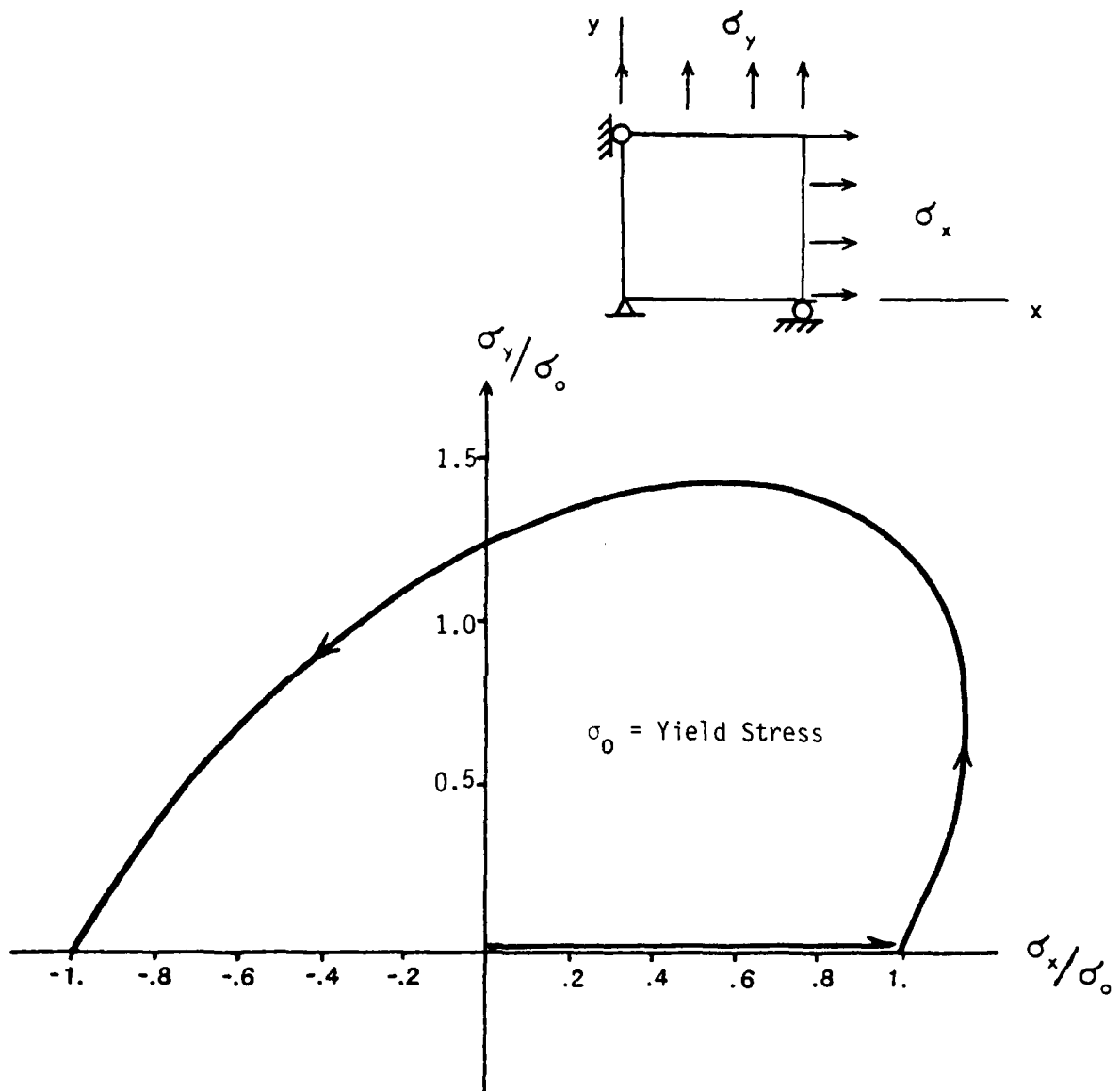


Fig. 6.4. Biaxial Loading Path of a Plate Problem

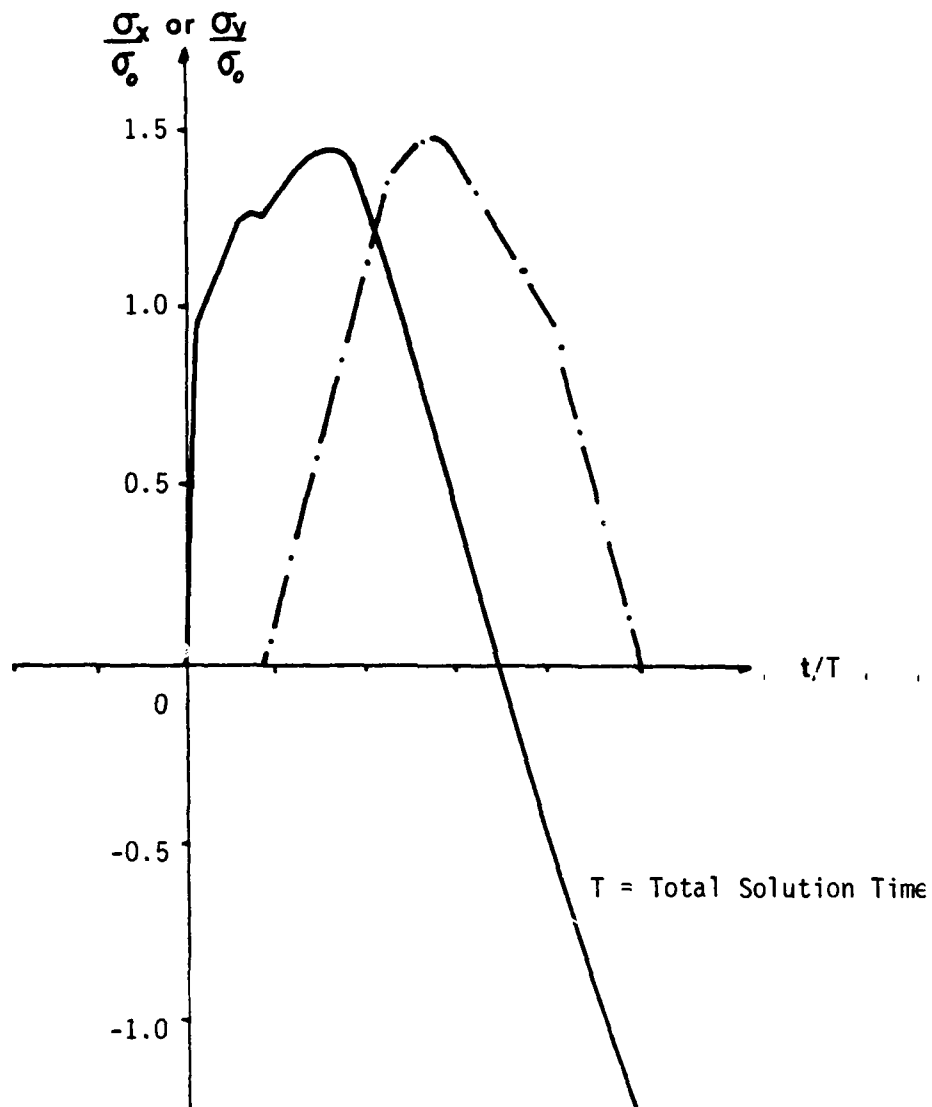


Fig. 6.5. Loading History of  $\sigma_x$  and  $\sigma_y$ .

AD-A128 788

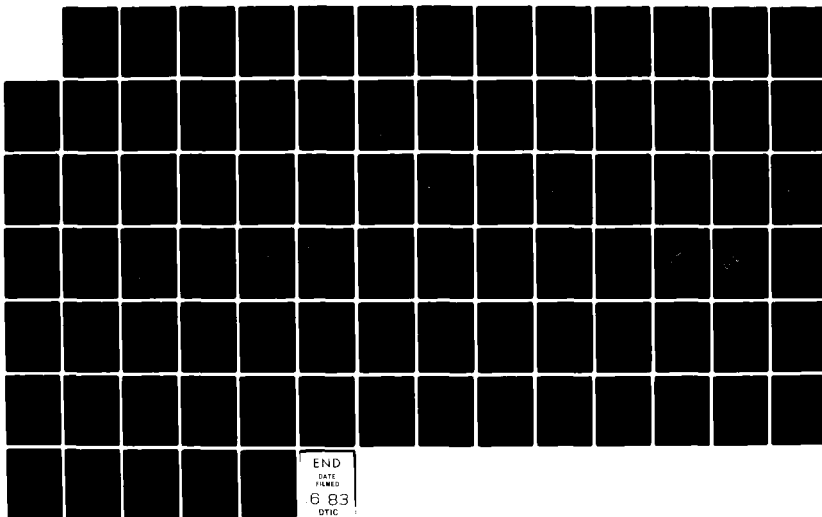
EVALUATION OF A NONLINEAR FINITE ELEMENT PROGRAM -  
ABAQUS(U) AKRON UNIV OH DEPT OF CIVIL ENGINEERING  
T Y CHANG ET AL. 15 MAR 83 AUE-821 N00014-78-C-0691

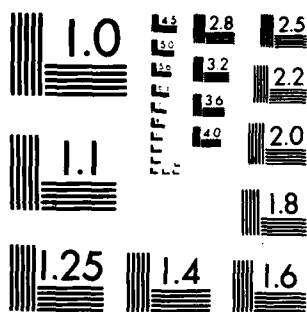
2/2

UNCLASSIFIED

F/G 9/2

NL





MICROCOPY RESOLUTION TEST CHART  
NATIONAL BUREAU OF STANDARDS-1963-A

Since the plate was subjected to a homogeneous state of stress, only one plane stress element, CPS4, was used. Initially, direct procedure with a loading increment  $\Delta P = 40000$  psi was specified. Although ABAQUS gave convergent solution, the solution deviates from the analytical result [33] as indicated in Fig. 6.6. Analysis was also done by using ADINA. Solution convergence could not be reached as soon as the plasticity was initiated.

In order to find a suitable loading increment, the automatic load incrementation option of ABAQUS was exercised for 7-load increments. The solution correlates with the analytical result, as shown in Fig. 6.6, very closely. Once a convergent load increment was found from the automatic incrementation option, a direct control was used to complete the analysis. Again, as seen in Figs. 6.6 and 6.7, the stress and strain printout from ABAQUS are indistinguishable from those of the analytical solution. The analysis was also conducted by using ADINA with the same loading increments. The strain output from ADINA are slightly different from those of ABAQUS as shown in Fig. 6.8.

From the experience of this example, it is felt that the automatic step control is an extremely desirable feature for searching for convergent load increment in nonlinear analysis.

### 6.3 A Cantilever Beam Subjected to an End Force

Large displacement of a cantilever beam was considered. The beam was subjected to a concentrated force at the free end (shown in Fig. 6.9) and two load cases were examined: Case a) Conservative load - load always remained vertical, and case b) Nonconservative load - load remained normal to the deformed neutral axis of the beam. The beam was assumed to have a rectangular

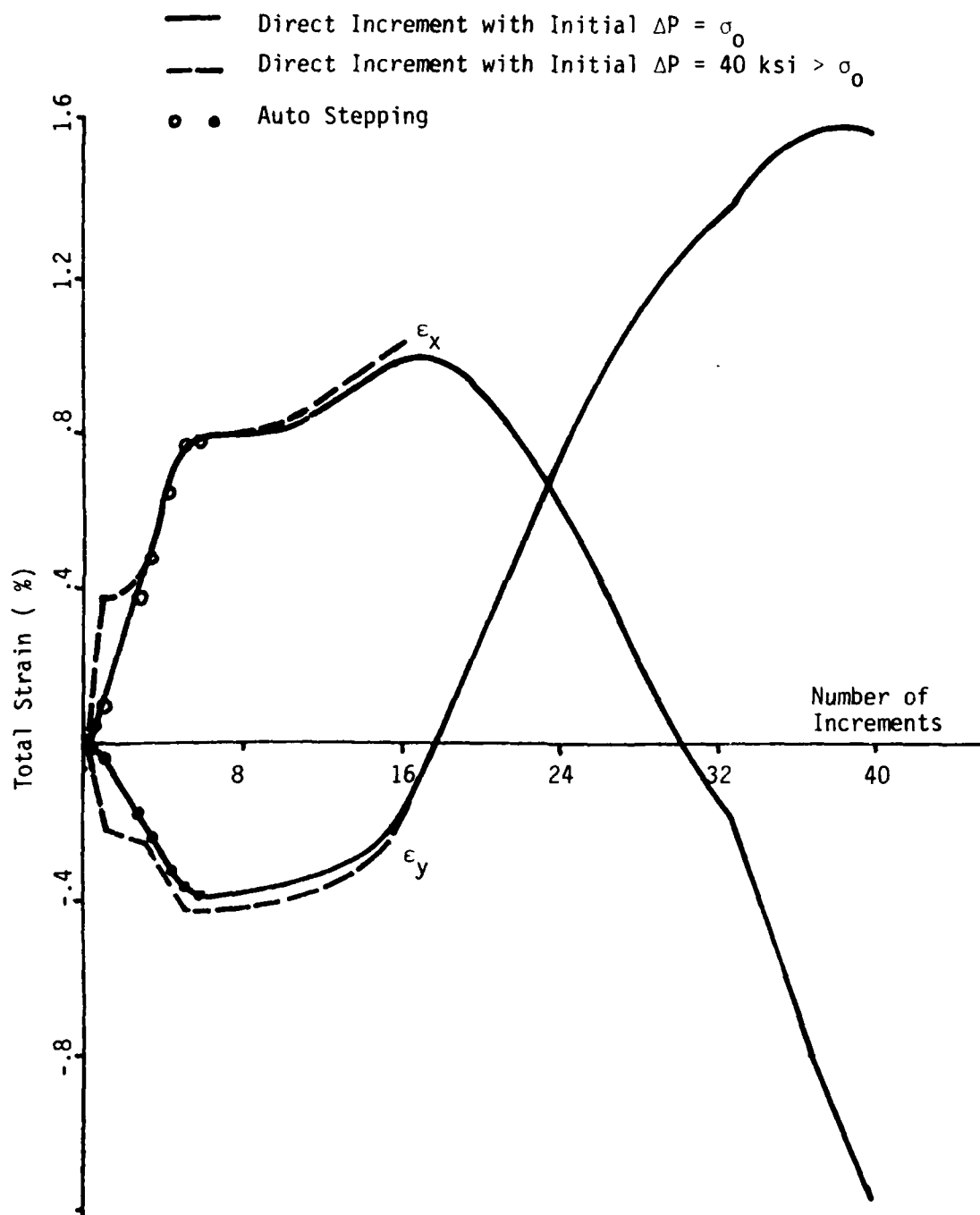


Fig. 6.6. Strains vs. Solution Increments of Biaxially Loaded Plate

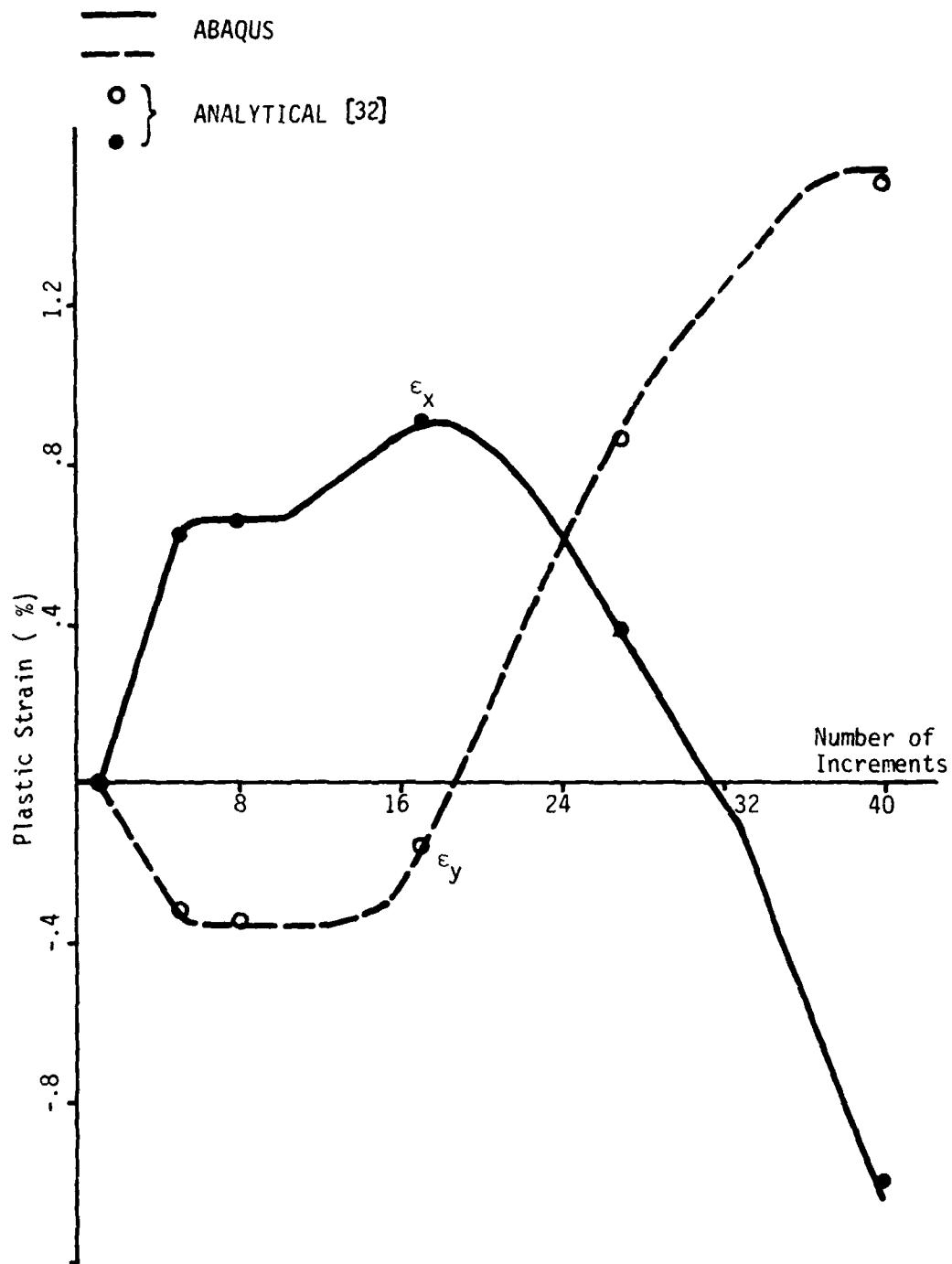


Fig. 6.7. Plastic Strains vs. Solution Increments of Biaxially Loaded Plate

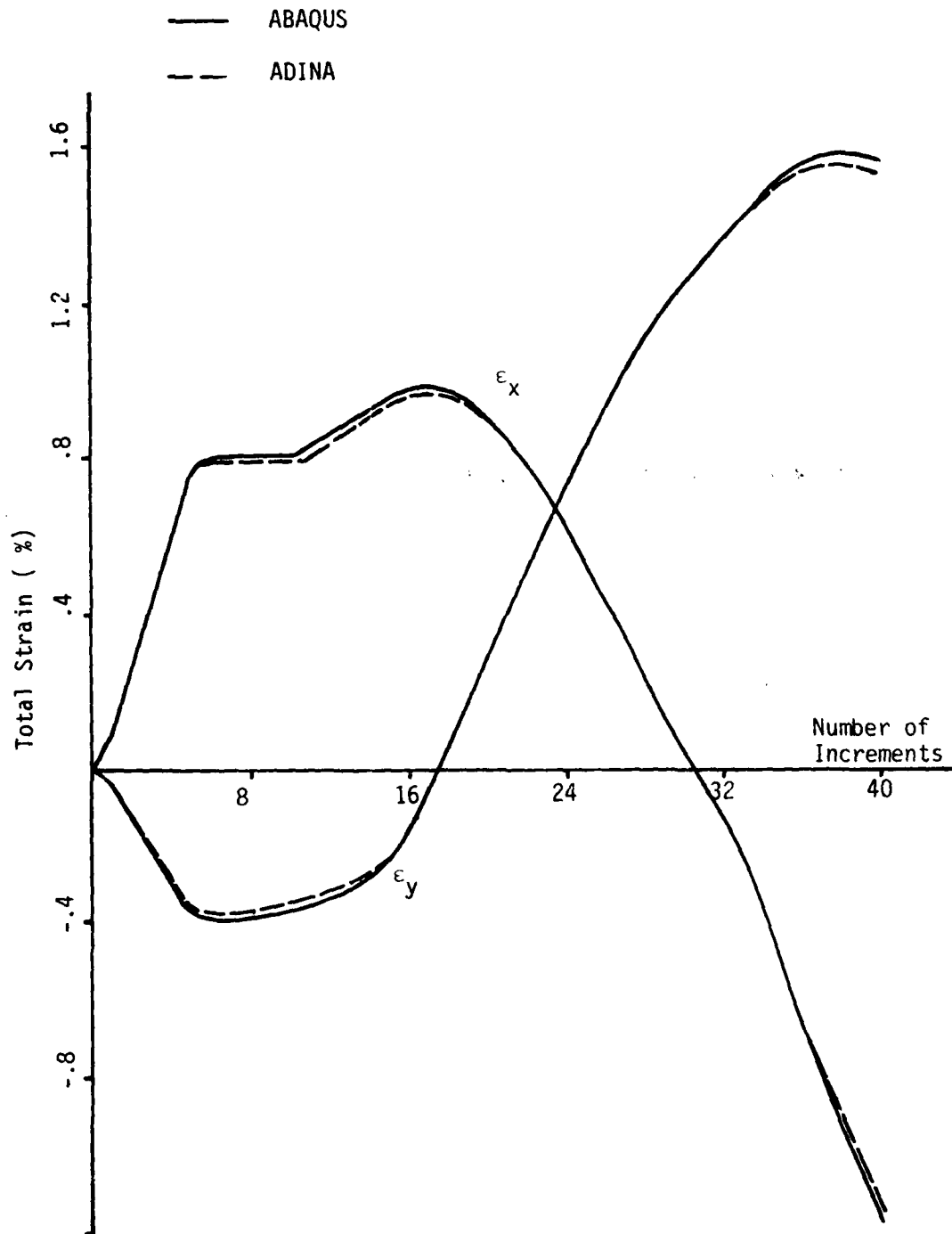


Fig. 6.8. Comparison of Results Between ABAQUS and ADINA



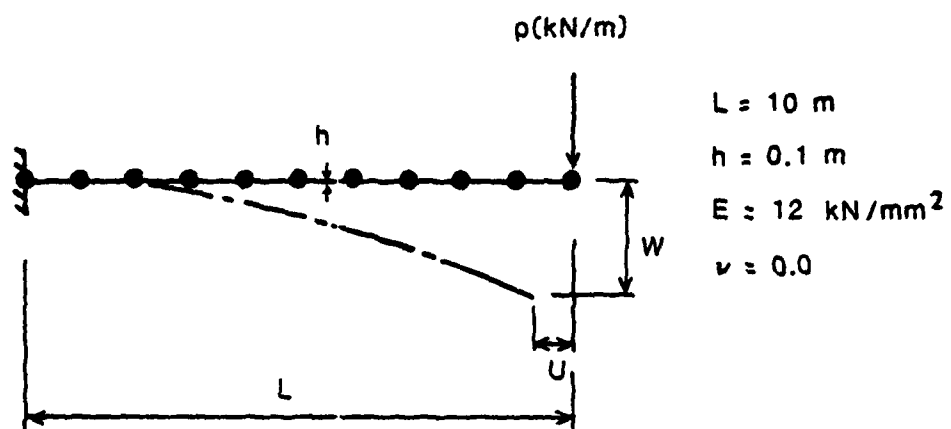


Fig. 6.9. A Cantilever Beam Subjected to a Concentrated Force.

cross section with linearly elastic material. The finite element model consisted of 10 B21 (beam) elements with 11 nodes.

When using ABAQUS, the automatic load control with fairly large convergence tolerances was specified, i.e.

$$PTOL = 15\% \cdot (\text{Max. Reaction Force})$$

$$MTOL = 2\% \cdot (\text{Max. Reaction Moment})$$

The horizontal and vertical displacements at the free end for the two load cases considered were plotted in Figs. 6.10 - 6.12 against the solution obtained by Horrigmoe [34].

Due to the difference in convergence characteristics, the non-conservative load case required much greater number of solution increments, thereby more CPU time, than the conservative load case. A comparison is given as the following:

	<u>No. of Increments</u>	<u>Total Iteration Cycles</u>
Conservative Load	10	30
Non-Conservative Load	30	115

It was somewhat surprising that the two load cases gave such remarkable difference in convergence.

The same problem was also run using ADINA. Since ADINA cannot handle deformation-dependent loading, only the conservative load case was considered. Due to the stiffening load-deflection response of this problem, solution convergence was extremely difficult to achieve when the MNR method with equilibrium iterations was optioned. After several unsuccessful trials finally a procedure with 800 load increments together with equilibrium iterations was necessary to obtain a convergent solution comparable to

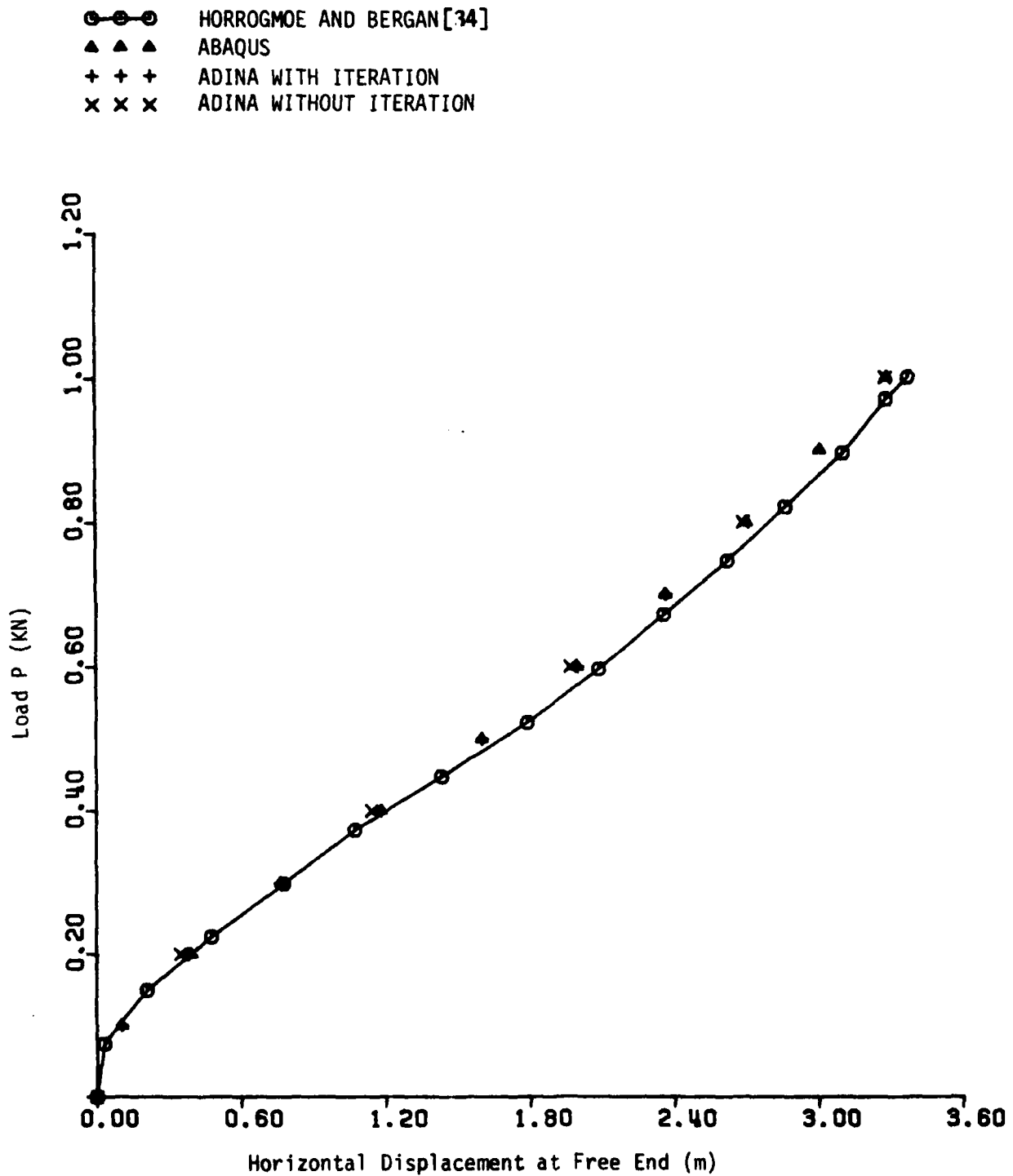


Fig. 6.10. Load-Displacement Response of a Cantilever Beam  
Subjected to a Vertical Force

- ○ ○ HORROGMOE AND BERGAN [34]
- ▲ ▲ ▲ ABAQUS
- + + + ADINA WITH ITERATION
- x x x ADINA WITHOUT ITERATION

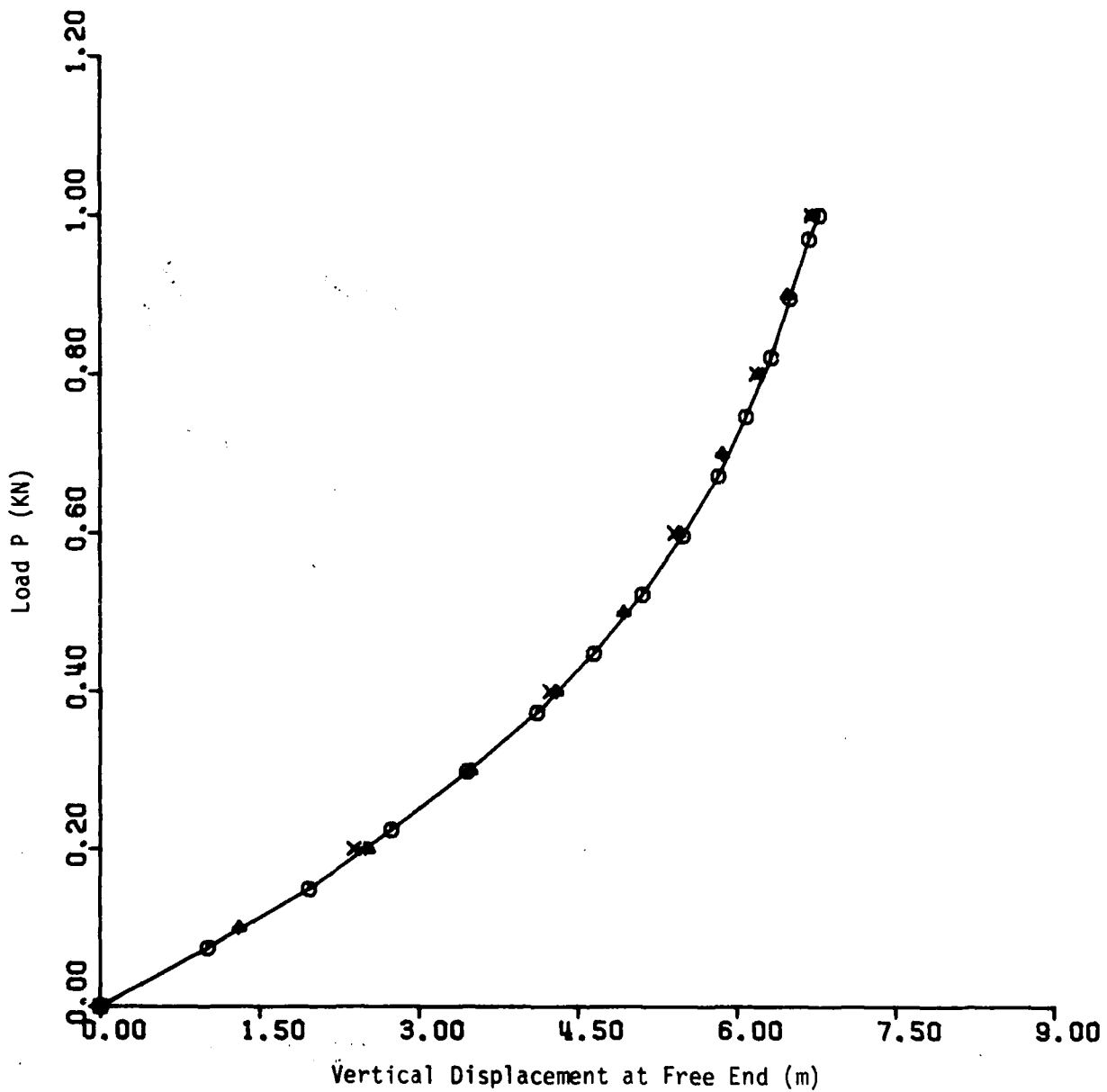


Fig. 6.11. Load-Displacement Response of a Cantilever Beam  
Subjected to a Vertical Force

- ○ ○ HORROGMOE AND BERGAN, HORIZONTAL [34]
- ▲ ▲ ▲ HORROGMOE AND BERGAN, VERTICAL
- + + + ABAQUS, HORIZONTAL
- x x x ABAQUS, VERTICAL

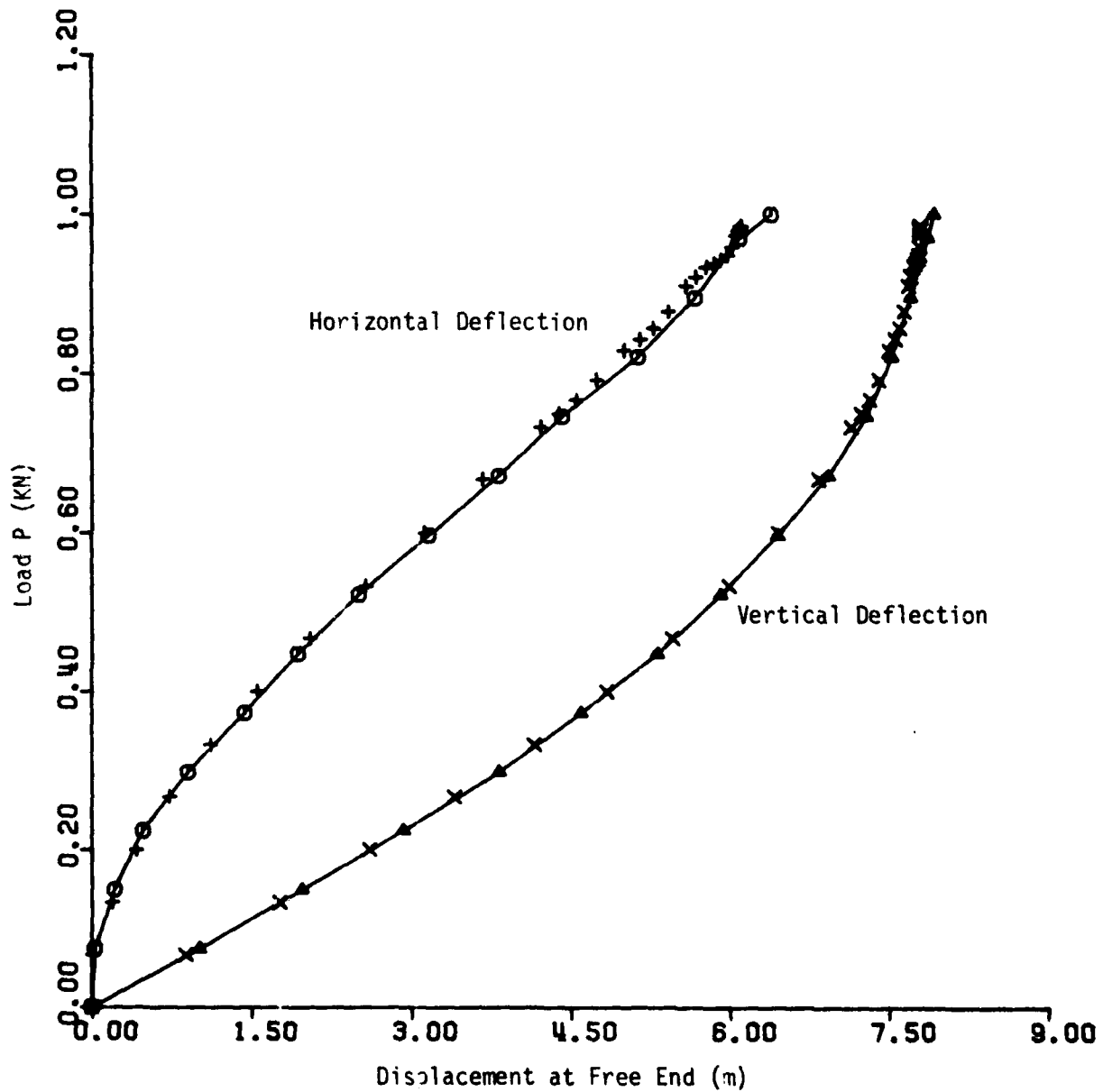


Fig. 6.12. Load-Deflection Response of a Cantilever Beam With a Follower Force

Horrigmoe's result. On the other hand, an ADINA run with 100 load increments and no equilibrium iterations was carried out and the result is similar to that of 800-increment analysis. This phenomenon illustrated the unpredictability of the MNR algorithm when it is applied to a nonlinear structural problem with stiffening effect.

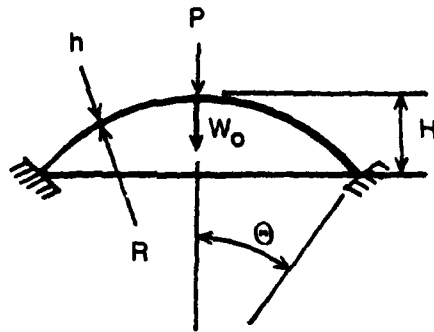
It is noted that both ABAQUS and ADINA results agree quite well; they are however slightly different from those obtained by Horrigmoe and Bergan [34], especially the horizontal component of the displacement at the free end (Fig. 4.10).

#### 6.4 Large Deformation of a Spherical Cap

A spherical cap subjected to a concentrated load at the crown as shown in Fig. 6.13 was analyzed using both ABAQUS and ADINA. Again, the purpose of this example is to demonstrate the relative merits between the full and modified Newton-Raphson algorithms.

The material of spherical cap was assumed to be linearly elastic. This problem was previously analyzed by Stricklin [35], Mescall [36], and Bathe in ADINA manual [11]. As seen in the load - deflection plot (Fig. 6.13), initially the cap exhibits softening behavior. After the apex is deformed to a point passing the baseline through the two supports, the bending action in the cap is transformed into the membrane action, and thus stiffening of the structure can be observed.

The cap was modeled by ten 8-node axisymmetric elements, i.e. CAX8R elements. To run ABAQUS, an automatic procedure with the following control parameters was used:



$R = 4.76$   
 $h = 0.01576 \text{ in}$   
 $H = 0.0859 \text{ in}$   
 $\Theta = 10.9^\circ$   
 $\lambda = 6$   
 $E = 10 \times 10^6 \text{ lb/in}^2$   
 $\nu = 0.3$   
 $\rho = 0.000245 \text{ lb-sec}^2/\text{in}^4$

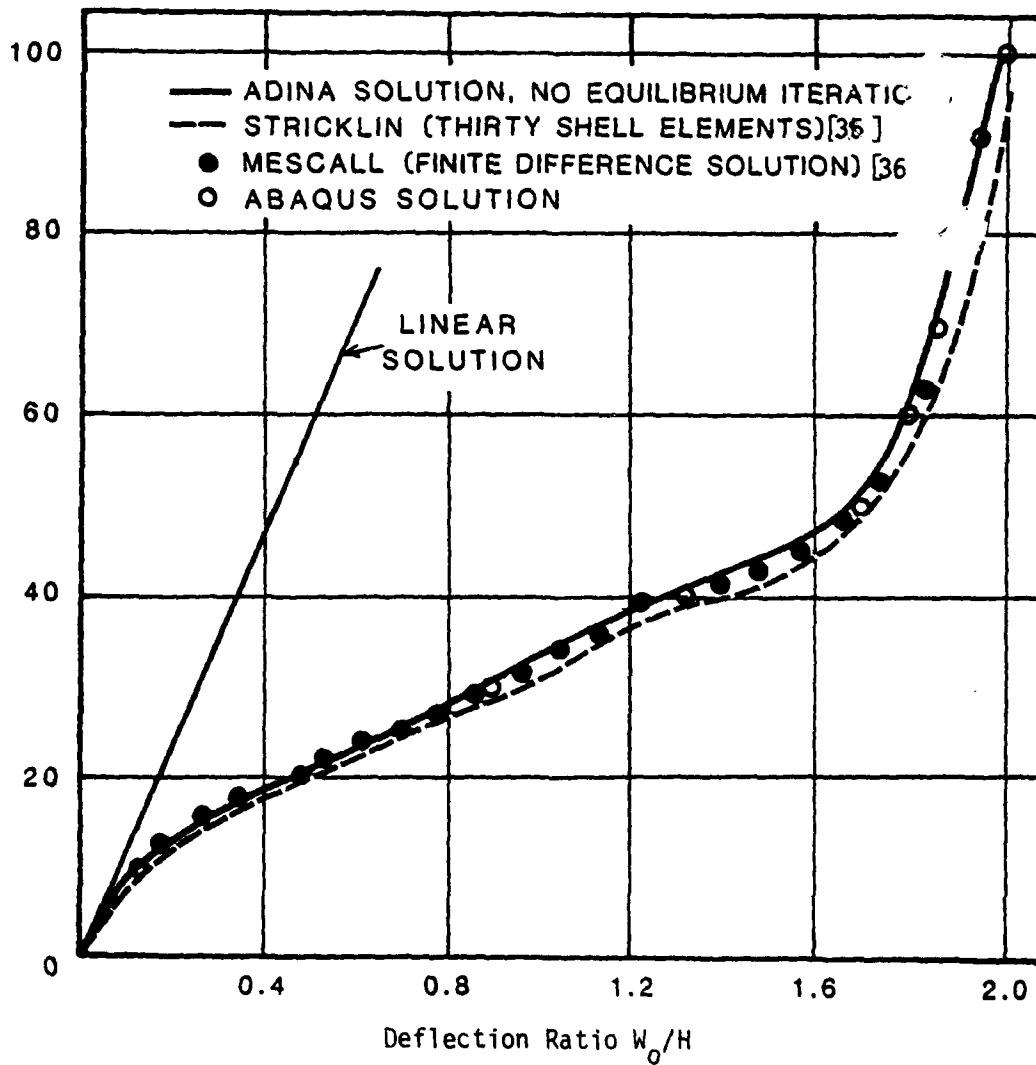


Fig. 6.13. Load-Deflection Curves for Spherical Shell

Suggested Number of Increments: NUM = 5

Force Tolerance: PTOL = 100 ( ~ 1% of Max. Reaction)

The analysis from ABAQUS was completed with a total of 36 solution increments (including iterations), and the results are shown in Fig. 6.13.

When ADINA was used to run the same problem, considerable difficulty in solution convergence was experienced if equilibrium iterations were exercised. Even with different specified values of convergence tolerance and maximum iteration cycles, the analyses were interrupted for loads between 20 - 50 lb. After several attempts, a procedure with 80 load increments and no iterations was successful to obtain a solution agreeable to the known results. Once again, this example demonstrated the numerical difficulty of the MNR algorithm whereas the FNR method appears to be superior.

#### 6.5 Buckling of A Spherical Shell

In general, ABAQUS cannot be used for post-buckling analysis, since the program does not have a special solution algorithm for handling such case. Nevertheless, post-buckling analysis can be performed for structures subjected to simple loadings, such as a concentrated force applied at the point of symmetry. For this purpose, a displacement control, as opposed to the load control, must be specified for the intended analysis.

A spherical shell with linearly elastic material properties was selected for buckling analysis. The purpose of such analysis is to determine the convergence characteristics of shell elements in ABAQUS when significant change of geometry is involved. The same problem has previously been analyzed



by several researchers [24, 34, 37] due to its simplicity in geometric shape and dramatic post-buckling features. Dimensions of material constants of the shell are given as below:

Radius	$R = 2450 \text{ mm}$
Side Dimension	$a = 754.9 \text{ mm}$
Thickness of Shell	$h = 99.45 \text{ mm}$
Young's Modulus	$E = 68.95 \text{ N/mm}^2$
Poisson's Ratio	$\nu = 0.3$

The shell is supported by hinges in such a way that it can rotate freely along the tangent direction to the curved edges, but no translation is allowed. With this boundary condition, coordinate transformation must be introduced in using ABAQUS, since the constrain conditions are specified in reference to the local coordinate at the boundary nodes.

Taking advantage of symmetry, only one-quarter of the shell surface was modeled by S8R shell elements. Three different meshes were considered for the intended analysis; namely  $2 \times 2$ ,  $3 \times 3$  and  $4 \times 4$  meshes. The load vs. maximum deflection responses of the three meshes are shown in Fig. 6.14. It is seen that the load-deflection responses obtained from the  $3 \times 3$  and  $4 \times 4$  meshes are identical; whereas the prebuckling response of  $2 \times 2$  mesh is similar to those of finer meshes, but the post-buckling response is far different. In fact, when the  $2 \times 2$  mesh was loaded near the critical value, the shell suddenly jumped to a new equilibrium state (membrane action), bypassed the lower post-buckling range. However, when the load was reduced from the membrane state, the lower post-buckling curve was traced, but quite different from those of the finer meshes. The implication of this phenomenon

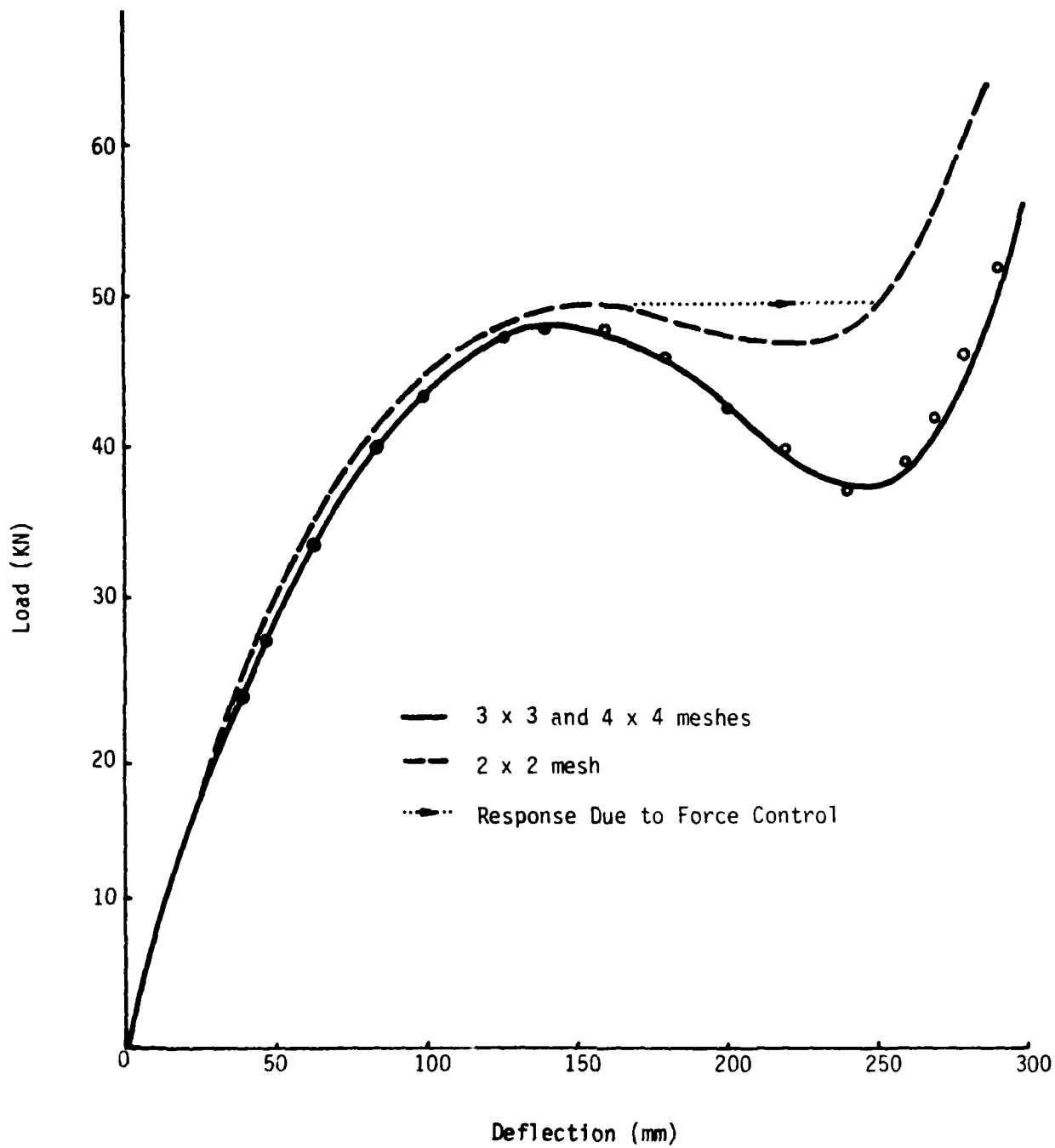


Fig. 6.14. Post-Buckling Behavior of a Spherical Shell  
With Different Mesh Sizes

is that a finite element mesh is sufficient for pre-buckling analysis, but may not be the case for representing post-buckling behavior.

For comparison, the load deflection response, obtained from ABAQUS using 4 x 4 mesh, was plotted in Fig. 6.15 together with those of Leicester [37] and Horrigmoe and Bergan [34]. Small, but significant deviation can be seen between ABAQUS results and others. Such deviation might have been caused by the use of TRANSFORM option in ABAQUS for defining the boundary restraints with respect to the local coordinates along the curved edge of the shell.

## 6.6 A Centrally Cracked Plate

A rectangular plate containing a plane crack at its center was considered as another example (Fig. 6.16). The plate is subjected to uniform pressure  $P_y$  at its two ends. The material properties were assumed to be elastic perfectly plastic obeying von Mises yield criterion and the material constants are

Young's Modulus:  $E = 27.4 \times 10^3$  ksi

Poisson's Ratio:  $\nu = 0.3$

Yield Stress:  $\sigma_0 = 10$  ksi

The purposes of this benchmark are two fold: 1) to check the correctness of 3/D solid element in ABAQUS for elastic-plastic analysis, and 2) to determine the sensitivity of solutions corresponding to different specified force tolerance values. The same problem was previously analyzed in [38].

The plate was represented by both 2/D (CPE8) and 3/D (C3020) solid elements, respectively. From symmetry, only one-quarter of the plate was modeled. For the 3/D elements, three layers of nodes were used. To utilize the node and element generation features in ABAQUS, the node number starts at the crack tip in the plane of symmetry and increases circumferentially

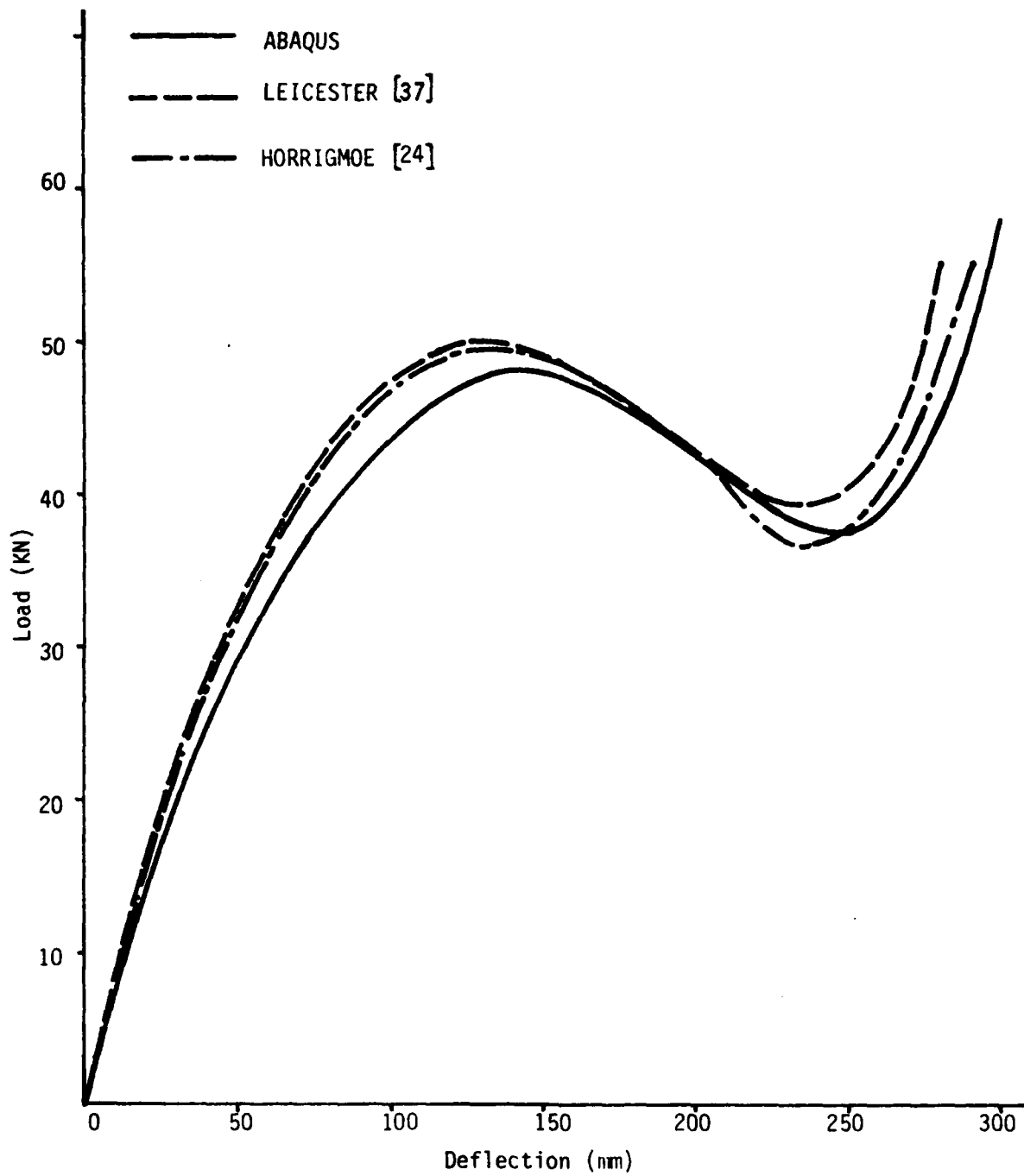


Fig. 6.15. Load vs. Deflection at the Center of Shell

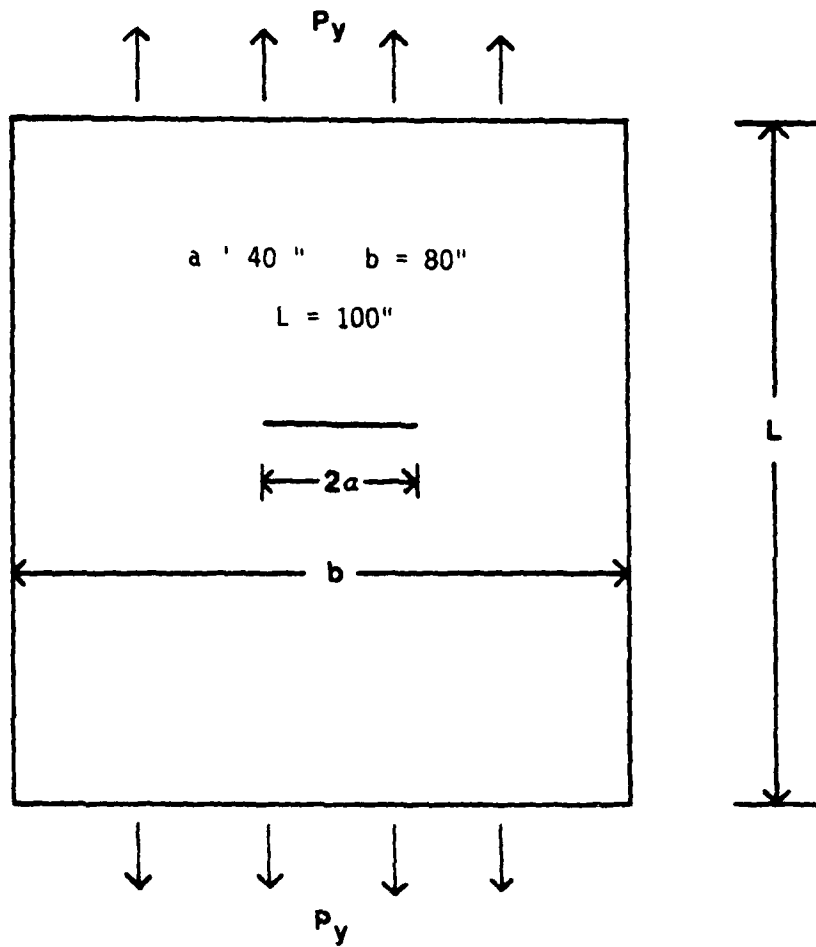


Fig. 6.16. A Centrally Cracked Plate

outward (Fig. 6.17). All nodes are restrained from movement in the thickness direction so that a plane strain state prevails. The same mesh and similar boundary conditions were used for the 2/D model.

In running this problem, the following solution parameters were specified for both 2/D and 3/D analyses:

- a) Automatic loading increment
- b) Maximum number of increments: INC = 50
- c) Maximum number of iteration cycles in an increment:  
CYCLE = 6 (Default value)
- d) Suggested number of increments: NUM = 5
- e) Force tolerance : PTOL = varied.

Several runs were made for both 2/D and 3/D models by varying the force tolerances to control solution convergence. The values of tolerance (PTOL) used are specified in Table 6.2.

Some of the analysis results corresponding to the above runs were plotted against the load for comparison, i.e.

- a) Load vs. vertical deflection of node #41 (center of crack) - Figs. 6.18 and 6.19.
- b) Vertical normal stress  $\sigma_y$  near crack tip ( $x_0 = 0.1"$  ,  $y_0 = 0.07"$ , from the tip) - Figs. 6.20 and 6.21.
- c) Horizontal stress  $\sigma_z$  (thickness direction) at the same location as b - Figs. 6.22 and 6.23.

It is seen from Fig. 6.18 that the vertical component of displacement at node #41 obtained from the 2/D model was not sensitive to the convergence tolerance. The same phenomenon can be said for the stresses (Figs. 6.20 and 6.22). On the other hand, the results obtained from the 3/D model for the

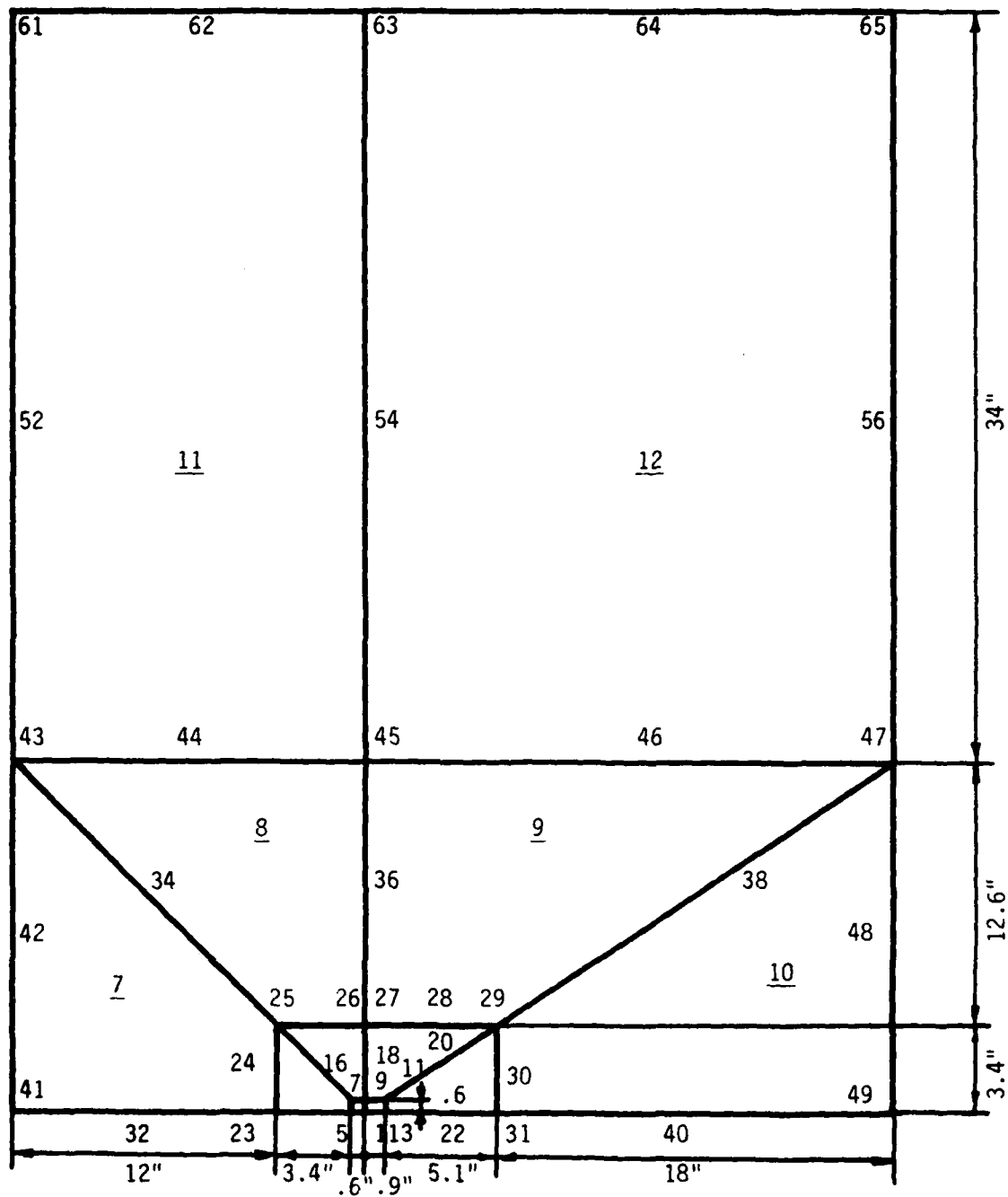


Fig. 6.17. Finite Element Model for the Cracked Plate

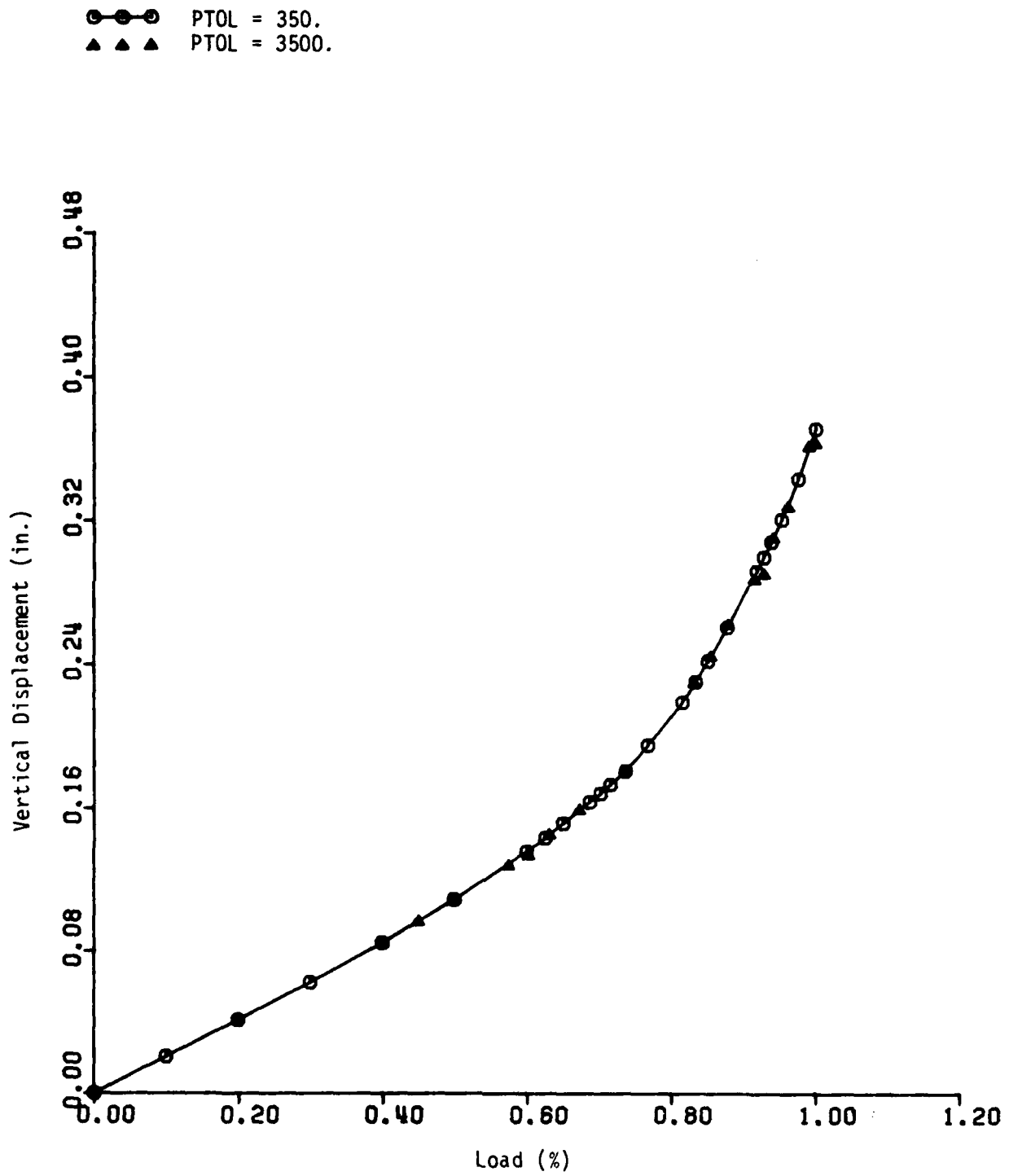


Fig. 6.18. Displacement Variations vs. Load of 2/D Model



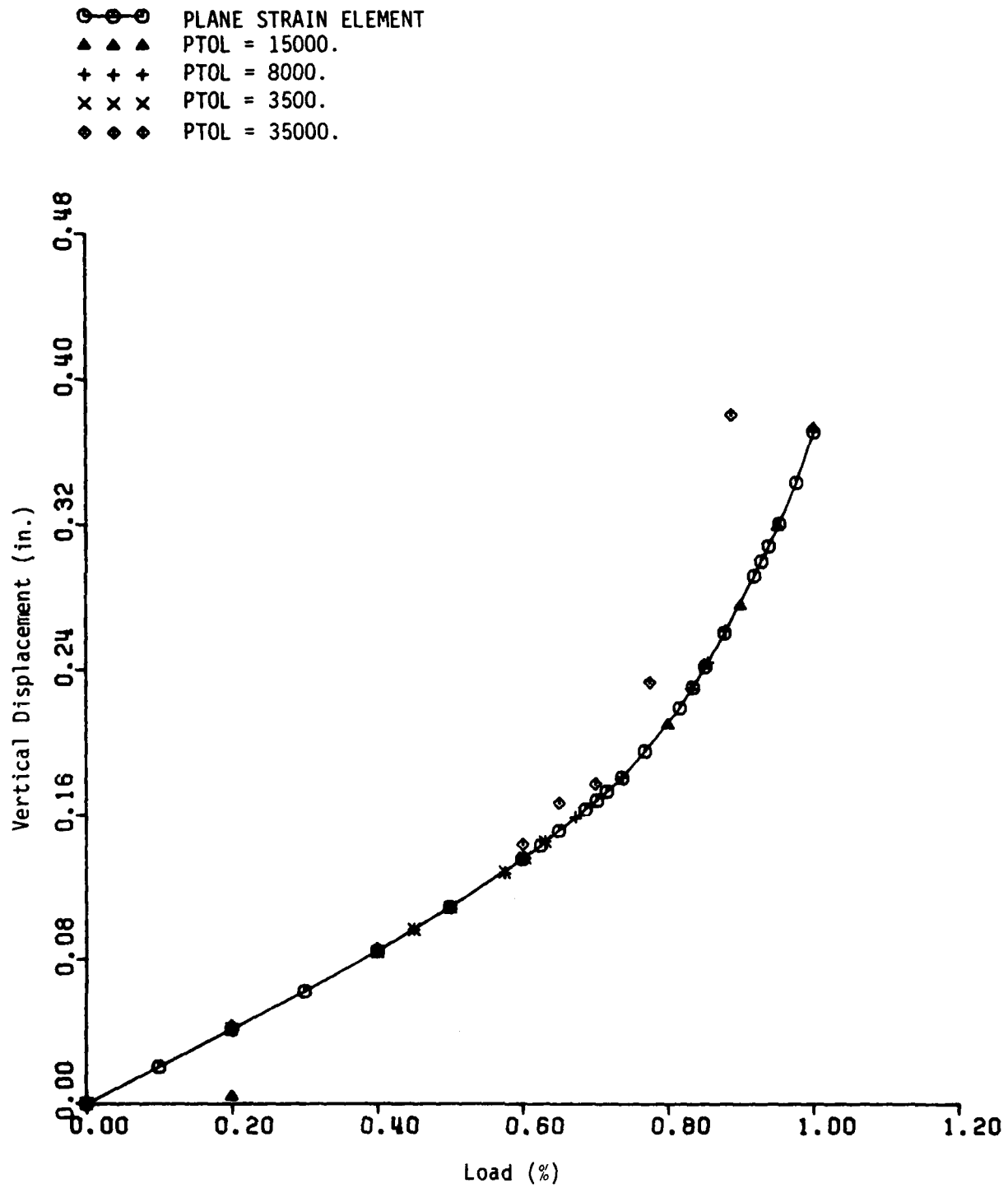


Fig. 6.19. Displacement Variations vs. Load of 3/D Model

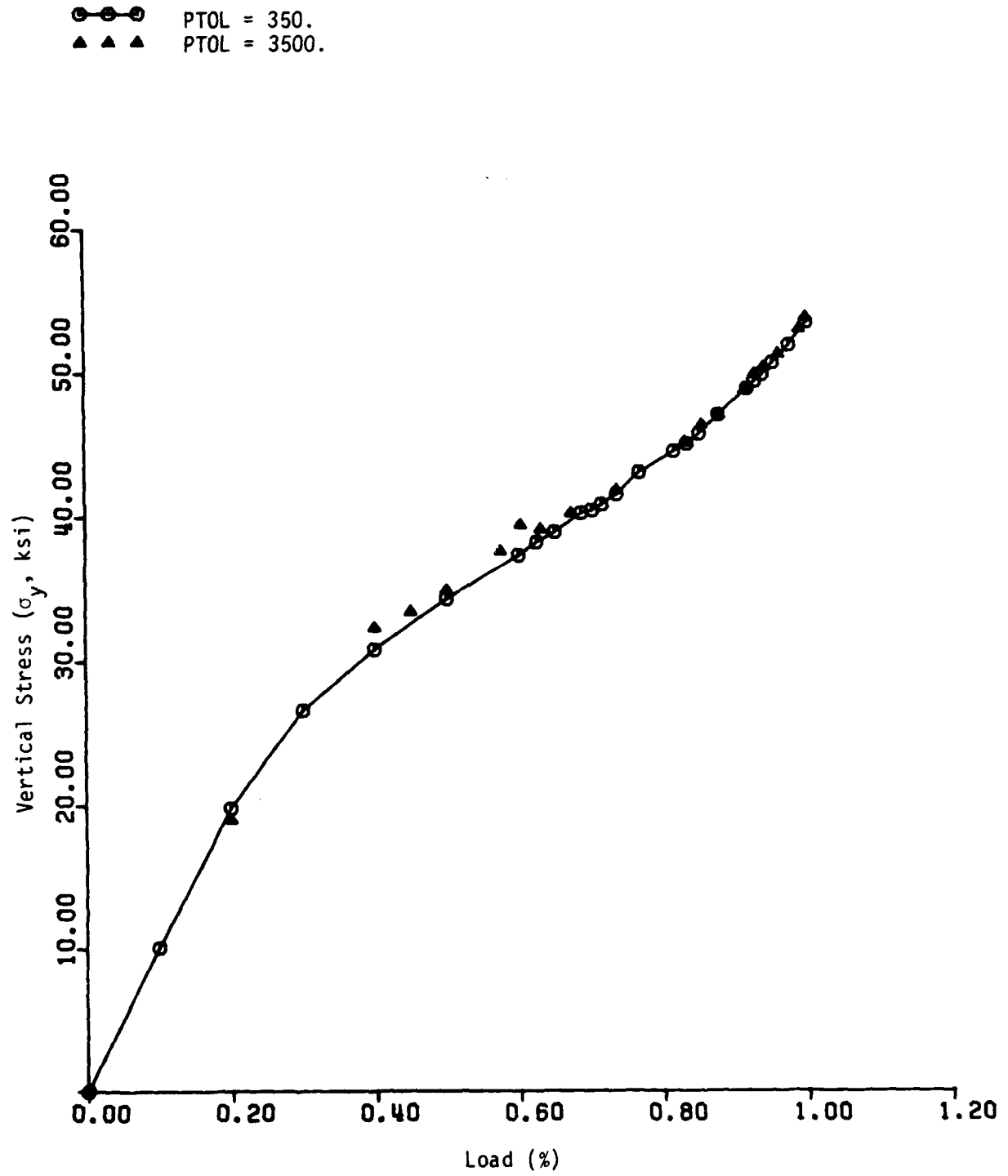


Fig. 6.20. Stress Variations vs. Load of 2/D Model

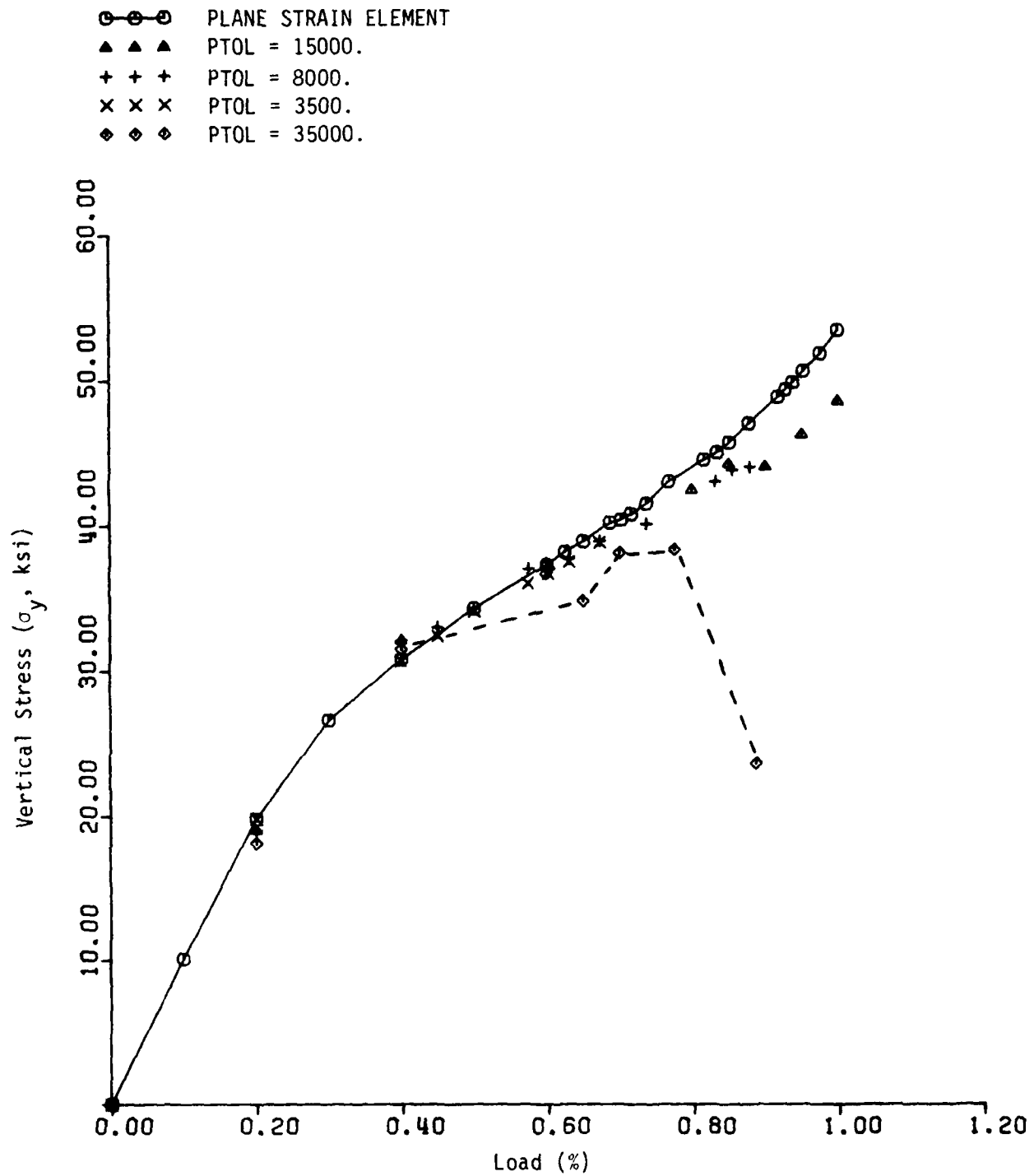


Fig. 6.21. Stress Variations vs. Load of 3/D Model

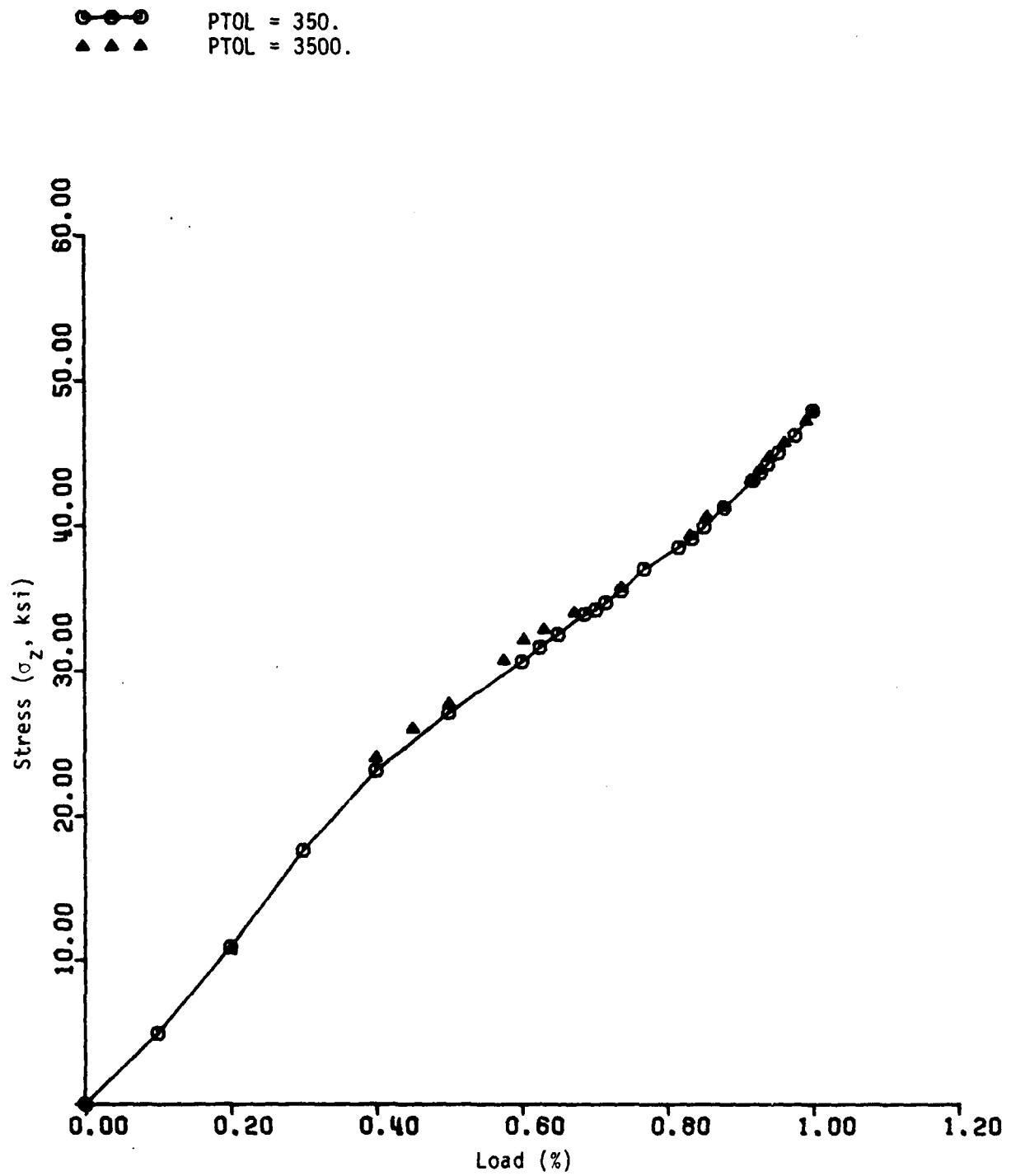


Fig. 6.22. Stress Variations vs. Load of 2/D Model

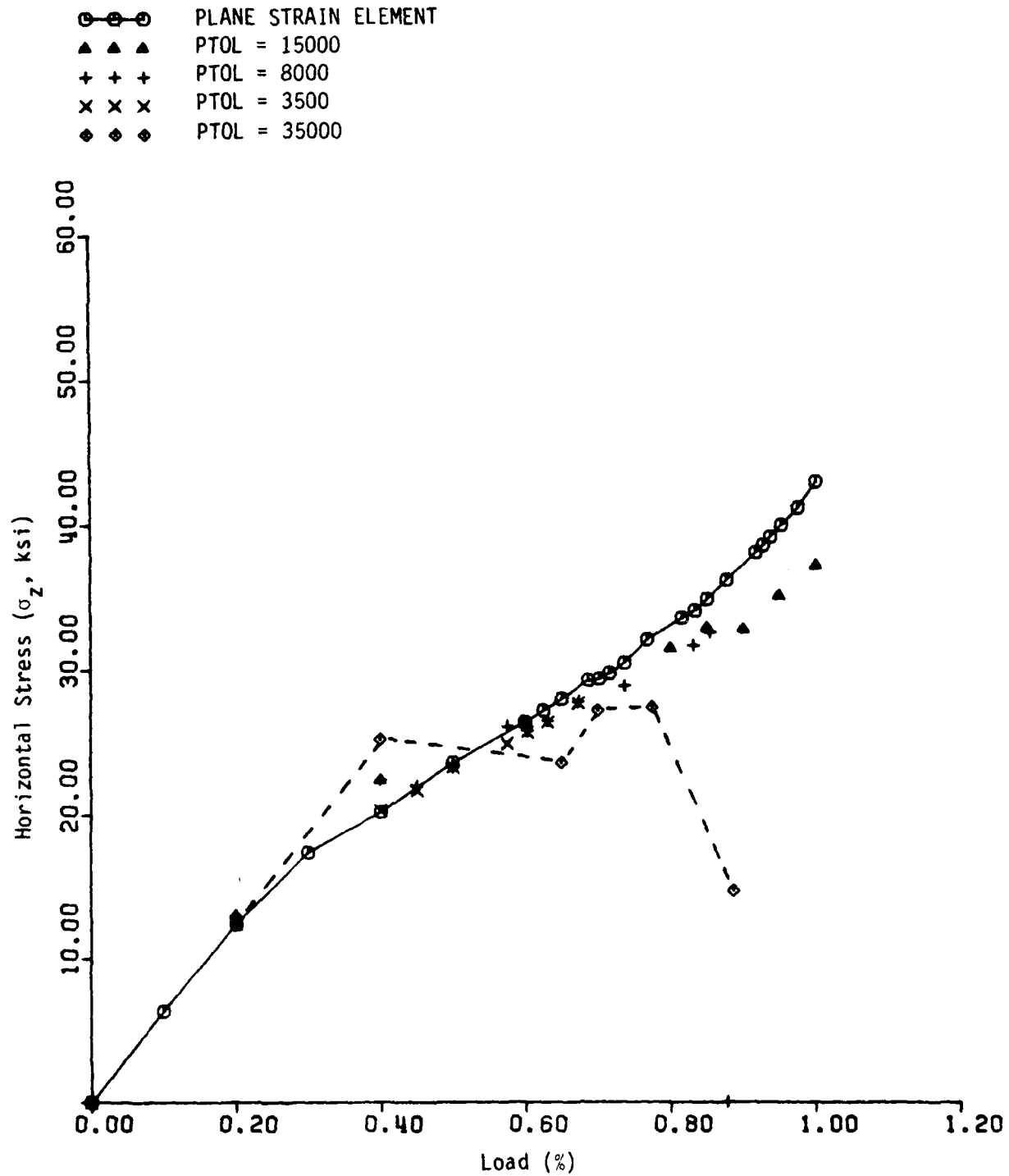


Fig. 6.23. Stress Variations vs. Load of 3/D Crack

Table 6.2      Different Tolerance Values  
for the Crack Problem

<u>Run No.</u>	<u>Description</u>	<u>Force Tolerance</u>
1	2/D Model	350 lb (.42%)*
2	2/D Model	3,500    (4.25%)
3	3/D Model	3,500    (0.17%)
4	3/D Model	8,000    (0.4%)
5	3/D Model	15,000   (0.75%)
6	3/D Model	35,000   (1.7%)

---

\*Note:

Percentage for force tolerance was calculated on the basis of maximum reaction force (absolute value) at supports.

same problem is rather sensitive to the tolerance values (note that the value  $PTOL = 35,000$  lb is only 1.7% of the maximum reaction force, well within the recommended range stated in ABAQUS manual). As the plastic zone was further spread out around the crack tip, the errors for near crack tip stresses are becoming even greater and erratic.

Another point of consideration is the computation (CPU) time required for solving a 3/D elastic-plastic crack problem. The CPU time increases significantly with the user's assigned convergence tolerance. A comparison of CPU's for different cases of 3/D runs is given in Table 6.3. Since the runs, except the case 5, were not completed at 100% of the intended loading, the CPU time for completing each problem was estimated in the last column of Table 6.3. It is seen clearly that the computer time required for analyzing this relatively small nonlinear 3/D problem is in the order of 1.5 - 4 hrs IBM CPU!

The iteration histories and automatic load cut-back in ABAQUS for the 3/D analyses are shown in Fig. 6.24. It is seen that more frequent load cut-back occurs for smaller force tolerances, and thereby it requires more iteration cycles to complete the problem.

From the experience of this example, the following comments are drawn:

- i) Analysis results for 3/D problems are sensitive to the convergence tolerance specified by the user. This phenomenon is especially acute for stresses (or strains) as opposed to the displacements. It is noted, however, that this numerical difficulty did not appear for the 2/D model.
- ii) For application problems, it is rather difficult for the user to come up with a tolerance value ( $PTOL$  or  $MTOL$ ) which would arrive at a reasonable solution accuracy and computation time.

Table 6.3 CPU Time  
vs. Tolerance of 3/D Crack Model

Case	PTOL	CPU Spent	No. of Iterations Completed	Ave. CPU Per Iteration	% of Total Load Completed	Estimated CPU
3	3,500 lb	120 min.	26	5.30 min	67%	230 min.
4	8,000	180	39	4.64	87.9%	205
5	15,000	130	28	4.62	100%	130
6	35,000	90	17	4.62	88.7%	95.3



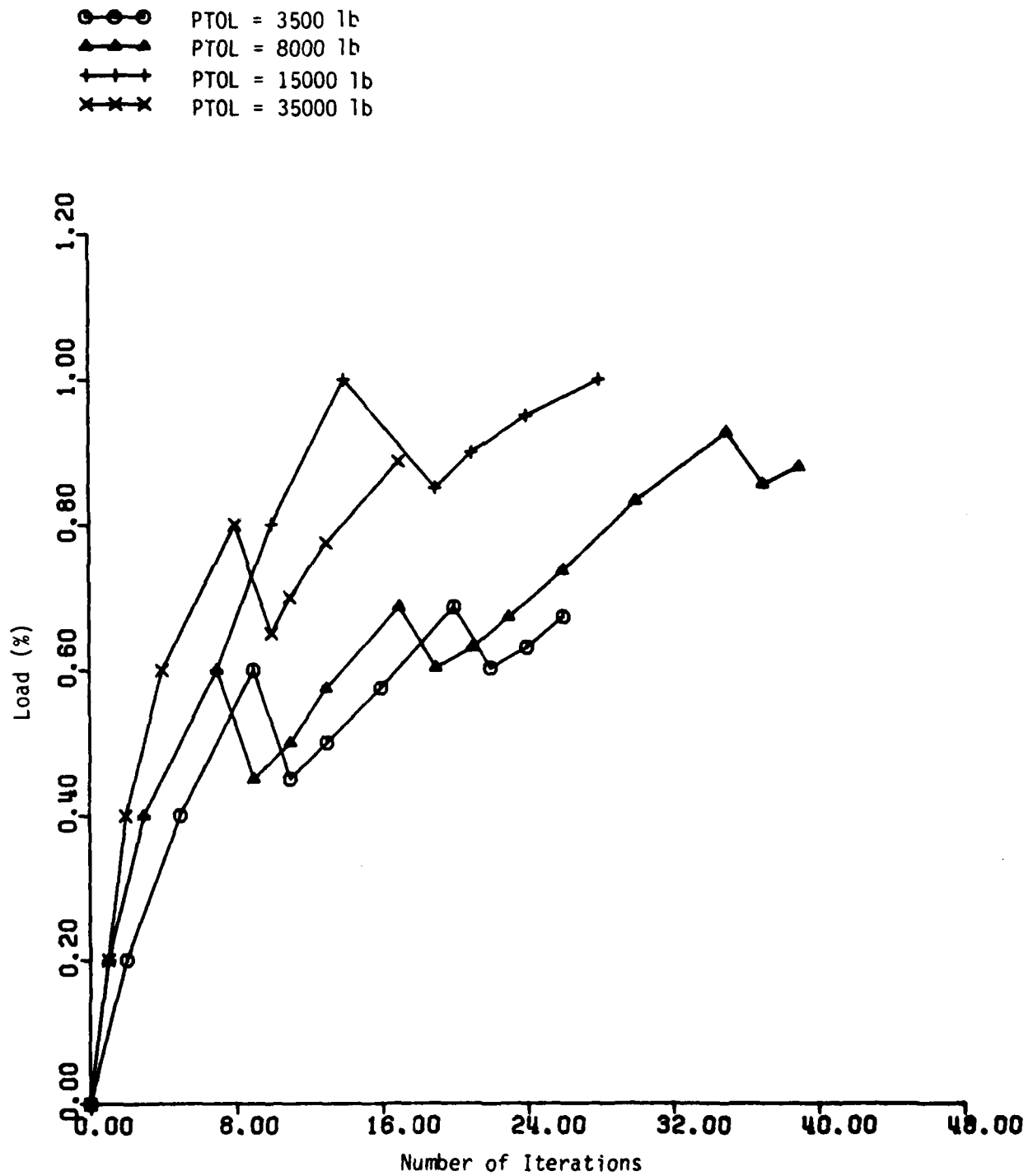


Fig. 6.24. Iteration History vs. Automatic Load Cut-Back

### 6.7 Dynamic Response of A Spherical Cap

A spherical cap subjected to uniform step pressure was considered as a benchmark to test the dynamic algorithms being used in ABAQUS. The same problem was previously analyzed by Bathe, Ramm and Wilson [39]. For the present study, the following three cases were considered:

Case 1. Linearly elastic material and small deformation

Case 2. Elastic-plastic material and small deformation

Case 3. Elastic-plastic material and large rotations

The primary purpose of this benchmark is to study the sensitivity of solution convergence to the parameters as below:

- i) Size of time increment  $\Delta t$
- ii) Artificial damping coefficient  $\alpha$
- iii) Convergence tolerances PTOL and HAFTOL.

In addition to ABAQUS runs, analyses were also performed using ADINA for the purpose of comparing results.

For case 1, i.e. linearly elastic, small deformation analysis, the material constants are

Young's modulus  $E = 10.5 \times 10^6$  psi

Poisson's ratio  $\nu = 0.3$

Density  $\rho = 2.45 \times 10^{-4}$  lb. sec<sup>2</sup>/in

The solution parameters used for ABAQUS and ADINA are shown in Table 6.5 by 10-axisymmetric elements and 63 nodes. The results obtained from both ABAQUS and ADINA are plotted in Fig. 6.25. Solutions from the two programs agree quite closely. Although the total number of time increments required for ABAQUS is only one-half of that needed by ADINA in order to achieve the same

Table 6.4 Solution Parameters

	<u>ABAQUS</u>	<u>ADINA</u>
Time integration	Hilber-Hughes operator $\alpha = -.05$	Newmark operator $\alpha = 0$
Convergence control	Residual Force: HTOL = 4000 lb.	Residual Energy ETOL = $10^{-3}$
Time Increment	$\Delta t = 10^{-4}$ sec.	$\Delta t = 0.5 \times 10^{-5}$ sec.

---

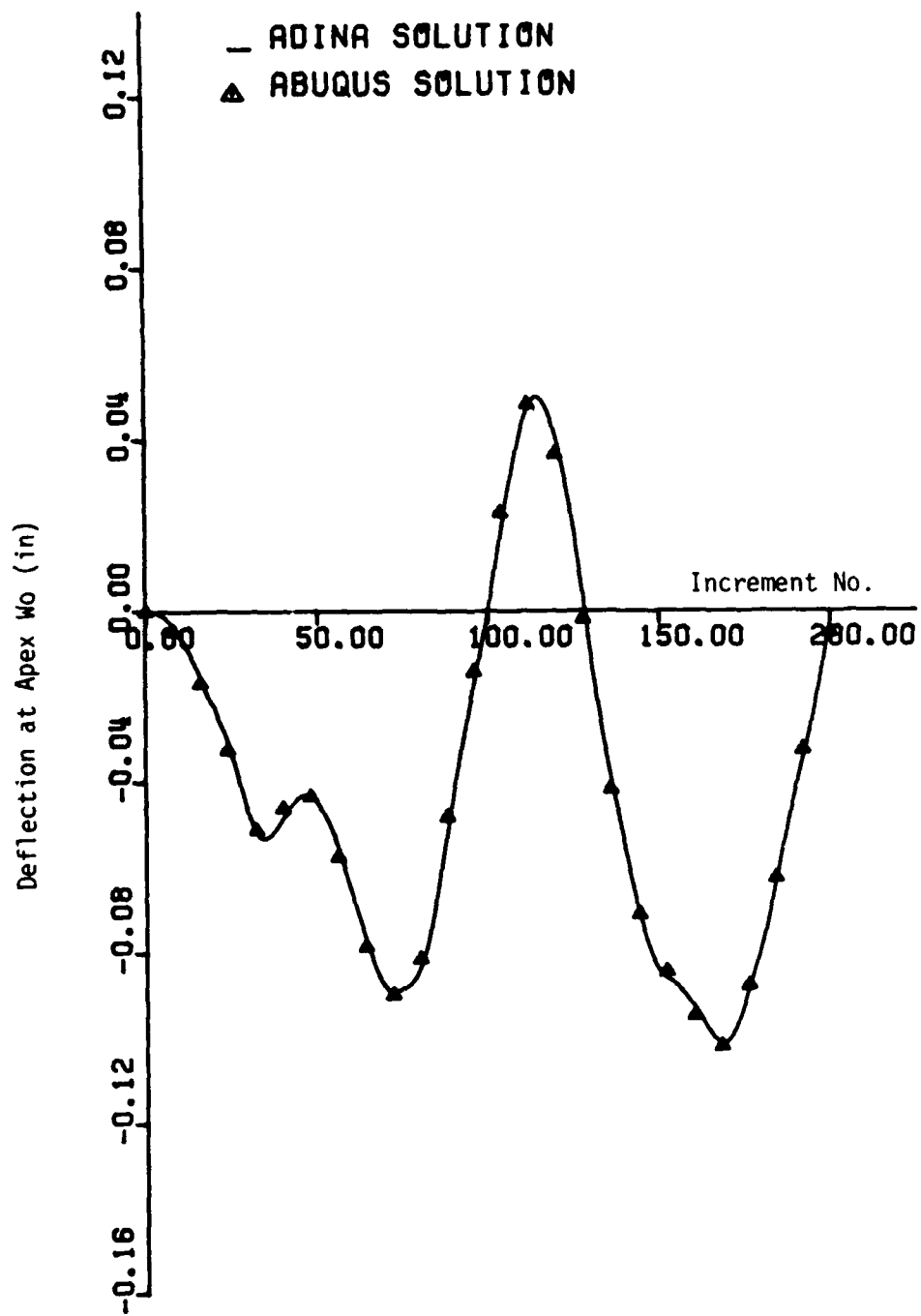


Fig. 6.25. Comparison of Linear Response of a Spherical Cap Between ABAQUS and ADINA

order of numerical accuracy, the actual CPU time of ABAQUS for this small problem is more than five times that of ADINA. Although ABAQUS appears to be slower than ADINA in handling small problems, it would be unfair to make a definite statement in regard to their relative numerical expediency for dynamic analysis due to the difference in their programming structure and intended purpose between these two codes.

By varying the size of time increment  $\Delta t$  but leaving other parameters in Table 6.5 unchanged, additional linear dynamic analyses were conducted to determine the solution sensitivity of ABAQUS and ADINA with respect to  $\Delta t$ . The deflection histories at the apex of the cap were plotted in Fig. 6.26 for ABAQUS and Fig. 6.27 for ADINA, respectively. It is seen that ABAQUS solution starts to deteriorate when  $\Delta t$  was increased to  $5 \times 10^{-5}$  sec; whereas the solution from ADINA starts to deviate for  $\Delta t = 2 \times 10^{-5}$  sec. This comparison indicates that the numerical algorithm for dynamic analysis in ADINA is slightly more sensitive to the increment size  $\Delta t$  than that in ABAQUS.

The second parameter to be investigated is the use of artificial damping coefficient  $\alpha$  in ABAQUS. Three different damping values were chosen, namely  $\alpha = 0$ ,  $-.05$ ,  $-1/3$ , and the linear analyses were made with a constant time increment  $\Delta t = 10^{-5}$  sec and the direct incrementing procedure. The displacements at the apex vs. time are shown in Fig. 6.28 and the damping coefficient did not seem to cause any significant difference in results. This is, of course, expected since  $\Delta t/T$  ( $T$  = fundamental period) ratio is less than  $1/40$ , well below the range where numerical dissipation may occur [12]. However, the damping ratio appears to have a profound effect on automatic incrementing procedure in ABAQUS. For example, when the same input data were run by switching from direct to automatic procedure, solution convergence becomes extremely difficult for  $\alpha = 0$ . For this case, ABAQUS cut back the

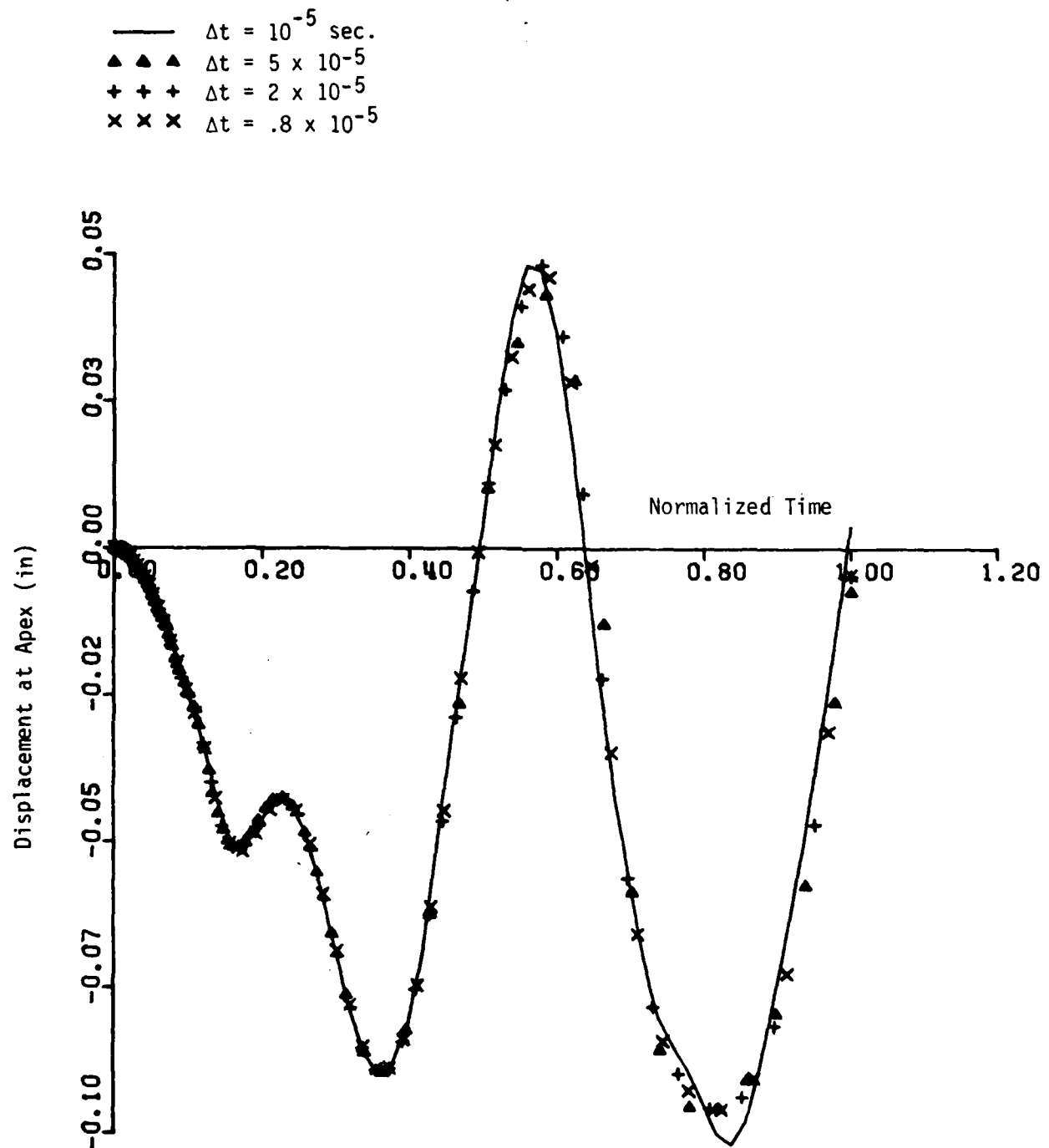


Fig. 6.26. Linear Dynamic Response of a Spherical Cap With Different Time Increments

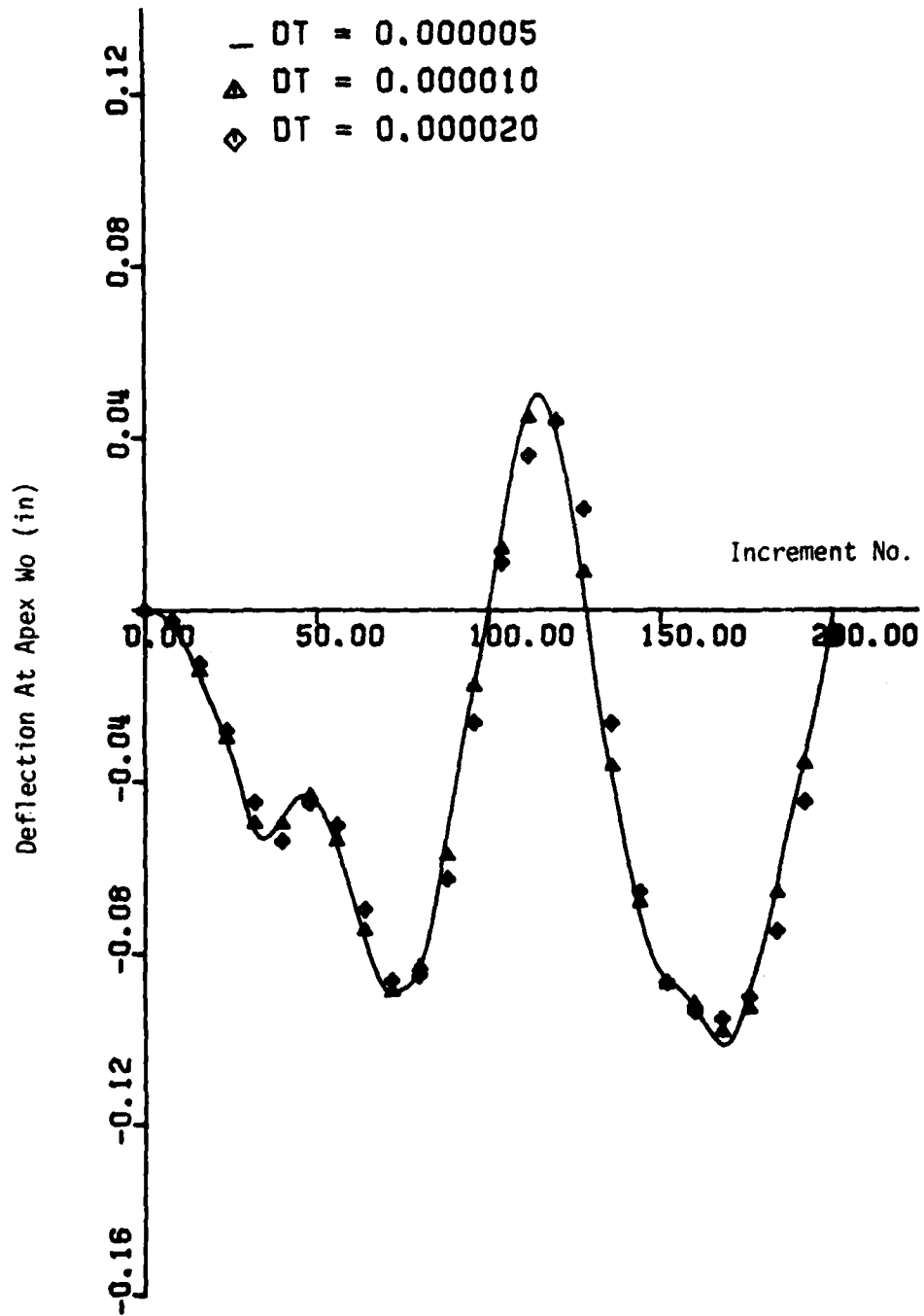


Fig. 6.27. Linear Dynamic Response of a Cap Using ADINA

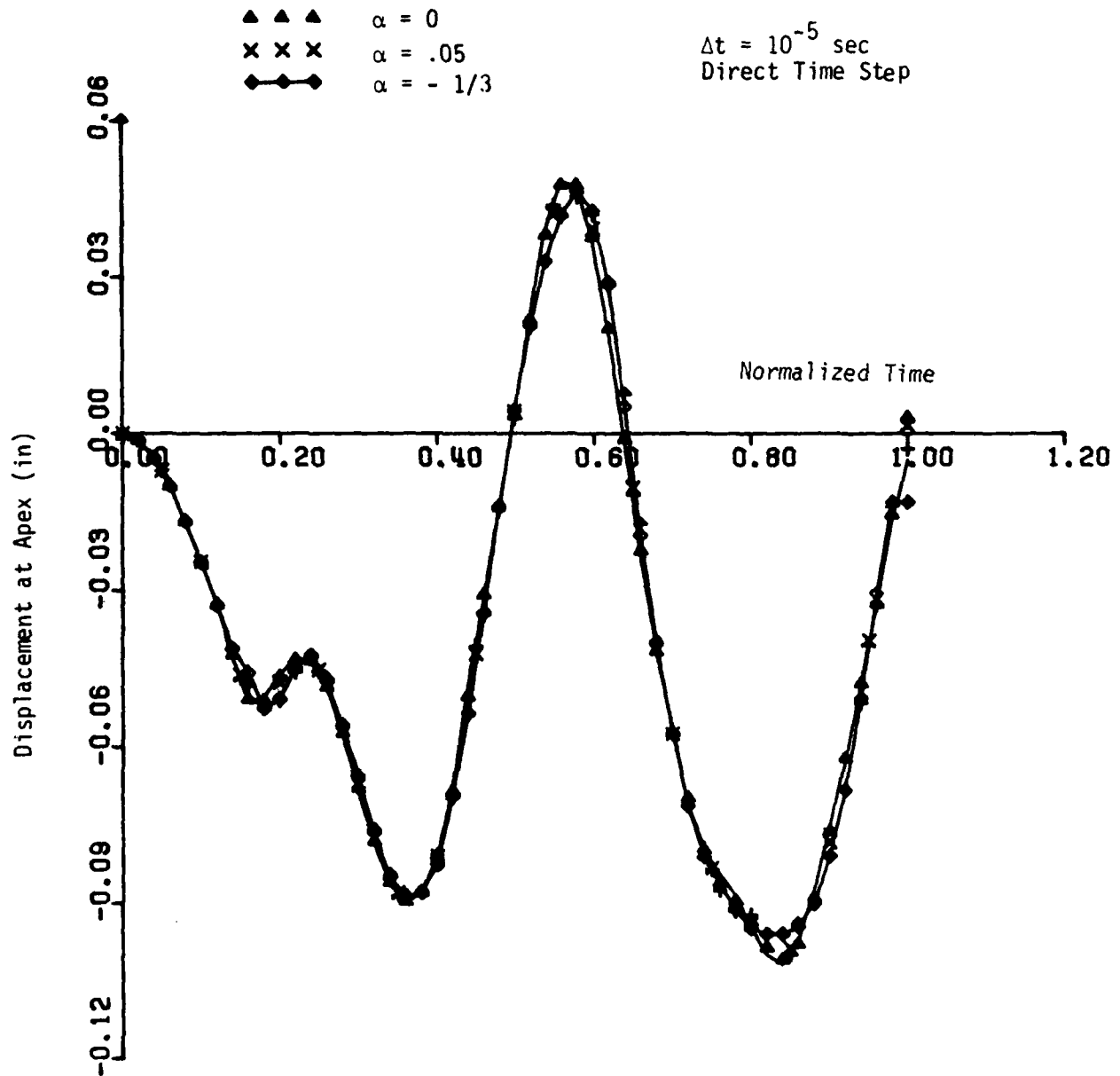


Fig. 6.28. Linear Dynamic Response of a Spherical Cap for Different Damping Ratios (ABAQUS)



suggested time increment  $\Delta t = 10^{-5}$  sec to 10 - subincrements so that the calculated half-step residue force,  $R(1/2)$ , was within the assigned tolerance. The changes in  $R(1/2)$  and the vertical deflections at the apex of the cap vs. time during the first increment cut-back are shown in Table 6.5. One can see that the maximum  $R(1/2)$  at the initial step was  $2.56 \times 10^6$  lbs, much greater than the assigned tolerance 20,000 lbs. Figs. 6.29-31 show the plots of the maximum  $R(1/2)$  vs. time for  $\alpha = 0, -0.05, -1/3$ , respectively. It is clear that the calculated  $R(1/2)$  is very sensitive to the damping  $\alpha$ . On the one hand, if a zero or small damping ratio is used, the number of time increments required for automatic procedure in ABAQUS would be enormous. On the other hand, if a large damping ratio is used, ABAQUS will increase the size of  $\Delta t$  automatically, thereby introducing significant numerical errors for the long time response as seen in Fig. 6.32, for  $\alpha = -1/3$ . The manner of step changes (i.e. time vs. increment numbers) is also shown in Fig. 6.33. Therefore, as suggested in ABAQUS manual, the best damping ratio appears to be  $\alpha = -0.05$  when the automatic incrementing is exercised. However, for direct procedure the value of damping ratio has no significant effect on the analysis results so long as  $\Delta t/T < .1$ .

For the case 2, elastic-plastic material with small deformation was considered and the material constants are

Initial yield stress  $\sigma_0 = 24$  ksi

Plastic modulus  $E_p = 0.21 \times 10^3$  ksi

(Isotropic strain hardening rule)

Solution parameters used for ABAQUS are

$\Delta T = 10^{-5}$  sec.

$\alpha = -0.05$

$R(1/2) = 20,000$  lbs.

Table 6.5 Change of HAFTOL and Vertical Displacement  
at the Apex During the First Increment Cut-Back

T(*)	DT	R(1/2)	U
1.000E-5	1.56E-7	2560000	(**)
1.560E-6	8.85E-7	706	-1.569E-6
1.040E-6	"	27100	-1.266E-5
2.026E-6	"	11500	-2.129E-5
2.822E-6	"	11500	-3.055E-5
3.917E-6	1.11E-6	31800	-5.142E-5
5.023E-6	"	27500	-8.473E-5
6.129E-6	"	8590	-1.261E-4
7.335E-6		12500	-1.653E-4
8.616E-6	1.38E-6	33100	-2.299E-4
1.000E-5	"	33800	-3.144E-4

(\*) T ..... Real Time

T(%)..... Normalized Time

DT ..... Time Increment

R(1/2) .. Half Residual

(\*\*) Cut back due to excessive residual

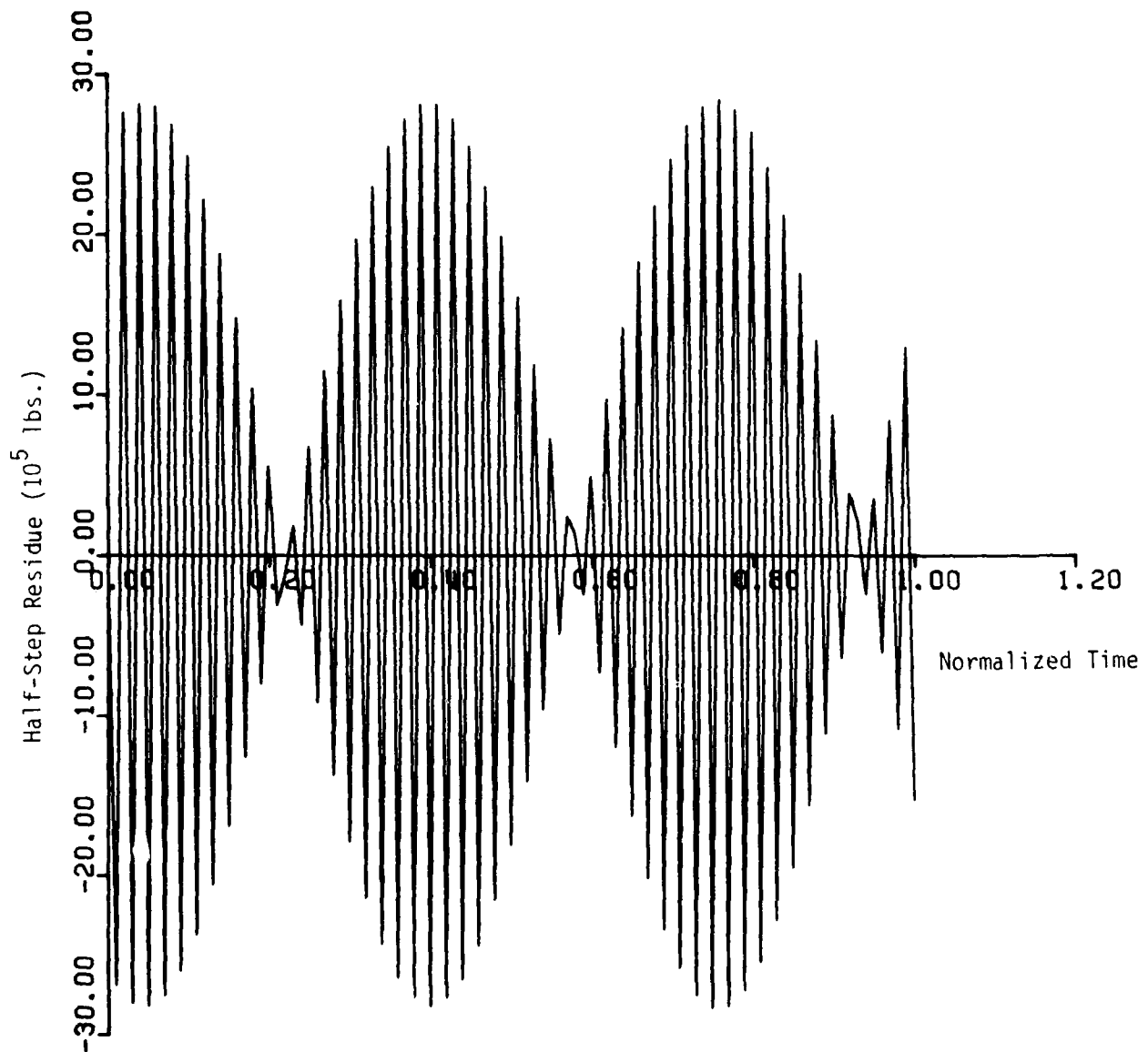


Fig. 6 29. Half-Step Residue vs. Time for  $\alpha = 0$

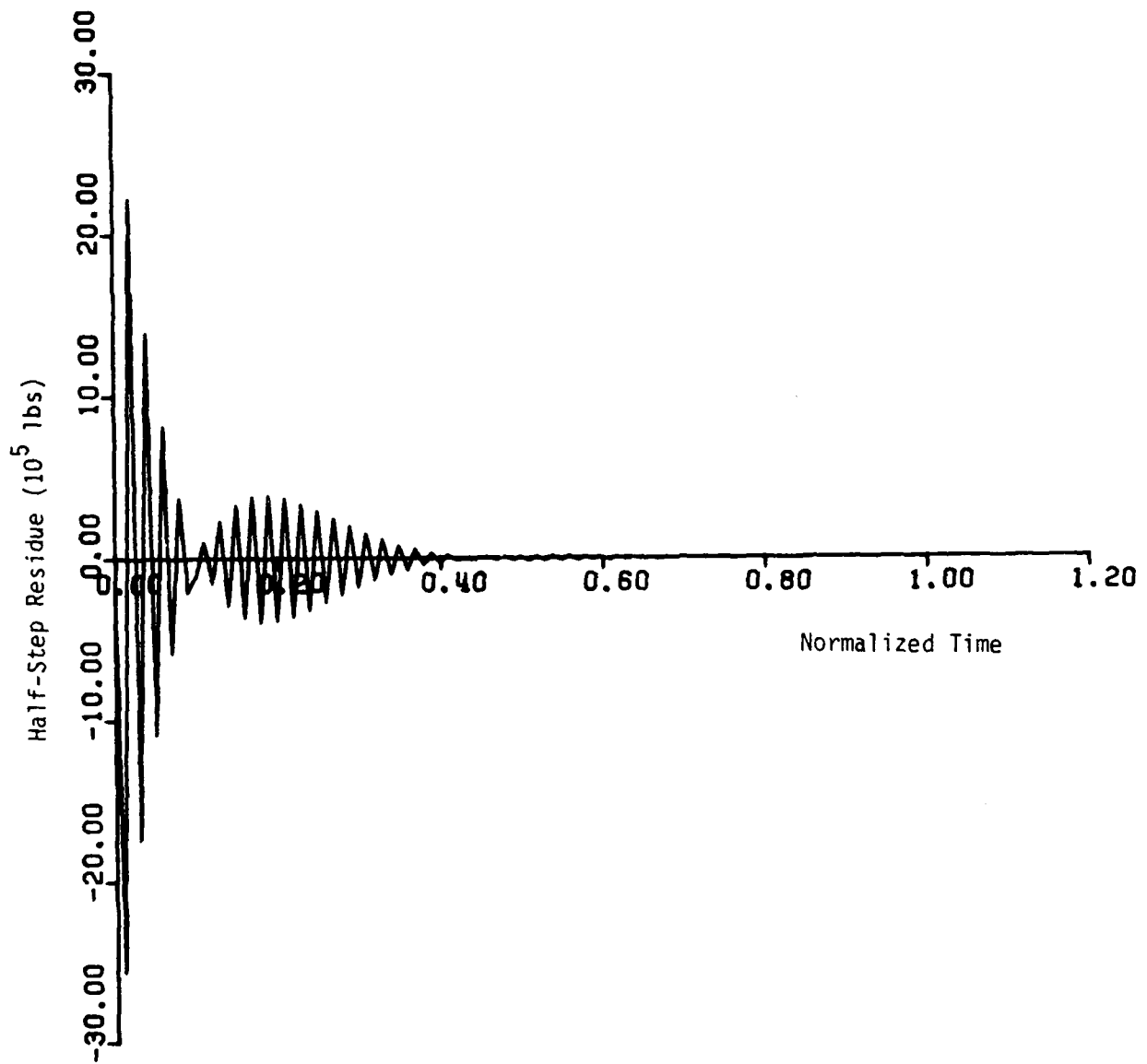


Fig. 6.30. Half-Step Residue vs Time for  $\alpha = -.05$

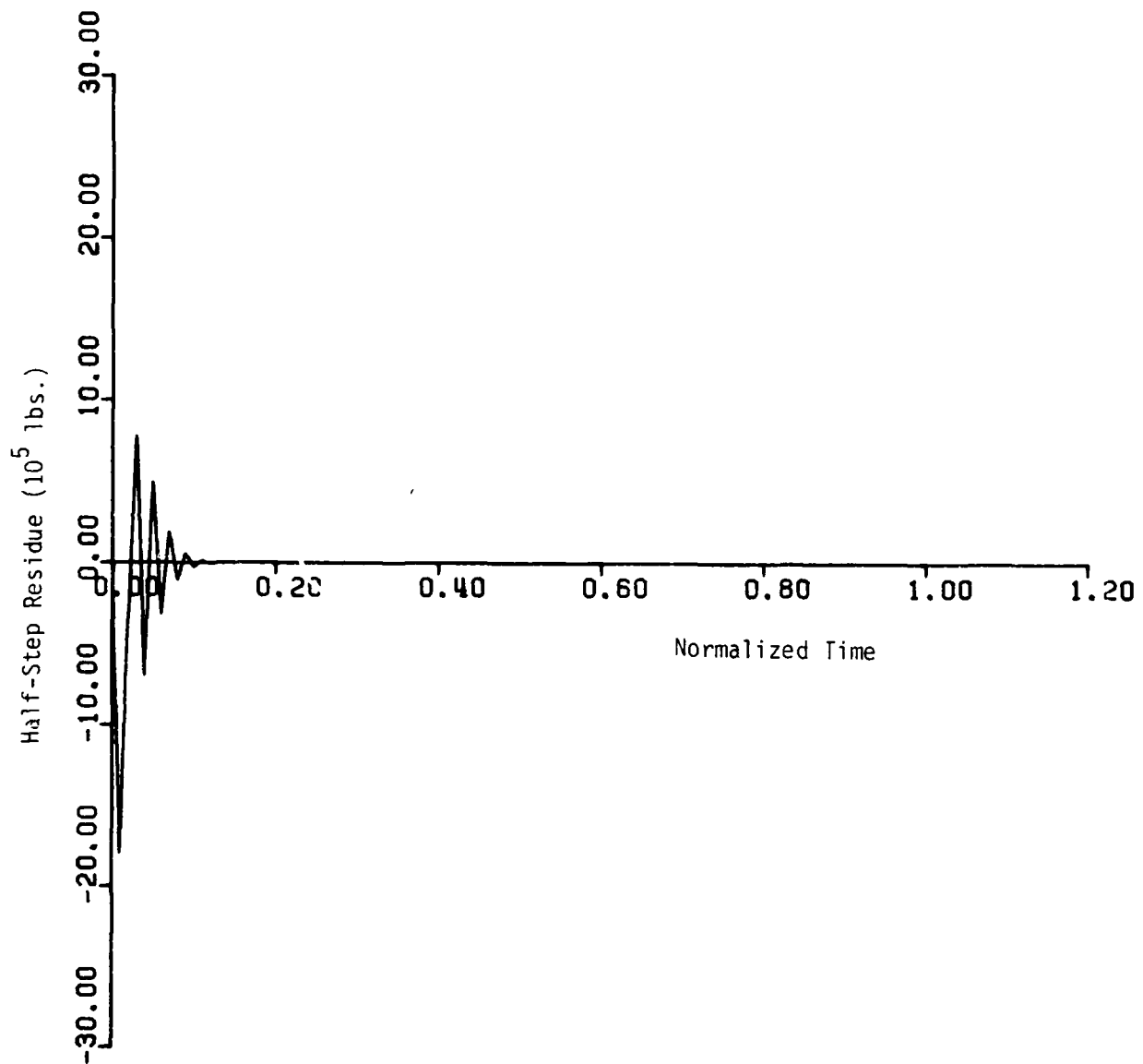


Fig. 6.31. Half-Step Residue vs. Time for  $\alpha = -1/3$ .

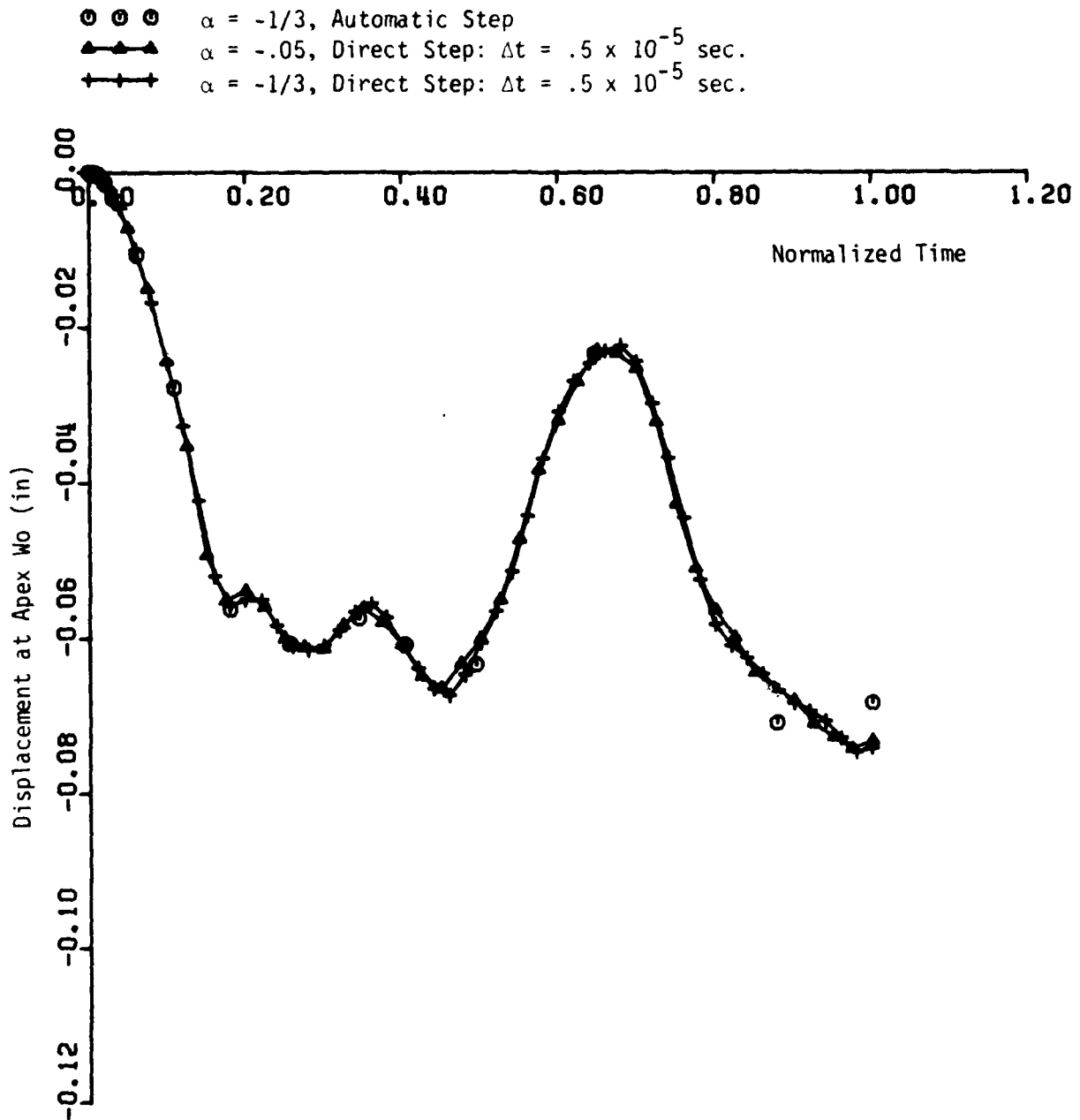


Fig. 6.32. Effect of Algorithmic Damping vs. Stepping Method

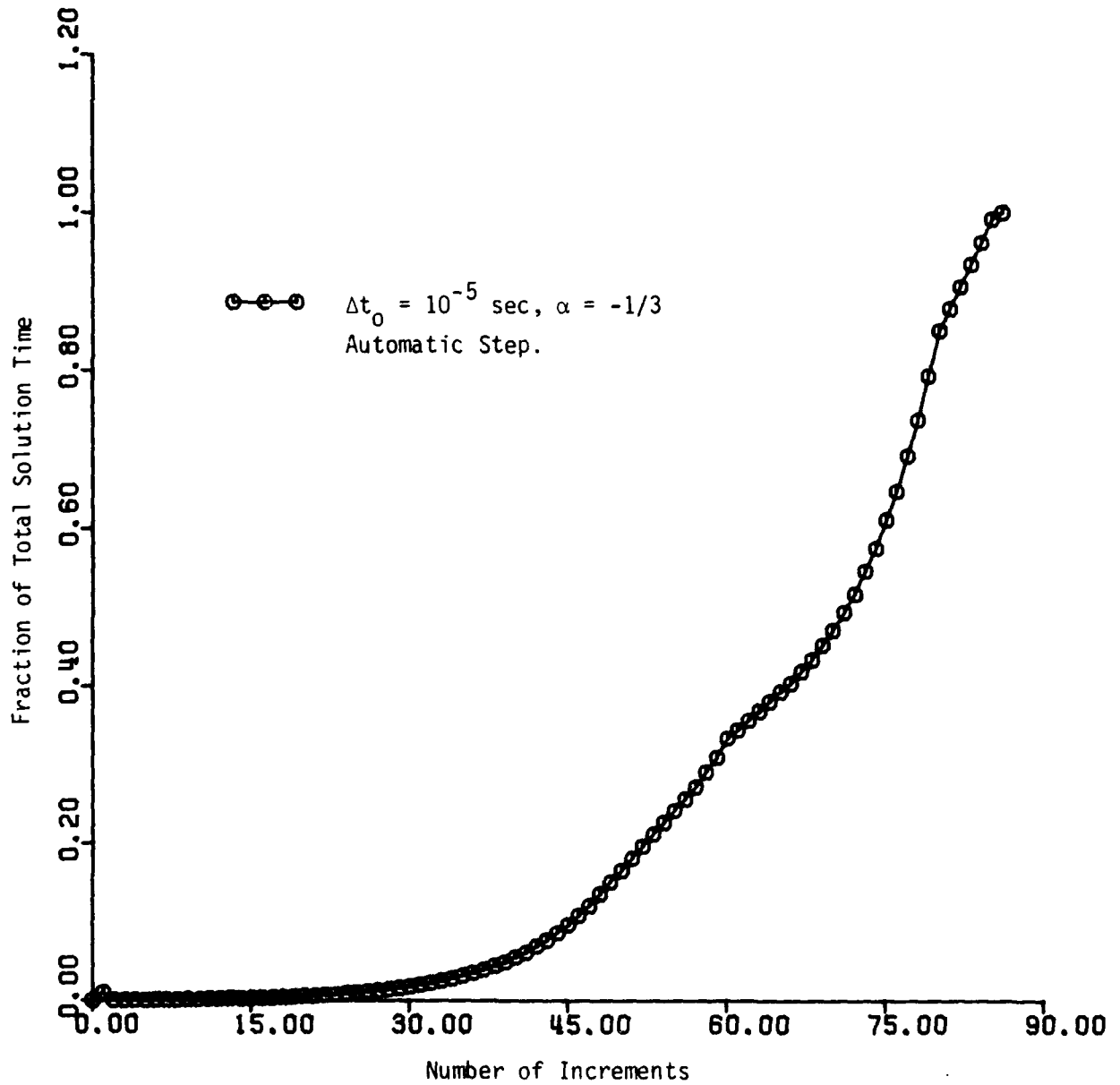


Fig. 6.33. Advance of Solution Time vs. Step Size Changes.

and direct procedure was exercised. The displacement history at the apex obtained from ABAQUS is compared with that of ADINA in Fig. 6.34. Both results appear to agree quite closely.

The third case is to consider both the geometric (large rotations) and material nonlinearities. For this case, both the automatic and direct incrementing procedures were employed and results are plotted in Figs. 6.35. Again, ABAQUS results are in general agreement with ADINA, although some minor difference can be seen. It is noted, however, that when the automatic procedure was used for ABAQUS, some unnecessary increment cut-back was experienced in the same way as the linear case. This is considered to be the shortcoming of the automatic procedure. Nevertheless, the reviewer still believes that this option is very helpful for handling a nonlinear problem in which case the convergent time increment is not known a priori.



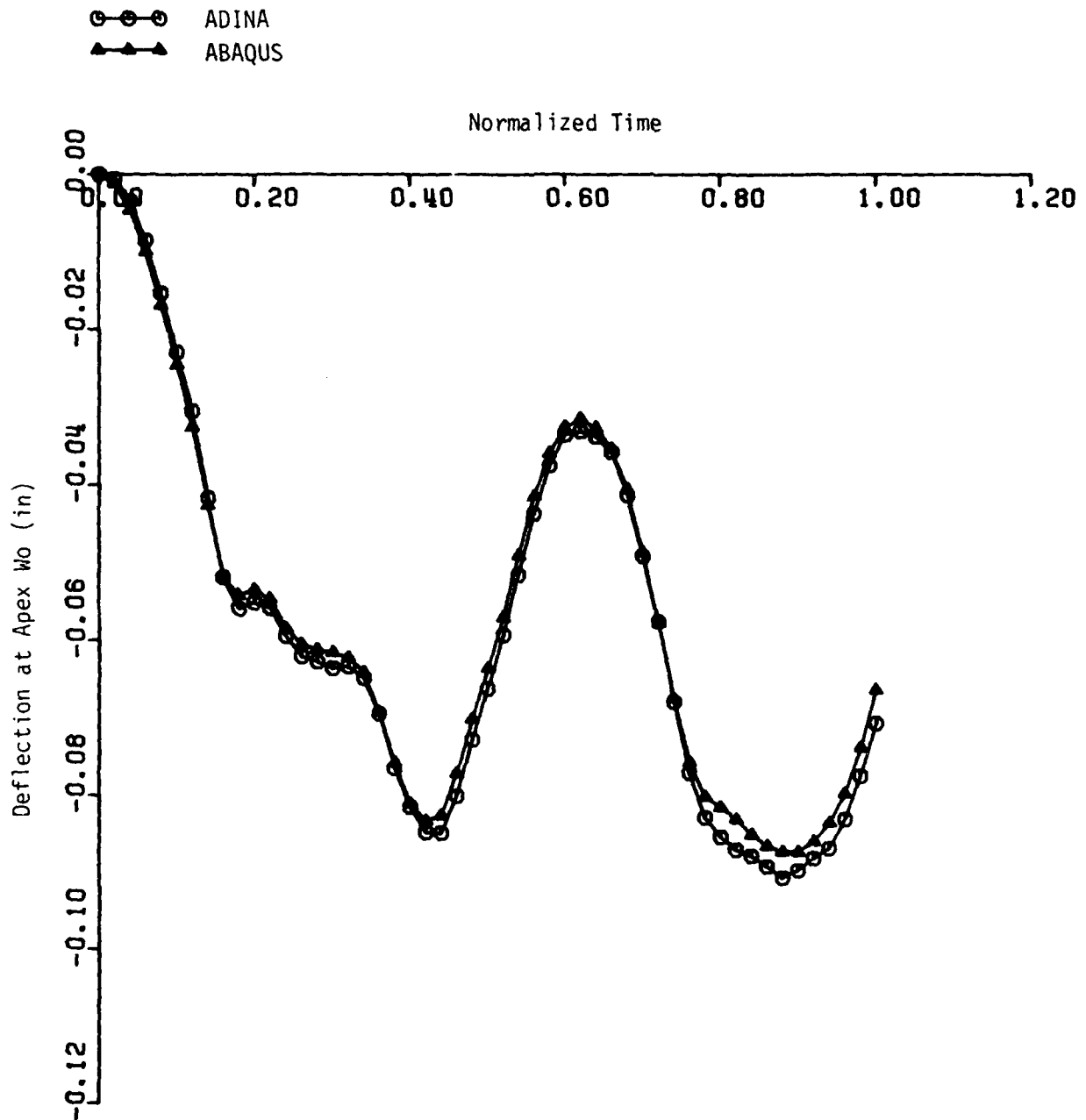


Fig. 6.34. Elastic-Plastic Deformation of Spherical Cap Using ABAQUS and ADINA

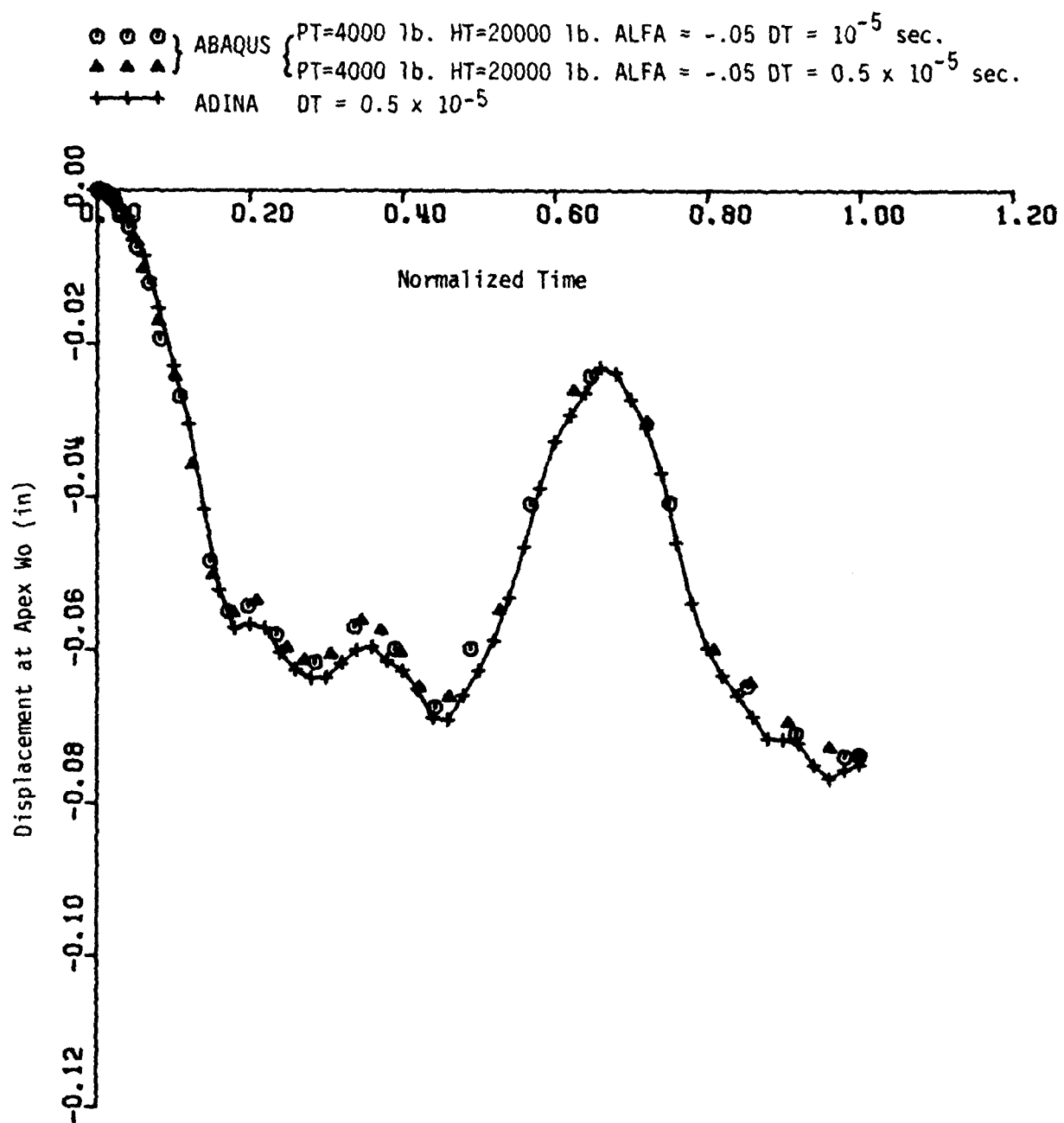


Fig. 6.35. Nonlinear Response of a Spherical Cap

### 6.8 Dynamic Analysis of A Semi-Spherical Shell

The linear dynamic response of a semi-spherical shell subjected to uniform pressure was considered as another dynamic case. The unique part of this problem is that its dynamic response involves a wide spread of frequencies and mode shapes. The motives of this benchmark are two-fold:

i) To compare the results obtained from both ABAQUS and ADINA with existing analytical solution [22], and ii) to examine the effect of numerical dissipation when a range of vibration modes are involved.

The benchmark under consideration was previously solved by Kraus and Kalnins [40]. The geometry and coordinate system of the shell are shown in Fig. 6.36. The general solution for displacement of the shell was given in [39] and it is outlined in the Appendix A. For a specific geometry and material, i.e.

$$\begin{aligned} h &= 1 \text{ in} & a &= 20 \text{ in} \\ E &= 30 \times 10^6 \text{ psi} & \nu &= 0.3 & \rho &= 1 \text{ lb-sec}^2/\text{in}^4 \end{aligned}$$

and simply supported condition, the vertical displacement at the crown has the expression

$$w = 1.33 \times 10^{-5} P_0 \sum_{i=1}^{\infty} \frac{m_i}{\Omega_i} (1 - \cos 273.86 \Omega_i t) \quad (1)$$

where  $P_0$  is the applied uniform pressure;  $m_i$ , the modal participation factor;  $\Omega_i$ , non-dimensionalized frequency defined in Appendix A. In order to obtain a sufficiently accurate solution, a total of 15-mode shapes are required. This problem was analyzed by both ABAQUS and ADINA. The finite element model used is a uniform mesh consisting of 20 - axisymmetric elements and 123 nodes. Finite element results in the form of displacement and velocity histories at the apex are compared with the analytical solution as seen in Figs. 6.37 - 38.

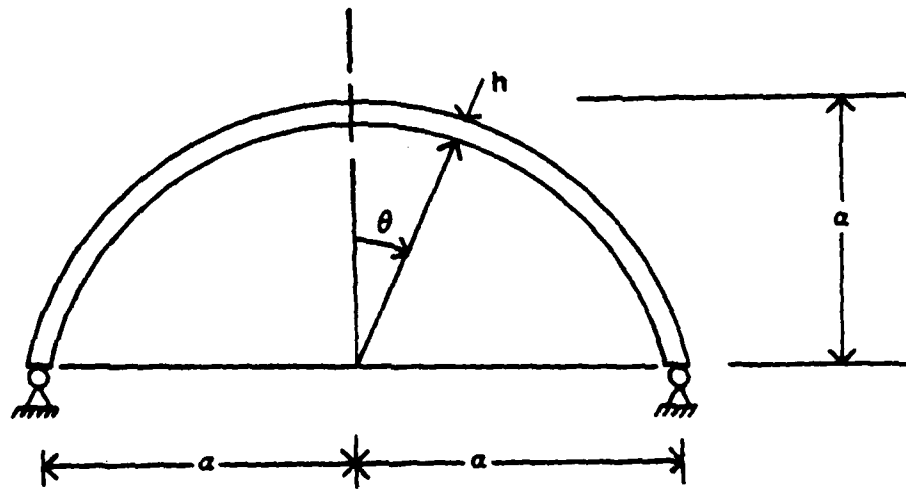


Fig. 6.36. A Semi-Spherical Shell

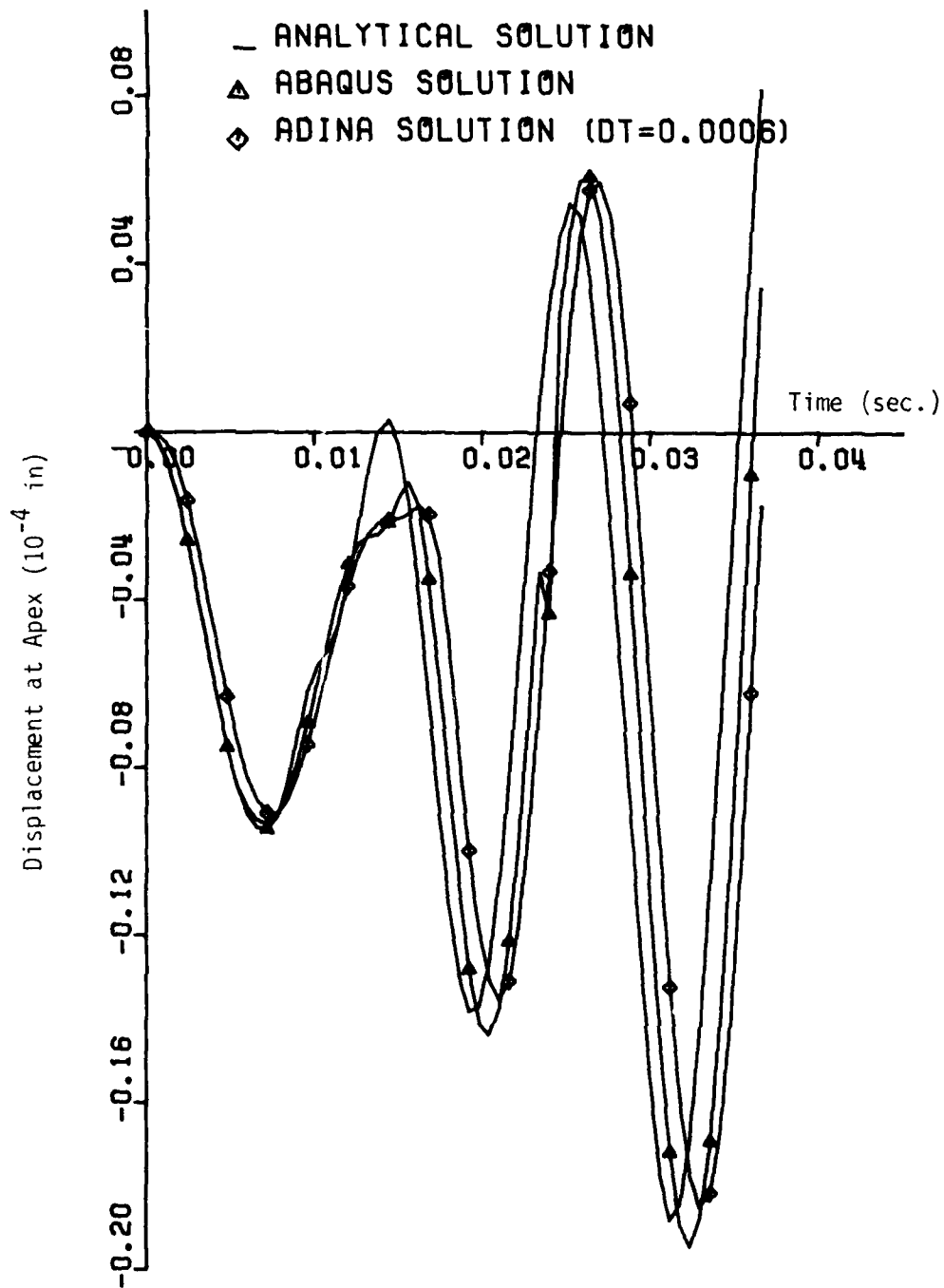


Fig. 6.37. Displacement History at the Apex of a Semi-Spherical Shell

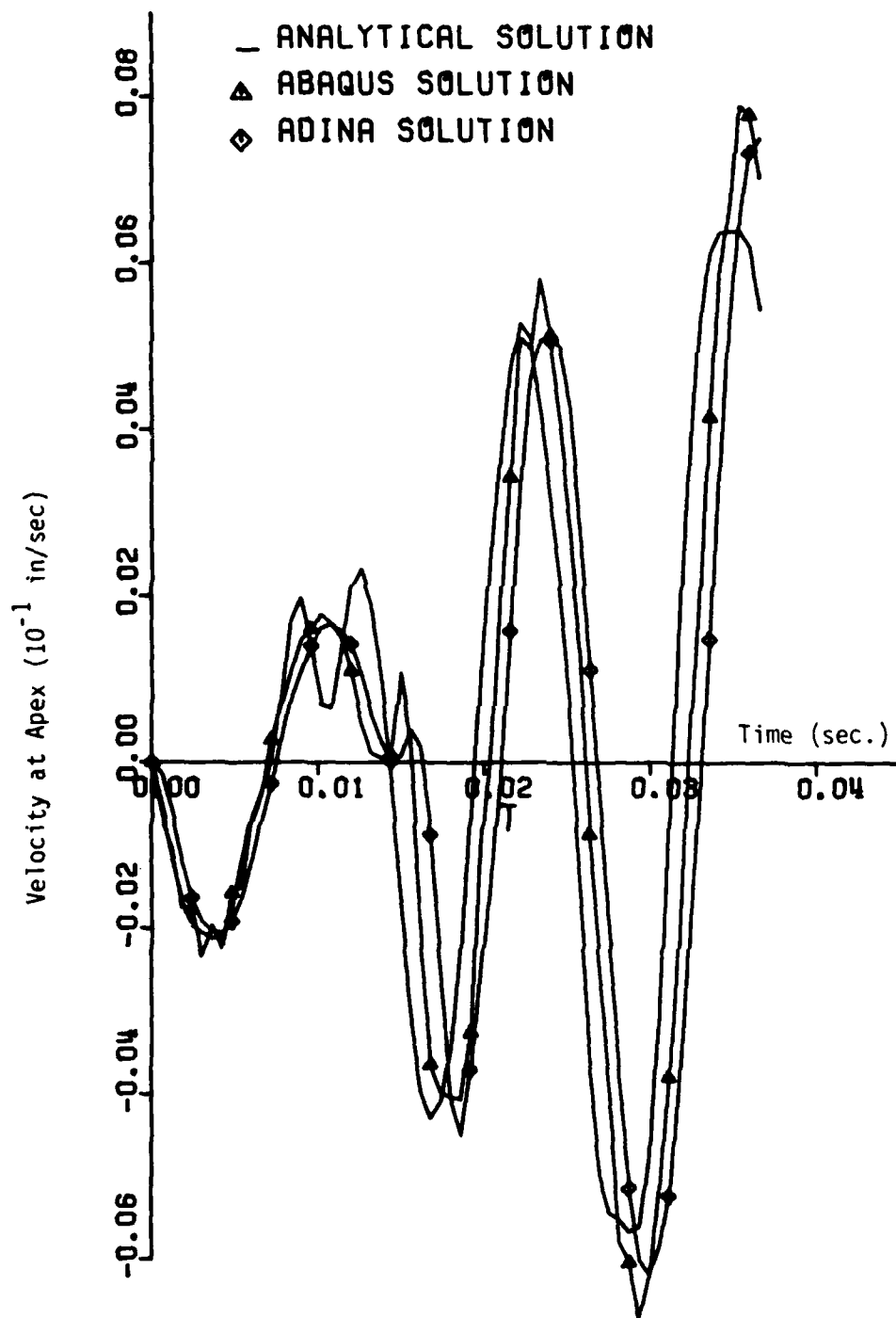


Fig. 6.38. Velocity History at the Apex of a Semi-Spherical Shell

It is seen that other than spurious oscillations and a small amount of period elongation from ADINA solution (due to Wilson  $\theta$  operator), all solutions are generally in good agreement.

Additional runs were made with ABAQUS by varying the increment size  $\Delta t$  and damping ratio  $\alpha$ , i.e.,

$$\Delta t = 3 \times 10^{-4} \text{ sec.}, \quad 6 \times 10^{-6} \text{ sec.}, \quad 12 \times 10^{-4} \text{ sec.}$$

$$\alpha = 0., \quad -1/3$$

As seen in Figs. 6.39 and 6.40, the solution is slightly affected by the increment size, but rather insensitive to the damping ratio as found out from the previously example.

#### 6.9 Longitudinal Pulse in a Prismatic Bar

For dynamic analysis, ABAQUS adopted a numerical operator called " $\alpha$  - method" proposed by Hilber and Hughes [12, 13]. This operator, as described previously, possesses a single parameter, namely  $\alpha$ , which is adjustable for controlling numerical damping. With an appropriate  $\alpha$ -value, the operator damps out the higher frequency components and preserve all the necessary low frequency modes.

To test the numerical performance of ABAQUS in dynamic analysis, longitudinal wave propagations in a prismatic bar are considered. Two different cases were analyzed by ABAQUS:

Case 1 - Elastic wave of a triangular pulse (Fig. 6.41a)

Case 2 - Elastic-plastic wave of a ramp pulse (Fig. 6.41b)

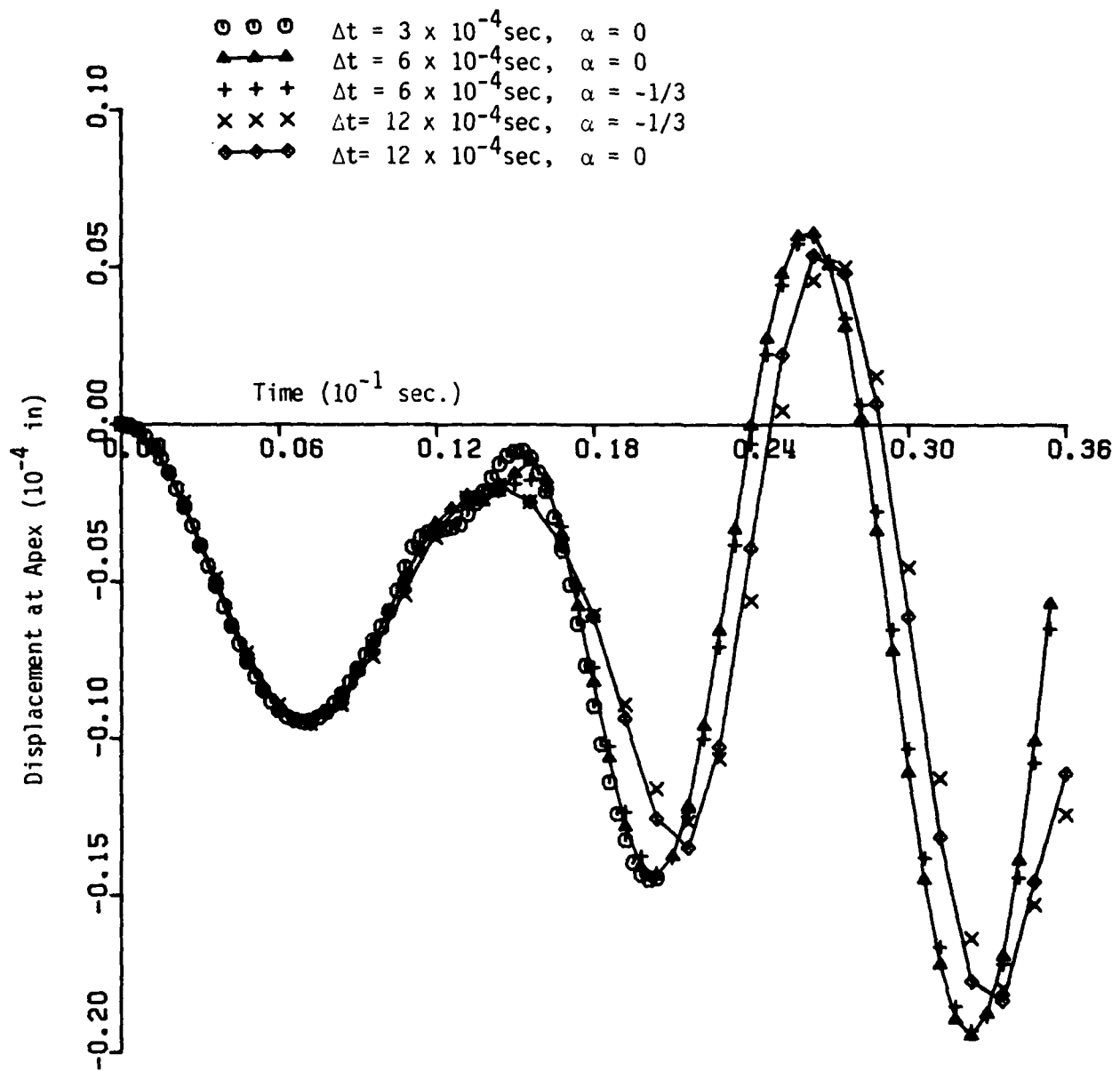


Fig. 6.39. Displacement Response vs. Different Time Increments and Damping Ratios



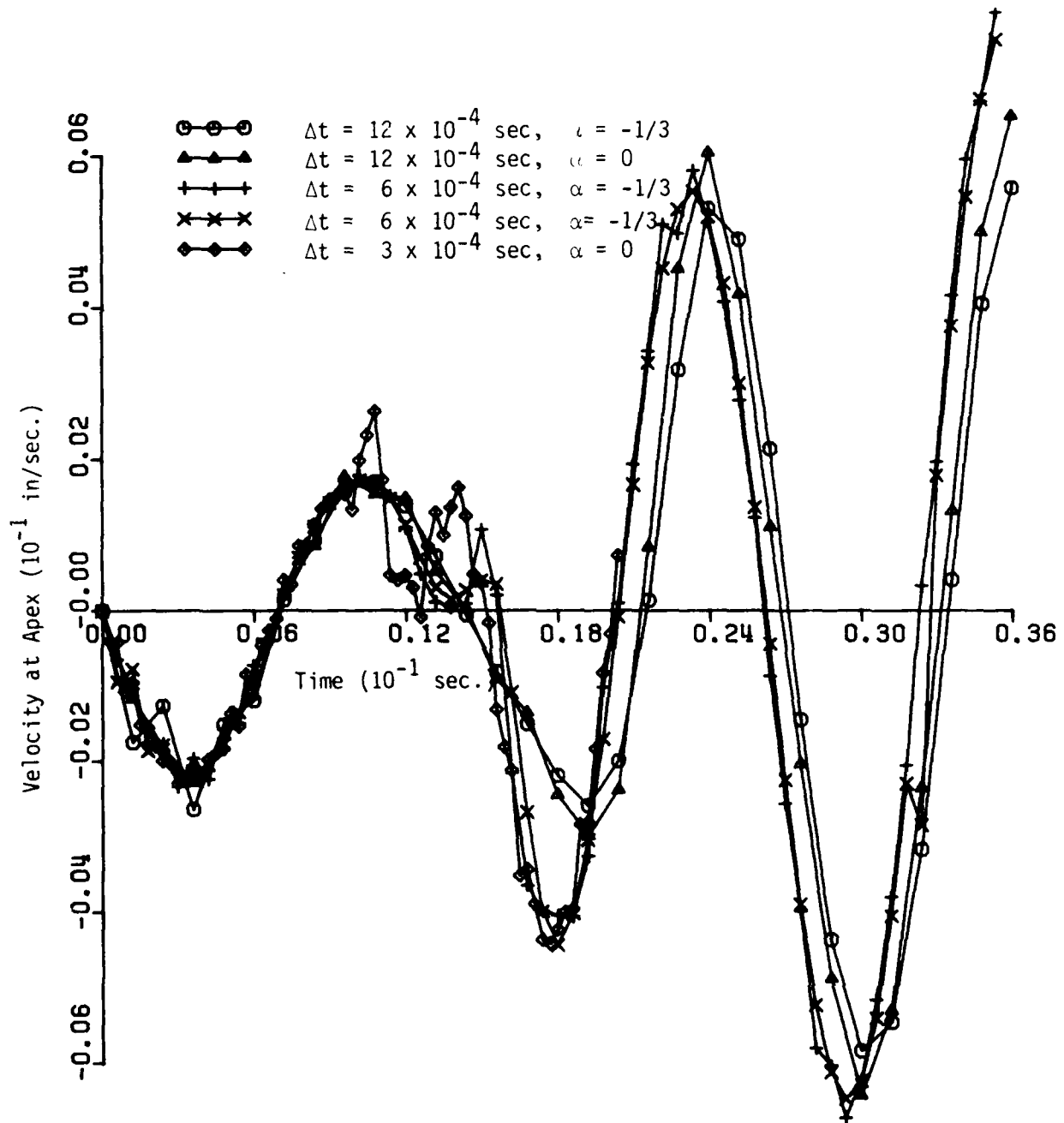
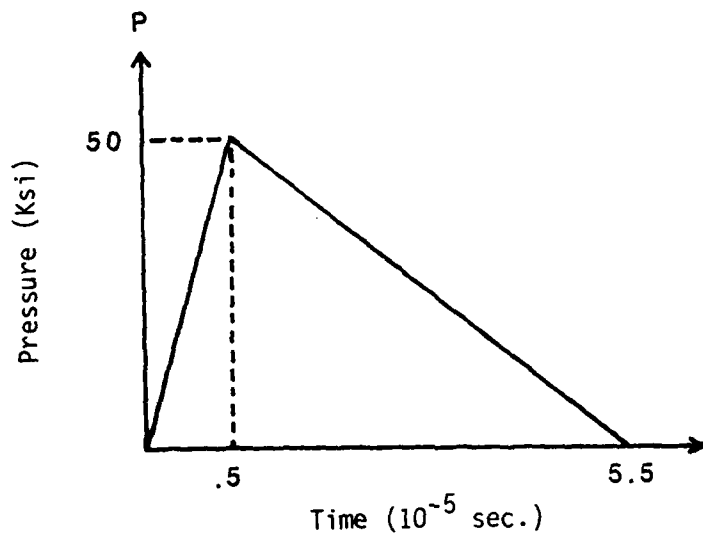
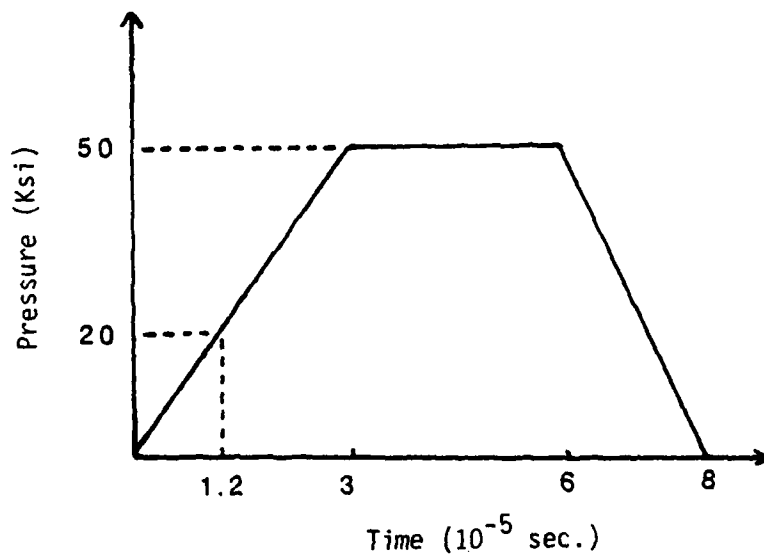


Fig. 6.40. Velocity vs. Different Time Increments and Damping Ratios



(a) Elastic Pulse



(b) Elastic-Plastic Pulse

Fig. 6.41. Applied Pressure Pulse at the End of a Prismatic Bar.

Material properties of the bar are

$$\begin{aligned} E &= 10^4 \text{ Ksi} & , & & E_p &= 2 \times 10^3 \text{ Ksi} \\ \sigma_0 &= 20 \text{ Ksi} & , & & \rho &= 2.5 \times 10^{-4} \text{ lb-sec}^2/\text{in}^4 \end{aligned}$$

To prepare the finite element model, some consideration must be given in the determination of mesh size. Basically, there should be sufficient elements to capture the profile of the wave front, namely the rising pulse. Using the elastic wave as a basis of calculation, we find

$$\text{Longitudinal wave velocity: } C_e = \sqrt{E/\rho} = w \times 10^5 \text{ in/sec.}$$

$$\text{Rising time of the pulse: } t_r = 5 \times 10^{-6} \text{ sec.}$$

$$\text{Length of the wave front: } L_f = t_r C_e = 1 \text{ in.}$$

We used 2-elements to cover the wave front, hence the mesh size in the region of propagating wave is  $\Delta x = 0.5 \text{ in.}$

The next point of consideration is the use of time increment  $\Delta t$ . For wave propagation analysis,  $\Delta t$  was suggested to be in the range:  $T_n/10 \leq \Delta t \leq T_n/2$ ,  $T_n$  = highest period of the system. For the triangular pulse, we found  $T_n = T_{200} = 5 \times 10^{-6} \text{ sec.}$  Therefore, a  $\Delta t = .5 \times 10^{-6} \text{ sec.}$  was selected for the analysis.

After the mesh size and time increment were determined, solution of this simple wave problem from AIAQUS was rather straightforward. Fig. 6.42 shows the elastic stress pulse in the bar for  $t = 30 \mu\text{s}$ . Elastic-plastic wave propagations are shown in Figs. 6.43-46 for instants  $t = 30, 60, 90$  and  $120 \mu\text{ sec}$ , respectively. It is seen that ABAQUS gave almost identical results as the analytical solutions (Appendix B).

As we consider the results of Case 2, the elastic-plastic wave consists of three parts: elastic wave front (Fig. 6.43) travelling at a speed  $C_e$ ,

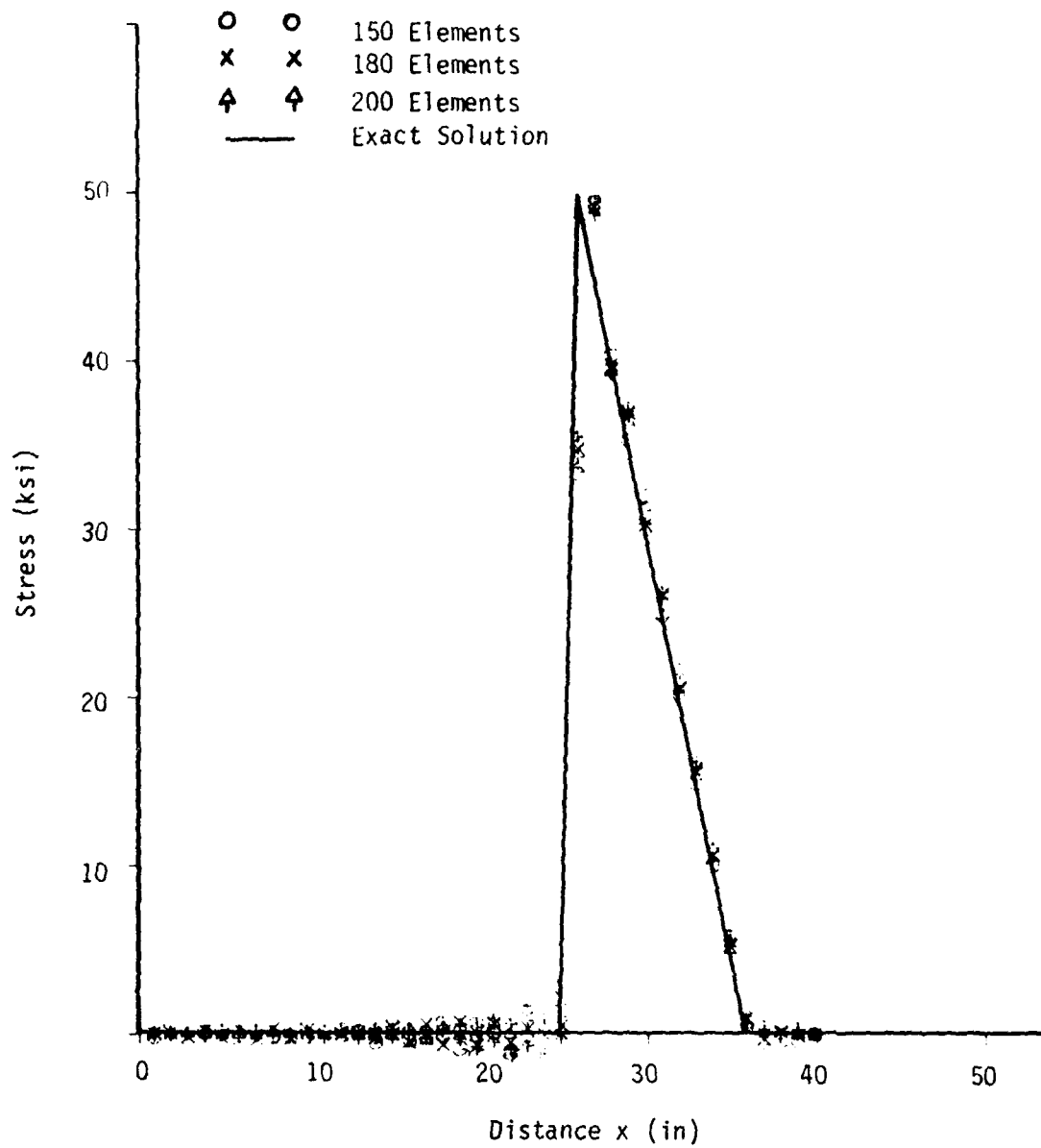


Fig. 6.42. Elastic Stress Pulse

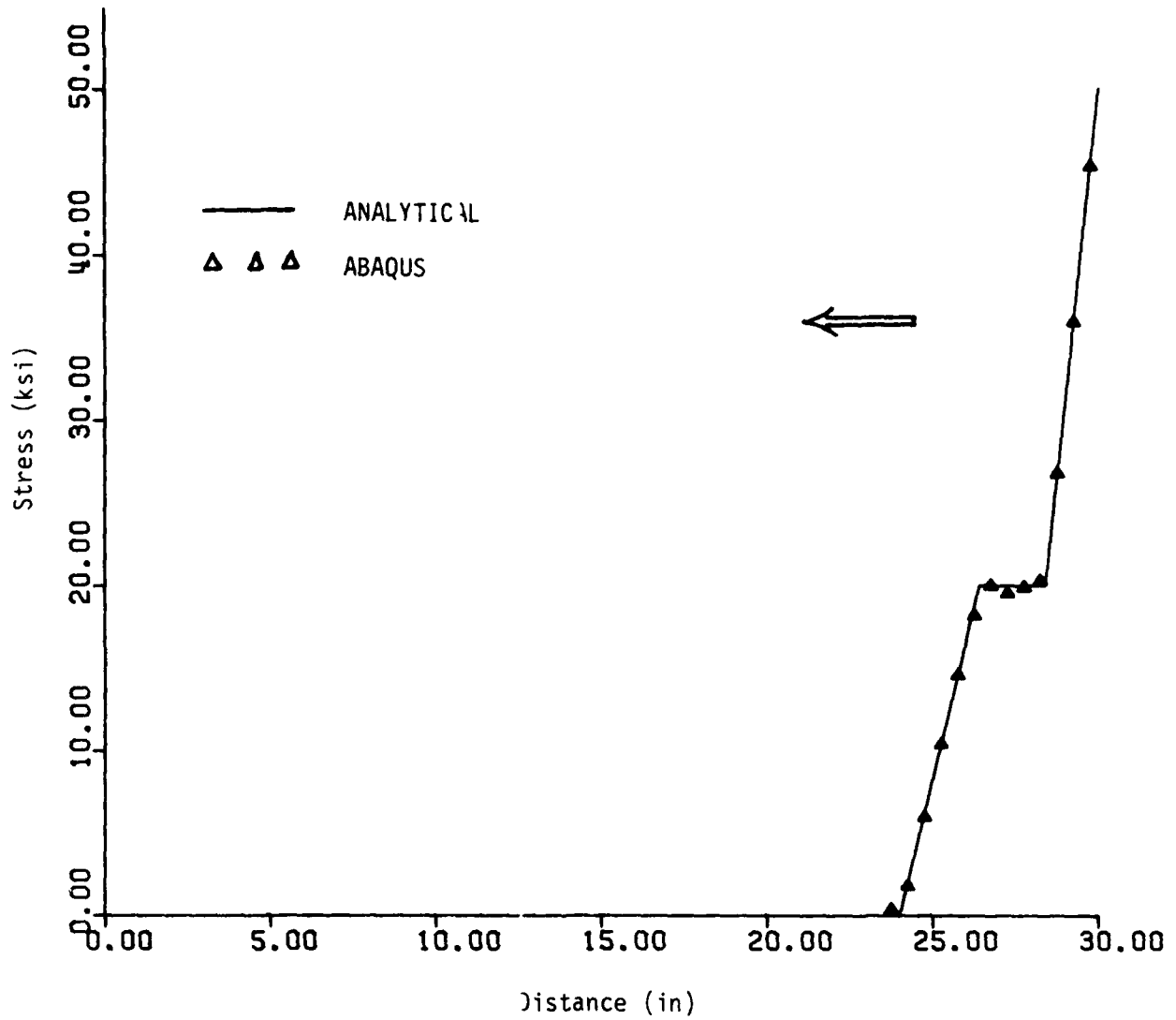


Fig. 6.43

Elastic-Plastic Pulse,  $t = 30 \mu \text{ Sec.}$

plastic wave front at speed  $C_p$  (Fig. 6.44) and elastic wave back due to plastic unloading (Fig. 6.45). At a certain point, the wave back begins to cut-off the plastic front and causes a secondary wave, as seen in Fig. 6.46, which induces a stress

$$S = \frac{1}{2} \left( \frac{C_e}{C_p} - 1 \right) (\bar{\sigma} - \sigma)$$

where  $\sigma = 50$  ksi;  $\sigma$ , stress at an instant  $t$  after plastic unloading. The secondary wave propagated both forward and backward at a speed  $C_e$ .

The same problem was previously analyzed by Hartzman and Hutchinson [23] by using 2/D 4-node elements and explicit integration scheme. In their solutions, considerable spurious oscillations were indicated in both elastic and elastic-plastic waves. From ABAQUS runs, no spurious modes were seen when a small damping ration,  $\alpha = -0.05$ , was imposed. The CPU time required for solving this small nonlinear dynamic problem was quite excessive on the IBM 370-158 :

Case 1 = 25 min., Case 2 = 17 min.

#### 6.10 Execution Time

One question that would have been asked by many users is how efficient is ABAQUS, say, as compared to ADINA? It is difficult to answer this question without some sort of qualified statement.

First of all, one must keep in mind that the computational efficiency of a finite element software is affected by several factors. These include:

- i) Program architecture and coding style
- ii) Numerical algorithm adopted
- iii) Application problem size
- iv) Hardware environment

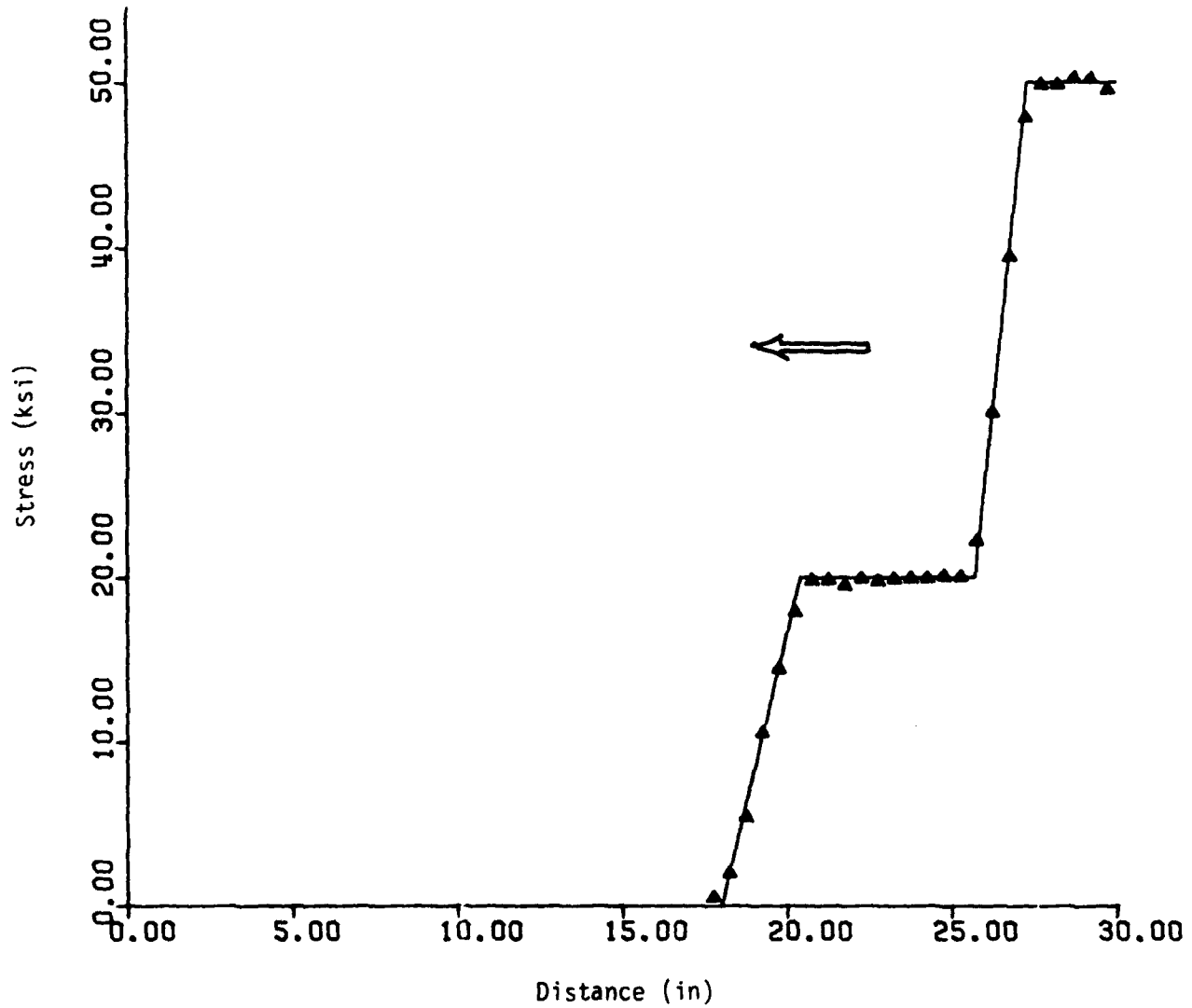


Fig. 6.44

Elastic-Plastic Pulse,  $t = 60 \mu \text{ Sec.}$

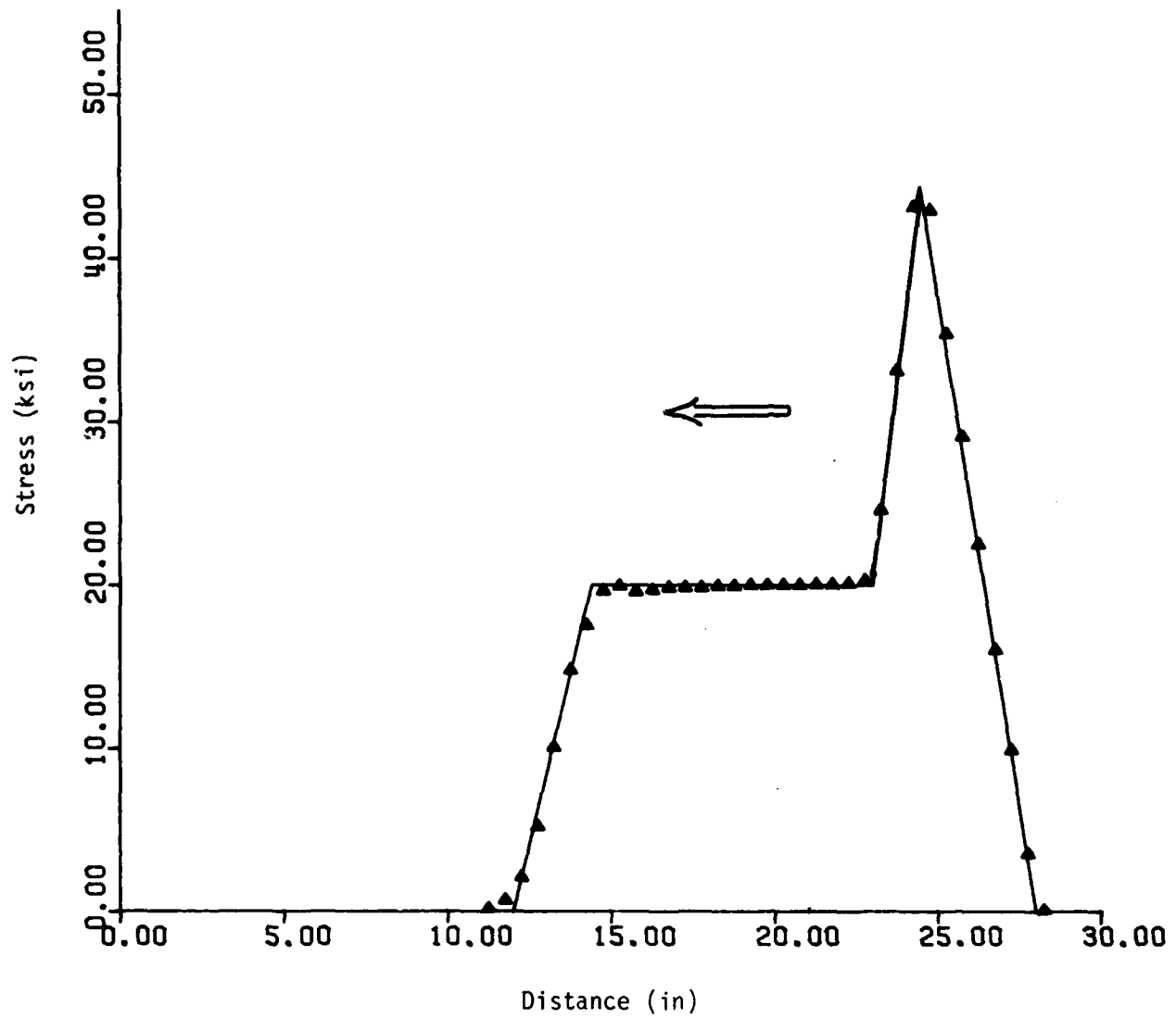


Fig. 6.45 Elastic-Plastic Pulse,  $t = 90 \mu \text{ Sec.}$



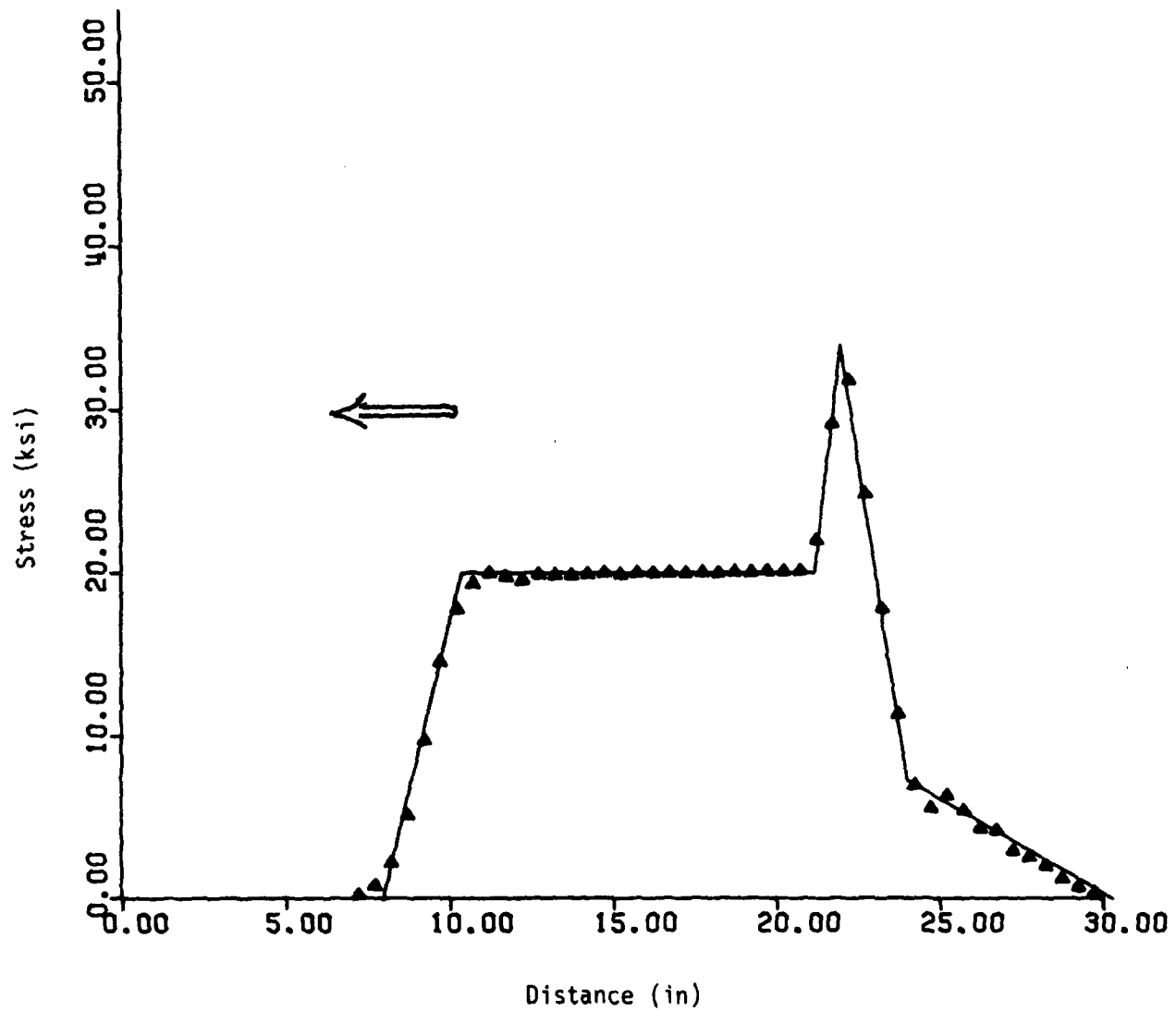


Fig. 6.46 Elastic-Plastic Pulse,  $t = 120 \mu \text{ Sec.}$

First, since ABAQUS was developed using a data base management procedure for the purpose of coding reliability, invariably some degree of overhead must be paid whenever running a problem. This overhead may become insignificant for large application problems, but it is a significant portion of the total CPU time for small size problems. Secondly, the nonlinear solution algorithm adopted in ABAQUS is based on the full Newton-Raphson method. Although this method gives better convergence characteristic as compared to the modified Newton-Raphson, this advantage is often off-set by its excessive computing effort. Based on the above two points, it appears that ABAQUS would be less computationally efficient than ADINA. This observation was also agreed upon by ABAQUS developers. However, it was argued that ABAQUS becomes more CPU competitive for large size problems. The question still remains that how large a problem has to be in order for ABAQUS to gain its CPU-competitiveness?

To answer the above question, two benchmark problems were run using both ABAQUS and ADINA: i) Elastic-plastic analysis of a cantilever beam and ii) Elastic response of a Rubik Cube. Each of the two problems is described as below.

i) A Cantilever Beam

The cantilever beam was modeled by two rows of 8-node plane stress elements as shown in Fig. 6.47. The number of elements were increased progressively along the axis of the beam, thereby the number of nodes were increased accordingly. Since only two rows of elements are involved for this problem, the wave front for ABAQUS, or bandwidth for ADINA is rather small, even though the total number of degrees of freedom can be expanded.

The beam was subjected to a concentrated force at its free end and the material constants used for the analysis are

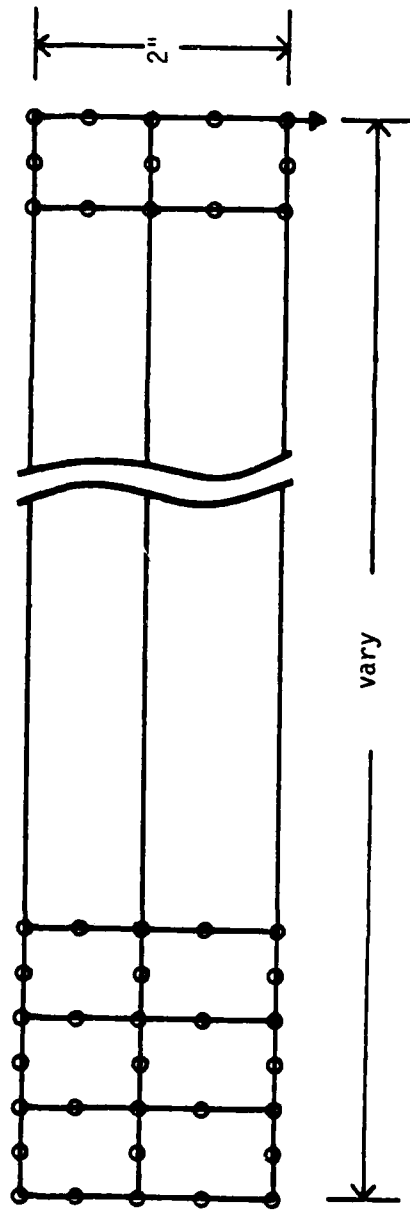


Fig. 6.47. A Cantilever Beam Modeled by 8-Node Plane Stress Elements.

Young's modulus	$E = 30 \times 10^3 \text{ Ksi}$
Poisson's ratio	$\nu = 0.3$
Initial yield stress	$\sigma_0 = 30 \text{ Ksi}$
Plastic modulus	$E_p = 1500 \text{ Ksi}$

Both the material and geometric nonlinearities were optioned with 20-load increments. Plasticity was initiated during the second load increment. For ABAQUS, direct incrementing procedure was used. The total number of elements varied from 100 to 400. Correspondingly, the number of degrees of freedom varied between 810 to 3210. For this problem, the CPU time on IBM 370-158 computer for both ABAQUS and ADINA is plotted against the number of elements as shown in Fig. 6.48. The CPU for ABAQUS increases linearly with the model size. For ADINA, two different sizes of workspace (master A-array) were specified; namely 45 K and 90 K (words). It is seen that the efficiency of ADINA strongly depends on the size of workspace allocated. This is due to the fact that the code uses an out-of-core blocking technique in which the structural stiffness is partitioned into several blocks and a great deal of CPU is consumed in transferring data from the fast core to low-speed disk or tape units or vice versa. Obviously, ADINA is quite efficient for small size models. As the number of elements was increased, ADINA loses its advantage over ABAQUS. One way to improve ADINA's efficiency is to increase the core size for execution. Even with a virtual memory system, there is always an upper limit on the maximum core size that can be allocated.

#### ii) A Rubik Cube

Differing from the preceding benchmark, both the number of degrees of freedom and its bandwidth increase as the mesh size is expanded. The cube is subjected to a concentrated force at the center and symmetric boundary

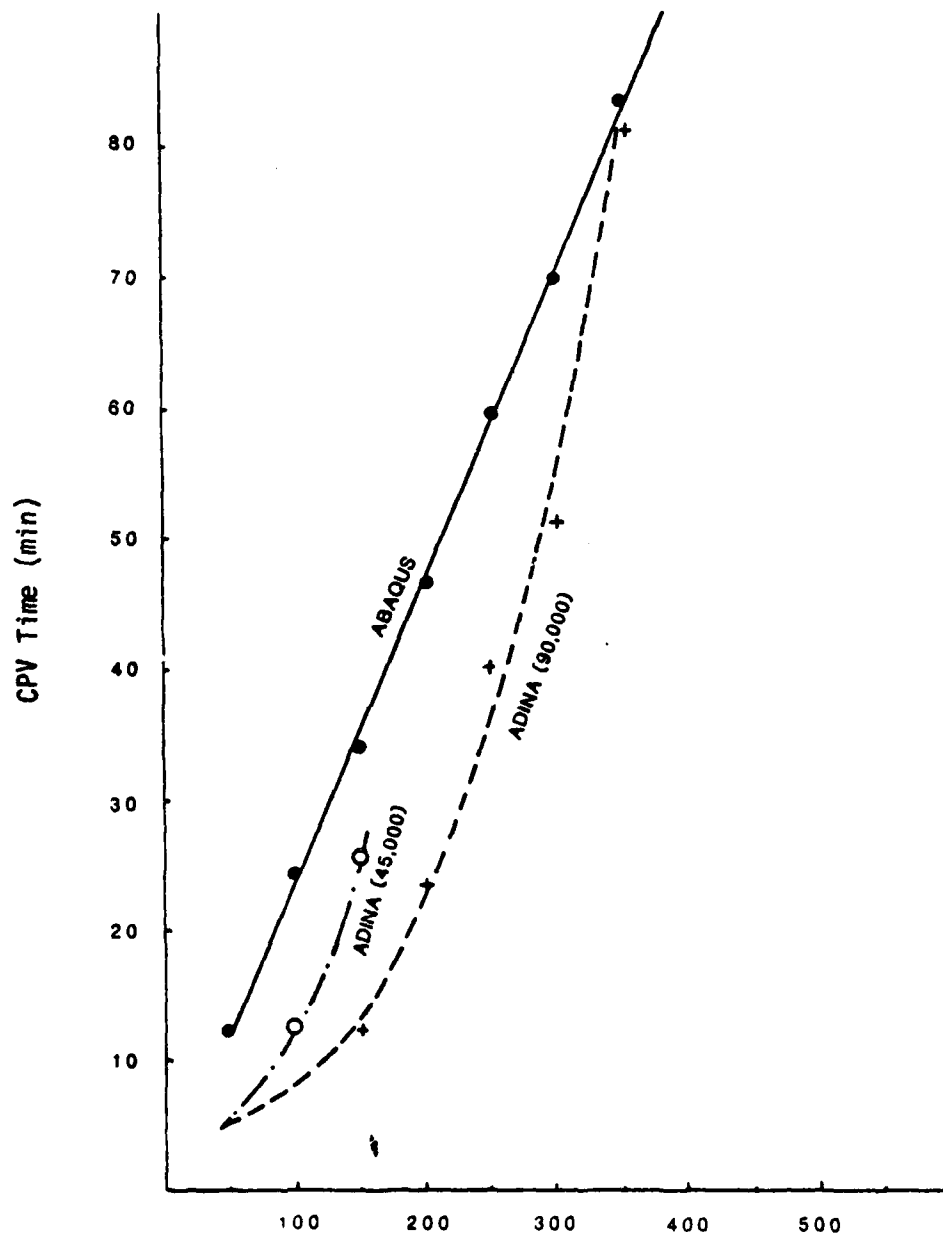


Fig. 6.48. Comparison of CPU Time Between ABAQUS and ADINA for a 2/D Problem

Table 6.6 ADINA Runs for Elastic-Plastic Beam Problem

<u>Problem Size</u>	<u>Workspace</u>	<u>Number of Blocks</u>	<u>CPU for Stiffness Formation</u>	<u>CPU for Triangu- larize</u>	<u>Step-by- step Total</u>	<u>Total C P U</u>
50	45,000	1	0*	0*	4min 54 sec	5min 31.95sec
50	90,000	1	1 sec	0	4min 42 sec	5min 20.69sec
100	45,000	3	1 sec	0	11min 56sec	12min35.99sec
100	90,000	1	0	0	7 min 42sec	8min 3.36sec
150	45,000	8	1 sec	0	25min 1 sec	25min41.28sec
150	90,000	1	0	0	11min 49sec	12min12.39sec
200	90,000	3	1 sec	0	22min 48sec	23min30.51sec
250	90,000	5	1 sec	0	39min 45sec	40min10.81sec
300	90,000	8	1 sec	0	50min 54sec	51min21.19sec
350	90,000	19	2 sec	0	80min 15sec	81min 0.23sec
350	1,000,000	1	1 sec	0	34min 24sec	35min 8.73sec

---

\*Less than .1 second.

conditions were enforced. Since full nonlinear analysis of this problem is prohibitively expensive, only linearly elastic response was considered. The mesh size was varied from two to five divisions in all three directions and a mesh of  $5 \times 5 \times 5$  is shown in Fig. 6.49. The workspaces specified for ABAQUS were 50 K bytes and 300 K; for ADINA, 90 K and 300 K. The CPU time vs. mesh size is plotted in Fig. 4. Again, for small problems ADINA is more efficient than ABAQUS. However, as the size of the problem was increased to be  $5 \times 5 \times 5$  i.e. 125 elements and 156 nodes ( = 2268 degrees of freedom), the CPU time required by ADINA is about the same as that by ABAQUS. Table 6.7 shows additional CPU detail of ADINA for analyzing the 3/D problem. Apparently, the requested workspace has some effect on the CPU time, but not as significant as the 2/D problem. In summary, we may draw the following commentary remarks:

- i) For small size problems, ABAQUS is not as efficient as ADINA. However for large size problems, the two codes seem to have similar efficiency.
- ii) The execution time of ADINA is quite sensitive to the workspace allocated. That is to say, the bigger core size is allocated to ADINA, the better its computational efficiency becomes. On the contrary, ABAQUS is not so sensitive to the size of workspace, so long as it is sufficient for the analysis.

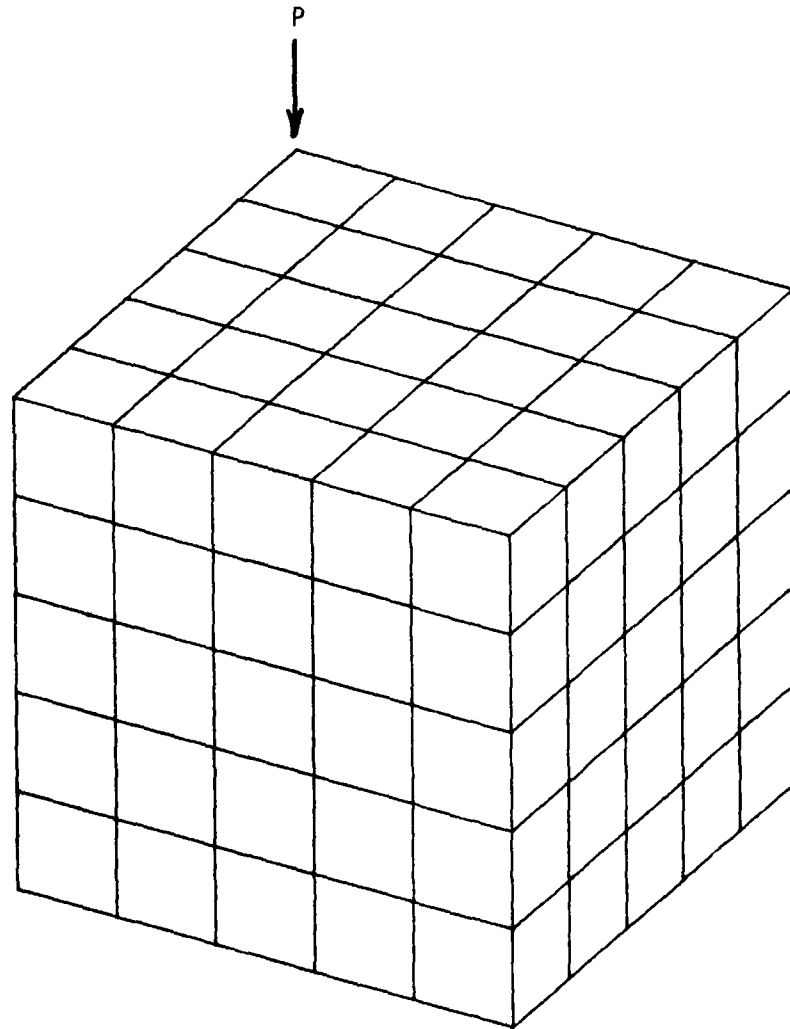


Fig. 6.49. A 3/D Rubik Cube



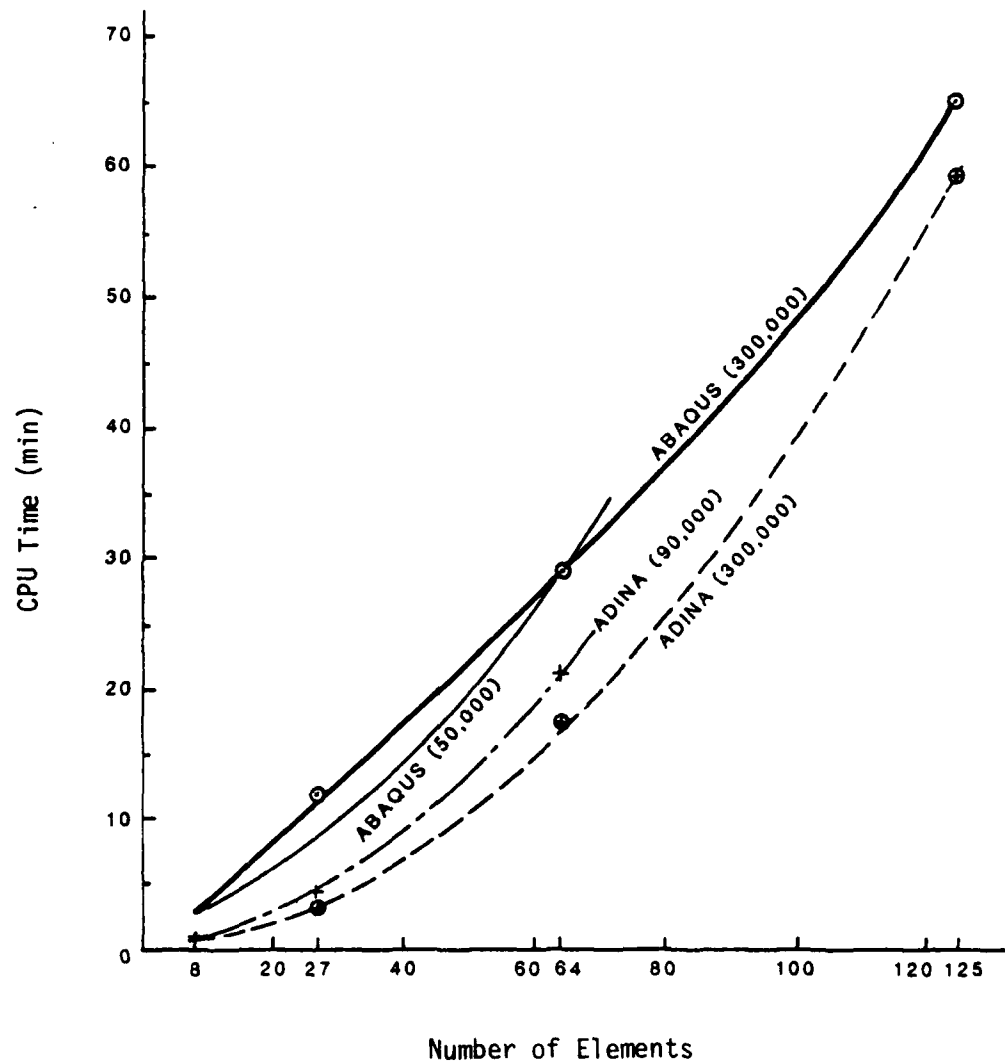


Fig. 6.50. Comparison of CPU Time Between ABAQUS and ADINA for a 3/D Problem.

Table 6.7 ADINA Runs for the 3/D Linear Problem

<u>Problem Size</u>	<u>Workspace</u>	<u>Number of Blocks</u>	<u>CPU for Stiffness Formation</u>	<u>CPU for Triangu- larize</u>	<u>Step-by- step Total</u>	<u>Total C P U</u>
2x2x2	90,000	1	13.0sec	14sec	1 sec	47.9 sec
3x3x3	90,000	4	1min18sec	2min17sec	22 sec	4min 20.32sec
3x3x3	300,000	1	41sec	1min55sec	3 sec	3min 20.13sec
4x4x4	90,000	16	5min50sec	13min37sec	1min 9sec	21min 9.19sec
4x4x4	300,000	4	2min48sec	12min17sec	1min17sec	17min14.08sec
5x5x5	90,000	66*	--	--	--	--
5x5x5	300,000	11	46min4sec	46min8sec	3min 7sec	59min30.11sec

\* Run failed due to too many blocks that the structural stiffness was partitioned.

## 7. SUMMARY AND CONCLUSION

A general purpose nonlinear finite element program ABAQUS was reviewed and evaluated with respect to its documentation, program architecture and analysis capability. In addition, its operating characteristics were also studied by running several representative benchmark problems and the results are given in the advanced evaluation section.

Based on our evaluation work, some specific points about ABAQUS are summarized as below:

- 1) ABAQUS is supported by four documents: User's Manual, Theory Manual, Systems Manual and Example Problems Manual. Both the User's Manual and Theory Manual are rated excellent in terms of their clarity and information included. The Systems Manual, although it has high quality, is outdated. The Example Problems Manual does not have sufficient representative problems to demonstrate different aspects of the code.
- 2) Division of the code into two distinct parts, the PRE and the MAIN programs, is an efficient approach for data check runs and quick computer turn around time. Moreover, the PRE program can be run on a stand-alone mini- or micro - computer for finite element model preparation purpose.
- 3) The coding structure is highly modularized so that future extension or modification becomes relatively easy for the developers. For example, the material module (or library) is completely independent from the element module. This is distinctly different from ADINA.

- 4) Since the code was written by using the data base management and separate workspace in the central memory for processing data, all data are well protected from accidental over-writing or deletion.
- 5) The Version 3 of ABAQUS has a fairly extensive element library. But its material library is somewhat limited.
- 6) For loading (or time) increment control, the user has two options to choose from: either direct stepping or automatic stepping. Automatic stepping is extremely useful to start-up a new problem for which the user does not have any experience in its nonlinear behavior. However, indiscriminate use of this option often causes excessive CPU time.
- 7) The code is relatively machine independent (primarily for main frames). Any coding differences for various machines were prepared in a master copy of the code. A special version for a given machine can be obtained using text editor to extract appropriate coding statements.
- 8) The solution algorithm adopted in ABAQUS is the full Newton-Raphson method which can handle a wide range of nonlinear problems.
- 9) Logical input sequence with the use of key-word cards and free field format is indeed one of the desirable user-friendly features.
- 10) The finite element formulations of ABAQUS were consistently derived on a firm theoretical basis. All assumptions were clearly stated in the theory manual.

- 11) By examining the programming architecture of ABAQUS, the reviewers found that it has very high quality coding style and programming discipline.

In addition to the above comments, several areas may deserve some attention for future improvement:

- 1) The nonlinear solution algorithm adopted in ABAQUS is a full Newton-Raphson base. Other algorithms, such as modified and quasi Newton-Raphson methods, should be included in the code for user's choice.
- 2) Solution convergence during iterations is controlled by two user specified parameters: PTOL (force tolerance) and MTOL (moment tolerance). These are the absolute physical quantities of force and moment, respectively. After some extensive usage of the code, the reviewers still feel uncertain on the question of specifying the right values of PTOL and MTOL when a new nonlinear problem is encountered.
- 3) The automatic stepping method, although very useful for starting up a new problem, is inefficient when used indiscriminately. A self-adaptive procedure with some degree of intelligence would be most desirable.
- 4) More sophisticated pre- and post-processors are needed for ABAQUS. Or, as an alternative, its interface with commercial finite element graphics packages would be adequate for application purposes.

In conclusion, it is the reviewers' opinion that ABAQUS is a strong contender in the nonlinear engineering analysis market-place. The program is considered primarily as a production code, with user's heavy reliance on the developers for software support. Any coding changes or modifications by the user appear to be difficult, since the code is not transparent to the common users.

## 8. REFERENCES

1. Nickell, R.E., "The Interagency Software Evaluation Group: A Critical Structural Mechanics Software Evaluation Concept," Report PT-U78-0246, Pacifica Technology, Del Mar, California, 1978.
2. Nickell, R.E., "The Interagency Software Evaluation Group: A Critical Evaluation of the ADINA, NASTRAN, and STAGS Structural Mechanics Computer Programs," Final Report Submitted to the Office of Naval Research, Applied Science & Technology, Poway, California, December, 1981.
3. Chang, T.Y. and Padovan, J., "Evaluation of ADINA: Part I and Part II," Report No. AUE-801, The University of Akron, Akron, Ohio, June 8, 1980.
4. Jones, J.W., Fong, H.H., and Blehm, D.A., "Evaluation of the NASTRAN General Purpose Computer Program," SSC Report No. 81980, Swanson Service Corporation, Huntington Beach, California, August 1980.
5. Thomas, K. and Sobel, L.H., "Evaluation of the STAGSC-1 Shell Analysis Computer Program," Report No. WARD-10881, Westinghouse Electric Corporation, Advanced Reactors Division, Madison, PA, August, 1981.
6. MARC Analysis Research Corporation, "MARC General Purpose Finite Element Program, Vol. A-E, Rev. J.2," 1981.
7. "ABAQUS User's Manual - Version 3," Hibbitt and Karlsson, Inc., June 1979 (Revised September 1980).
8. "ABAQUS Theory Manual," Hibbitt and Karlsson, Inc., January, 1981.
9. "ABAQUS Systems Manual," Hibbitt and Karlsson, Inc., September, 1980.
10. "ABAQUS Example Problems Manual," Hibbitt and Karlsson, Inc., September, 1980.
11. Bathe, K.J., "ADINA - A Finite Element Program for Automatic Dynamic Incremental Nonlinear Analysis," Report 82448-1, Acoustic and Vibration Laboratory, Mechanical Engineering Department, M.I.T., September 1975, (revised December 1978).
12. Hilber, H.M., Hughes, T.J.R. and Taylor, R.L., "Improved Numerical Dissipation for Time Integration of Algorithms in Structural Dynamics," Earthq. Engng. Struct. Dyn., 5, 1977, pp. 283-292.
13. Hilber, H.M. and Hughes, T.J.R., Collocation, Dissipation and 'Overshoot' for Time Integration Schemes in Structural Dynamics," Earthq. Engng. Struct. Dyn., 6, 1978, pp. 99-117.

14. Wilson, E.L., "A Computer Program for the Dynamic Stress Analysis of Underground Structures," Report No. SESM 68-1, Department of Civil Engineering, University of California, Berkeley, 1968.
15. Budiansky, B. and Sanders, J.L., "On the 'Best' First-Order Linear Shell Theory", pp. 129-140, in Progress in Applied Mechanics, The Prager Anniversary Volume, Macmillan, London, 1963.
16. Zienkiewicz, O.C., "The Finite Element Method", McGraw-Hill Book Company, New York, 1977.
17. Dodge, W.G. and Moore, S.E., "Stress Indices and Flexibility Factors for Moment Loadings on Elbows and Curved Pipes", Welding Research Council Bulletin, No. 179, Dec. 1972.
18. Hibbitt, H.D., "Special Structural Elements of Piping Analysis" in Pressure Vessels and Piping: Analysis and Computers, ASME, NY, 1974.
19. Ohtsubo, H. and Watanabe, O., "Flexibility and Stress Factors for Pipe Bends - An Analysis by the Finite Ring Method", ASME paper 76-PVP-40, 1976.
20. Takeda, H., ASai, S. and Kwata, K., "A New Finite Element for Structural Analysis of Piping Systems", Proceedings of the 5th SMIRT Conference, Berlin, 1979.
21. Bathe, K-J., and Almeida, C.A., "A Simple and Effective Pipe Elbow Element - Linear Analysis", Trans. ASME, J. Appl. Mech., 47, No. 1, 1980.
22. Chang, T. Y., Prachuktam, S. and Reich, M., "Assessment of a Nonlinear Structural Analysis Finite Element Program (NONSAP) for Inelastic Analysis," Paper presented at the Energy Technology Conference, Houston, Texas, September 18-22, 1977, ASME Paper 77-PVP-10.
23. Felippa, C.A., "Refined Finite Element Analysis of Linear and Nonlinear Two-Dimensional Structures," Ph.D. Thesis, Univ. of California, Berkeley, Report 150, 76-22, 1966.
24. Horrigmoe, G., "Finite Element Instability Analysis of Free-form Shells," The Univ. of Trondheim, Norway, Report No. 77-2, 5, 1977.
25. Kao, P., "A Comparative Study on the Elastic-Plastic Collapse Strength of Initially Imperfect Deep Spherical Shells," The George Washington University, Washington, D.C., 20052.
26. Horrigmoe, G. and Eidsheim, O.M., "Hybrid Stress Finite Element Model for Elastic-Plastic Analysis," in Finite Elements in Nonlinear Mechanics, edited by P.G. Bergan, et al., Norwegian Institute of Technology, Trondheim, Norway, 1977.
27. Hodge, P.G., Jr. and Belytschko, T., "Numerical Methods for the Limit Analysis of Plates," J. Appl. Mech., Vol. 25, Series E, 1968, pp 796-802.



28. Popov, E.P., Khjogasteh-Bakht, M., and Yaghmai, S., "Bending of Circular Plates of Hardening Material," Int. J. Solids and Structures, Vol. 3, 1967, pp 975-988.
29. Sabir, A.B., and Lock, A.C., "The Application of Finite Elements to the Large Deflection Geometrically Non-Linear Behavior of Cylindrical Shells," in Variational Methods in Engineering, Ed. by C. A. Brebbia and H. Tottenham, Southampton Univ. Press, 1973, pp. 7166-7175.
30. Dhatt, G.S., "Instability of Thin Shell by The Finite Element Method," Proceeding of IASS Symposium for Folded Plates and Prismatic Structures, Vienna, 1970.
31. Timoshenko, S.P. and Gere, J.M., Theory of Elastic Stability, Second Ed., McGraw-Hill, New York, 1961.
32. Krakeland, B., "Nonlinear Analysis of Shells Using Degenerate Isoparametric Elements," in Finite Elements in Nonlinear Mechanics, edited by P. G. Bergon et al., Norwegian Institute of Technology, Trondheim, Norway, 1977.
33. "Evaluation of Inelastic Computer Program," A Report Prepared for Westinhouse Advanced Reactor Division by Foster Wheeler Corporation, Livingston, N.J., Contract No. 54-7WP-12177-B, March 1972.
34. Horrigmoe, G. and Bergan, P.G., "Nonlinear Analysis of Free Form Shells by Flat Finite Elements," Comp. Meth. Appl. Mech. Engng., 16, 1978. pp. 11-35.
35. Stricklin, J.A., "Geometrically Nonlinear Static and Dynamic Analysis of Shells of Revolution," High Speed Computing of Elastic Structures, Proc. of the Symposium of IUTAM, University of Liege, August 1970, pp. 383-411.
36. Mesall, J.F., "Large Deflections of Spherical Shells Under Concentrated Loads," J. Appl. Mech., Vol. 32, 1965, pp. 936-938.
37. Leicester, R.H., "Finite Deformations of Shallow Shells," J. Eng. Mech. Division, ASCE, Vol. 94, No. EM-2, 1968, pp. 1409-1423.
38. Money, H.A. and James, A.G., "Applications of BERSAFE in Nonlinear Stress Analysis Problems," in Nonlinear Problems in Stress Analysis, Ed. by P. Stanley, Applied Science Publishers, London, 1977.
39. Bathe, K.J., Ramm, E., and Wilson, E.L., "Finite Element Formulations for Large Deformation Dynamic Analysis," Int. J. Numerical Methods in Engng., Vol. 9, 1975, pp. 353-396.
40. Kraus, H. and Kalnins, A., "Transient Vibration of Thin Elastic Shells," J. Acoust. Soc. Amer., 38(6), 1965, pp. 994-1002.
41. Hartzman, M. and Hutchinson, J.R., "Nonlinear Dynamics of Solids by The Finite Element Method," J. Computers and Structures, 2, 1972, pp. 47-77.

## Appendix A - Dynamic Response of a Semi-Spherical Shell

(Problem 6.7)

The solution for dynamic response of a semi-spherical shell was obtained by Kraus and Kalnins [39]. The non-dimensionalized transverse displacement is given by

$$(WC\phi, T) = \sum_{i=1}^{\infty} \frac{w_i(\phi)}{w_i(0)} \cdot \frac{m_i F_i(T)}{\Gamma_i} \quad (A-1)$$

and

$$W = (D/a^4 P_0) w \quad (A-2)$$

where

$$\phi = \text{Angular coordinate, } 0 \leq \phi \leq 90^\circ$$

$$T = (D/a^4 \rho h)^{1/2} \cdot t \quad (A-3)$$

$$D = \frac{Eh^3}{12(1-\nu^2)} \quad (A-4)$$

$$a = \text{Radius of the shell}$$

$$h = \text{Thickness of the shell}$$

$$\rho = \text{Density}$$

$$t = \text{Time}$$

$$P_0 = \text{Uniform Pressure}$$

$$w = \text{Transverse deflection}$$

$$m_i = \text{Mode participation factor}$$

The function  $F_i$  in Eq. (A-1) has the expression

$$F_i = \{ T_i / [K + 12(1-\nu^2) \Omega_i^2 (a/h)^2] \} \cdot [1 - (e^{-T\Lambda}/T_i) (\Lambda \sin T_i T + T_i \cos T_i T)] \quad (A-5)$$

and

$$T_i = [K + 12(1-\nu^2) \Omega_i^2 (a/h)^2 - \Lambda^2]^{1/2} \quad (A-6)$$

$$K = (a^4/D) k \quad (A-7)$$

$$\Omega_i = (\rho/E)^{1/2} a \omega_i \quad (A-8)$$

$$\Lambda = (a^4/\rho h D)^{1/2} \cdot \lambda/2 \quad (A-9)$$

where

$k$  = Elastic parameter of viscoelastic foundation

$\omega_i$  = Natural frequency

$\lambda$  = Viscous damping of the foundation

For the following specialized values of parameters:

$$h = 1 \text{ in.} \quad a = 20 \text{ in.} \quad P_o = 1 \text{ Psi}$$

$$E = 30 \times 10^6 \text{ Psi} \quad \nu = 0.3 \quad \rho = 1 \text{ lb-sec}^2/\text{in}^4$$

$$n = 0 \quad k = 0$$

and simply support condition, the transverse deflection at the corner of the shell (Fig. 6.36) is

$$w = 1.33 \times 10^{-5} \sum_{i=1}^{\infty} \frac{m_i}{\Omega_i} (1 - \cos 273.86 \Omega_i t) \quad (\text{A-10})$$

The values of  $m_i$  and  $\Omega_i$  are given as follows:

<u>i</u>	<u>m<sub>i</sub></u>	<u>Ω<sub>i</sub></u>
1	0.0480	0.773
2	-0.1048	1.010
3	0.3582	1.242
4	-1.5912	1.578
5	2.7978	1.720
6	-0.8794	2.192
7	0.3739	2.793
8	0.2619	2.941
9	-0.4800	3.733
10	0.3596	4.682
11	0.0477	4.843
12	-0.3783	5.804
13	0.0557	6.876
14	0.3063	7.047
15	-0.3411	8.366

---

## Appendix B - Longitudinal Wave Propagation in a Bar

The solution of elastic longitudinal wave propagation can be found from Reference [42]. Consider a semi-infinite bar subjected to an axial force  $P(t)$ , the displacement  $u$  is given by:

$$u = \frac{4}{\pi C_e \rho A} \sum_{i=1,3,5,\dots}^{\infty} \frac{(-1)^{(i-1)/2}}{i} \sin \frac{i\pi x}{2L} \int_0^t P(t') \sin \left[ \frac{i\pi C_e}{2L} (t-t') \right] dt' \quad (B-1)$$

where

$u$  = Axial displacement

$C_e$  = Elastic wave velocity

$$= \sqrt{E/\rho}$$

$A$  = Cross sectional area

$L$  = Length of the bar

$P$  = Pressure pulse applied at one end

For Problem 6.8, we consider the following pressure history

$$\begin{aligned} p &= P_0 \cdot t/\tau_1, \quad t \in [0, \tau_1] \\ &= P_0 (t-\tau_2)/(\tau_1-\tau_2), \quad t \in [\tau_1, \tau_2] \end{aligned} \quad (B-2)$$

where

$P_0$  = Peak pressure at  $t = \tau_1$ .

The stress pulse has the expression

$$= \frac{4 P_0}{\pi A} \sum_{i=1,3,5,\dots}^{\infty} \frac{(-1)^{(i-1)/2}}{i} F_i(t) \cos \frac{i\pi x}{2L} \quad (B-3)$$

where

$$\begin{aligned} F_i &= \frac{t}{\tau_1} - \frac{\sin p_i t}{p_i \tau_1}, \quad t \in [0, \tau_1] \\ &= \frac{t}{\tau_1} - \frac{\sin p_i t}{p_i \tau_1} - \frac{\tau_2 (t - \tau_1)}{\tau_1 (\tau_2 - \tau_1)} \\ &\quad + \frac{\tau_2 \sin p_i (t - \tau_1)}{p_i \tau_1 (\tau_2 - \tau_1)}, \quad t \in [\tau_1, \tau_2] \\ &= - \frac{\sin p_i t}{p_i \tau_1} + \frac{\tau_2 \sin p_i (t - \tau_1)}{p_i \tau_1 (\tau_2 - \tau_1)} - \frac{\sin p_i (t - \tau_2)}{p_i (\tau_2 - \tau_1)}, \quad t \geq \tau_2 \end{aligned}$$

(B-4)

The above series converges very slowly; it requires about 200 natural modes.

In the case of plastic wave propagation (for elastic-perfectly plastic material), let the stress pulse be denoted by (also shown in Fig. B-1).

$$\sigma_{\text{Front}} = k_F \tau + \sigma_F \quad (\text{B-5})$$

$$\sigma_{\text{Back}} = k_B \tau + \sigma_B$$

where  $\tau$  is the time at which the stress pulse is applied;  $k_F$  and  $k_B$  are the slopes of the front and back of the pulse. The stress profile travelling in the bar at different instants varies due to the difference in elastic wave speed  $C_E$  and plastic wave speed  $C_P$ . To determine the stress profiles, we consider the intersection of the plastic front and elastic back (corresponding to plastic unloading). The intersection has a stress value  $\bar{\sigma}$  and is located at a distance  $\bar{d}$  from the free end of the bar. Both  $\bar{\sigma}$  and  $\bar{d}$  can be expressed by

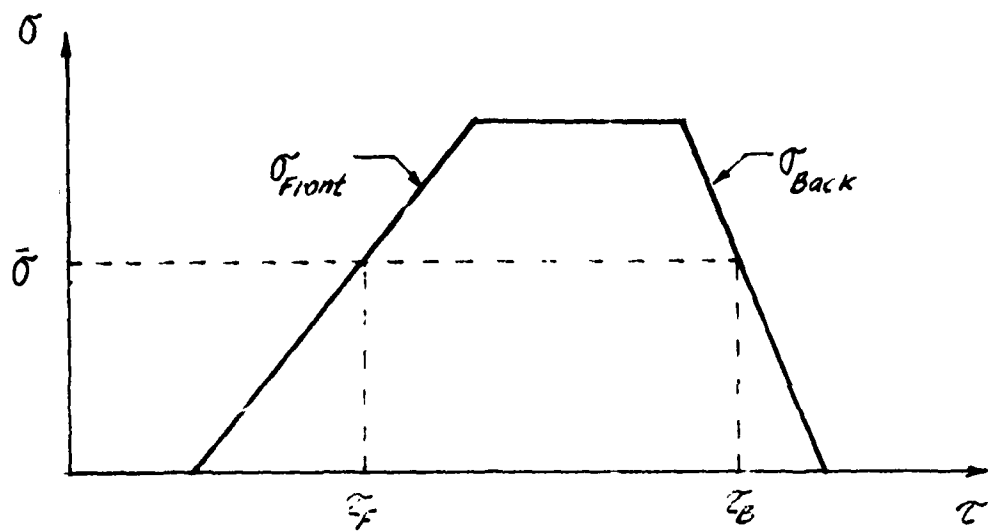
$$\bar{\sigma} = k_F \tau_F + \sigma_F = k_B \tau_B + \sigma_B \quad (\text{B-6})$$

$$\bar{d} = (t - \tau_F) C_P = (t - \tau_B) C_E$$

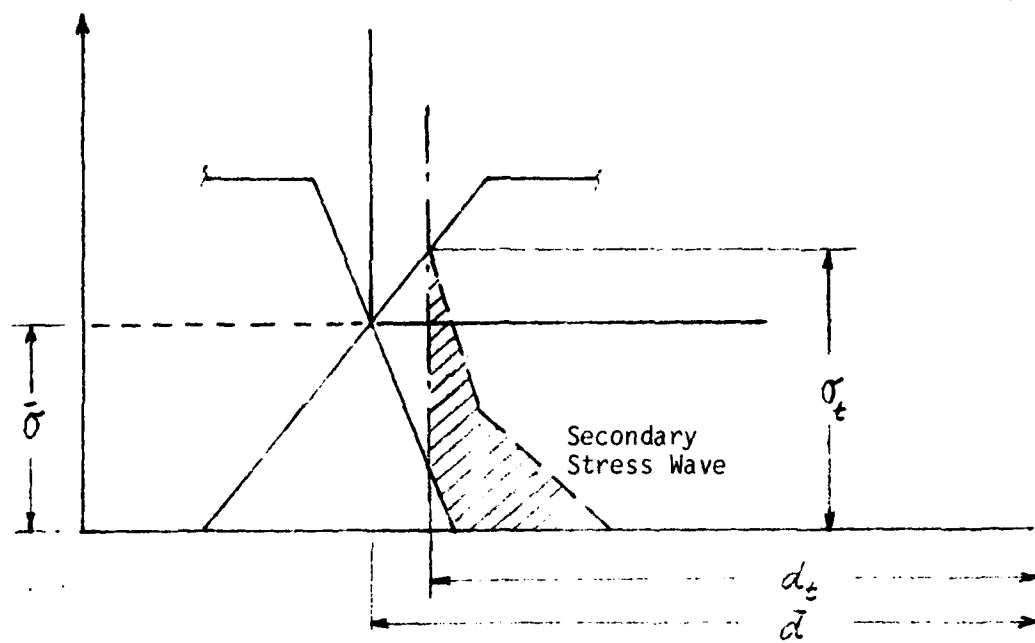
where  $\tau_F$  and  $\tau_B$  are the starting time of the stress pulse  $\bar{\sigma}$  on the front and back, respectively as shown in Fig. B-1. From Eqs. (B-5) and (B-6), solving for  $\tau_F$  and  $\tau_B$

$$\tau_F = \frac{(1 - \frac{C_E}{C_P}) t + \frac{C_E}{C_P} \cdot \frac{\sigma_F - \sigma_B}{k_B}}{1 - (\frac{C_E}{C_P})(\frac{k_F}{k_B})} \quad (\text{B-7})$$

$$\tau_B = \frac{\sigma_F - \sigma_B}{k_B} + \frac{k_F}{k_B} \sigma_F$$



(a) Stress Pulse



(b) Intersection of the Front and Back of Stress Pulse



Appendix C - Additional Analysis Capability of Version  
4 - ABAQUS.\*

For reader's information, additional analysis capabilities of version 4.5 ABAQUS over Version 3 are listed below:

Elements

- Continuum elements with finite strains
- Incompressible hybrid elements for plane strain, axisymmetric and three-dimensional analysis.
- Axisymmetric shells with finite strains
- Line Spring elements for modeling part-through cracks in shells
- Shell elements for heat - transfer analysis
- 2/D and 3/D elements with pore pressures for consideration analysis
- Interface elements (2/D and 3/D) for contact/friction stress problems
- Interface elements (2/D and 3/D) for heat transfer analysis
- Elements for coupled thermal-stress analysis (truss, 2/D, 3/D and shell elements)
- Pipe elements with the effect of internal pressure

Materials

- A hypoelastic model for soils
- Modified Cam Clay model
- ORNL creep and plasticity model for types 306 and 316 stainless steel

- Coulomb friction model for interface elements
- No-tension or no-compression material model
- Gap conductance and radiation for interface elements
- Latent heat model
- Permeability model (isotropic, orthotropic or anisotropic)  
for soils
- Chen and Chen concrete plasticity model
- hyperelastic model for elastomer

Procedures

- A modified Riks algorithm for structural instability analysis
- Consolidation analysis for soils
- Coupled temperature/displacement analysis
- Fluid-solid interaction analysis
- Superelement/substructuring capability
- J integral calculations with Park's node moving technique

---

\* The above information was supplied by Hibbitt, Karlsson & Sorensen, Inc.  
(March 30, 1983).

REPORT DOCUMENTATION PAGE		READ INSTRUCTIONS BEFORE COMPLETING FORM
1. REPORT NUMBER AUE - 821	2. GOVT ACCESSION NO. A128788	3. RECIPIENT'S CATALOG NUMBER
4. TITLE (and Subtitle)  Evaluation of a Nonlinear Finite Element Program: ABAQUS.		5. TYPE OF REPORT & PERIOD COVERED Technical Report
		6. PERFORMING ORG. REPORT NUMBER
7. AUTHOR(s)  T. Y. Chang, S. M. Wang		8. CONTRACT OR GRANT NUMBER(s) N0014-78-C-0691
9. PERFORMING ORGANIZATION NAME AND ADDRESS Department of Civil Engineering University of Akron Akron, OH 44325		10. PROGRAM ELEMENT, PROJECT, TASK AREA & WORK UNIT NUMBERS
11. CONTROLLING OFFICE NAME AND ADDRESS  Office of Naval Research Arlington, VA		12. REPORT DATE March 15, 1983
		13. NUMBER OF PAGES
14. MONITORING AGENCY NAME & ADDRESS (if different from Controlling Office)  Office of Naval Research-ONR Resident Representative Ohio State University Research Center 1314 Kinnear Road Columbus, OH 43212		15. SECURITY CLASS. (of this report) Unclassified
		15a. DECLASSIFICATION/DOWNGRADING SCHEDULE
16. DISTRIBUTION STATEMENT (of this Report)  Distribution of this report is unlimited.		
17. DISTRIBUTION STATEMENT (of the abstract entered in Block 20, if different from Report)		
18. SUPPLEMENTARY NOTES		
19. KEY WORDS (Continue on reverse side if necessary and identify by block number)  ABAQUS, Nonlinear Finite Element Analysis, Computer Program, Analysis Capability, Data Base Structure		
20. ABSTRACT (Continue on reverse side if necessary and identify by block number)  An evaluation of the version 3 - ABAQUS, a general purpose finite element program, was conducted. The evaluation work consists of the review of its documentation, functional capability, and programing structure. Work also includes a section on advanced evaluation to investigate the numerical performance of the program.		

DATE  
FILME